PhD degree in Molecular Medicine (curriculum in Molecular Oncology)

European School of Molecular Medicine (SEMM),

University of Milan and University of Naples "Federico II"

Settore disciplinare: Bio/10

Mitochondrial MARCH5 ubiquitin ligase abrogates MCL1-dependent resistance to BH3 mimetics via activation of NOXA

Aishwarya Subramanian

Center for Genomic Science of IIT@SEMM, Milan

R09854

Supervisor: Dr. MARK WADE, IIT@SEMM, Milan

Anno accademico 2014-2015

DEDICATION

This dissertation is dedicated to my grandmothers Janaki Raman and Pattamal Viswanathan, my dear friends Viswanathan Balakrishnan and Srinivasan Seshadri and to every individual fighting cancer.

Your strength and courage are a continuous source of inspiration

ACKNOWLEDGEMENTS

I would like to acknowledge and thank the people who have supported and guided me over the past four years. I would especially like to thank my PhD supervisor, Dr. Mark Wade for providing me with this opportunity and for his guidance and constant encouragement. All this cumulatively has allowed me to become a confident and independent researcher today. To all my colleagues- Michela Mattioli, Fernanda Ricci, Lisette Verhoef, Francesca Milanesi and Adrian Andronache, thank you for your help and putting my with my sometimes incessant doubts and questions. I have learnt a great deal from all of you.

I would also like to extend my appreciation to my external and internal PhD advisors- Dr. Damien Arnoult and Dr. Simona Polo. Thank you for the helpful feedback, experimental ideas and support. My thanks are also extended to Dr. Mohamed Elgendy for the innumerable MCL1 discussions that we have had and for his generosity in lending reagents. I would also like to thank the tissue culture and imaging facilities at the IFOM-IEO campus whose support has been critical for the completion of this work.

I would like to thank my parents, brother and other family members. Your constant support and belief in me has been the backbone of this work. To my fiancé Karthik, thank you foremost for putting up with me over the last difficult year. Your constant encouragement and positive outlook has made it easier for me to face stressful situations. Finally, to all the wonderful friends that I have gained here, thank you for the support over the past four years.

TABLE OF CONTENTS

LIST OF FIGURES PAGE

LIST OF ABBREVIATIONS

APAF1- Apoptotic Peptidase Activating Factor 1

ATP- Adenosine Triphosphate

BAD- Bcl-2 Antagonist Of Cell Death

BAK- Bcl-2 Antagonist/Killer

BARD1-Brca1 Associated Ring Domain 1

BAX- Bcl-2-Associated X Protein

BCL2- B Cell Lymphoma 2

BCLW- Bcl-2-Like Protein 2

BCLXL- Bcl-2-Related Gene, Long Isoform

BID- Bh3 Interacting Domain Death Agonist

BIM- Bcl-2-Interacting Mediator Of Cell Death

BRCA1- Breast Cancer 1

BTRCP- Beta-Transducin Repeat Containing Protein

CCCP- Carbonyl Cyanide M-Chlorophenyl Hydrazone

CIAP- Cellular Inhibitor Of Apoptosis

CLL- Chronic Lymphocytic Leukemia

CPT- Camptothecin

CYLD- Cylindromatosis

DMEM- Dulbecco's Modified Eagle's Medium

DMSO- Dimethyl Sulfoxide

DRP1- Dynamin-Related Protein 1

ERK- Extracellular Signal-Regulated Kinase

FADD- Fas Associated Via Death Domain

FBXW7- F-Box/Wd Repeat-Containing Protein 7

GSK3-Glycogen Synthase Kinase 3

HECT- Homologous To The E6-Ap Carboxyl Terminus

JNK- C-Jun N-Terminal Kinase

MAPK- Mitogen-Activated Protein Kinase

MARCH- Membrane-Associated Ring -Ch

MCL1-Myeloid Cell Leukemia 1

mdivi-1-Mitochondrial Division Inhibitor 1

MDM2- Mouse Double Minute 2 Homolog

MFN1- Mitofusin 1

MFN2-Mitofusin2

MLK1- Mixed-Lineage Kinase 1

MOMP- Mitochondrial Outer Membrane Permeabilization

MPT- Mitochondrial Permeability Transition Pore

MULAN- Mitochondrial E3 Ubiquitin Protein Ligase 1

NEMO- NF-Kappa-B Essential Modulator

NF-KB- Nuclear Factor Of Kappa Of Activated B Cells

OPA1- Optic Atrophy 1

PARP- Poly ADP-Ribose Polymerase

PEST- Proline (P), Glutamic Acid (E), Serine (S), And Threonine (T)

PINK1- Pten Induced Putative Kinase 1

PKA- Protein Kinase A

PKB-Protein Kinase B

PMA- Phorbol Myristate Acetate

PTEN- Phosphatase And Tensin Homolog

PUMA- p53-Upregulated Modulator Of Apoptosis

RING-Really Interesting New Gene

RIPK3- Receptor-Interacting Serine/Threonine-Protein Kinase 3

RMCE- Recombinase-Mediated Cassette Exchange

RNF144B- Ring Finger Protein 144b

SCF- Skp, Cullin, F-Box Containing Complex

SDS-PAGE- Sodium Dodecyl Sulphate - Polyacrylamide Gel Electrophoresis

TANK- TRAF Family Member-Associated Nfkb Activator

TCF3-Transcription Factor 3

TMRE- Tetramethylrhodamine, Ethyl Ester

TNF- Tumor Necrosis Factor

TOMM20- Translocase Of Outer Mitochondrial Membrane 20 Homolog

TRAF2/3/6- TNF Receptor-Associated Factor 2/3/6

TRIM17- Tripartite Motif Containing 17

USP13/21/22- Ubiquitin Carboxyl-Terminal Hydrolase 13/21/22

USP9X- Ubiquitin Specific Peptidase 9, X-Linked

VDAC- Voltage-Dependent Anion Channel

XIAP- X-Linked Inhibitor Of Apoptosis

ABSTRACT

BH3 mimetic compounds induce tumor cell death through targeted inhibition of anti-apoptotic BCL2 proteins. Resistance to one such compound, ABT-737, is due to increased levels of anti-apoptotic MCL1. Using chemical and genetic approaches, we show that resistance to ABT-737 is abrogated by inhibition of the mitochondrial RING E3 ligase, MARCH5. Mechanistically, this is due to increased expression of pro-apoptotic BCL2 family member, NOXA, and is associated with MARCH5 regulation of MCL1 ubiquitination and stability in a NOXA-dependent manner. *MARCH5* expression contributed to an 8-gene signature that correlates with sensitivity to the preclinical BH3 mimetic, navitoclax. Furthermore, we observed a synthetic lethal interaction between MCL1 and MARCH5 in MCL1-dependent breast cancer cells. Our data uncover a novel level at which the BCL2 family is regulated; furthermore, they suggest targeting MARCH5-dependent signaling will be an effective strategy for treatment of BH3 mimetic-resistant tumors.

CHAPTER 1. INTRODUCTION

Mitochondria regulate critical aspects of cellular function and homeostasis. Apart from generating energy required for cellular function, mitochondria also serve as major signaling hubs in pathways related to redox regulation, innate immune signaling, and apoptosis[1,2]. Mitochondria have also been implicated in retrograde signaling; during this process, metabolic changes are sensed by these organelles and relayed to the nucleus in order to mount a transcriptional response[3]. In line with these diverse functions, the mitochondrial outer membrane is equipped with numerous proteins that are required for processes such as energy conversion, transfer of metabolites, and membrane dynamics; all these processes are important for mediating signal transduction events.

Mitochondria and Cancer

As mitochondria are major cellular signaling platforms, their dysfunction plays a critical role in the etiology of diseases such as neurodegeneration, metabolic disorders, and cancer[1,4]. In cancer, virtually all tumors exhibit altered metabolic states. According to the theory put forward by Otto Warburg, cancer cells produce ATP through glycolysis even under aerobic conditions. In contrast, healthy cells generate energy from the oxidation of pyruvate, which is a glycolytic end-product that is oxidized within the mitochondria. According to Warburg, the switch from mitochondrial respiration to aerobic glycolysis, which may be due damaged or dysfunctional mitochondria, was a key driver of tumorigenesis[5].

However, it is now clear that the switch to glycolysis is predominantly due to the reprogramming of mitochondrial metabolic pathways by activated oncogenes such as *RAS*, *MYC*, and *AKT*, rather than being a default consequence of mitochondrial defects.

These oncogenes also render cancer cells resistant to programmed cell death through rewiring of the mitochondrial apoptotic pathway. Thus, many cancer cells are refractory to chemotherapeutics due to increased dependency on pro-survival pathways and altered metabolism[6–8].

Apoptosis

Apoptosis (or 'programmed cell death') is vital for the regulation of cell growth and maintenance of tissue homeostasis, and its evasion is one of the major hallmarks of cancer[9,10]. The reduced sensitivity of cancer cells to apoptosis is largely due to up regulation of anti-apoptotic genes and inactivation of genes crucial for mediating cell death. Characteristics of apoptosis include cell shrinkage, nuclear fragmentation, chromatin condensation and membrane blebbing, which are cumulatively mediated by a group of proteases called caspases[11]. The signaling cascades that lead to cell death are diverse and depend on the upstream death-inducing stimulus. The different categories of cell death pathways can be broadly categorized as follows-

(i) Extrinsic Apoptosis

The extrinsic apoptotic pathway initiates apoptosis through death receptors that are members of the tumor necrosis factor (TNF) receptor gene superfamily. These receptors transmit death-inducing signals from the cell surface to intracellular signaling pathways. Examples of ligands and corresponding death receptors include FasL/FasR, TNF-α/TNFR1, Apo3L/DR3, Apo2L/DR4 and Apo2L/DR5. The binding of ligands to receptors initiates the recruitment of adapator molecules such as the FAS-associated death domain protein (FADD) that can in turn dimerize and activate the initiator caspase 8. This protease can in turn cleave its substrates BID and caspase 3 to initiate cell death[11,12].

(ii) Intrinsic Apoptosis

The intrinsic signaling pathway instigates apoptosis through non-receptor-mediated stimuli that converge on the mitochondria. This pathway is predominantly activated by "intrinsic stimuli" such as oncogene activation, growth factor withdrawal, and DNA damage, and is characterized by mitochondrial outer membrane permeabilization (MOMP), release of cytochrome C and the formation of a cytosolic apoptosome complex consisting of adapter protein apoptotic protease activating factor 1 (Apaf1) and the activating protease caspase 9. This complex in turn mediates the activation of the downstream effector caspases such as caspase 3. The proteolytic activity of the caspase proteins serves to cleave substrates such as nuclear lamins, ICAD/DFF45 (inhibitor of caspase activated DNase or DNA fragmentation factor 45) and PARP (poly-ADP ribose polymerase). These cleaved proteins induce DNA fragmentation, leading to cell death. In the absence of apoptotic stimuli, caspase activation is blocked by the X-linked inhibitor of apoptosis protein (XIAP) and the cellular inhibitors of apoptosis I and II (cIAP I, II). Upon initiation of MOMP, the release of second mitochondria-derived activator of caspase (SMAC/DIABLO) blocks XIAP - mediated inhibition of caspase activity[11,12].

A great deal of cross talk exists between the extrinsic and intrinsic pathways. In certain types of cells (type I) extrinsic apoptosis involves the activation of the effector caspase 3 by caspase 8. In other types of cells (type II), the cleavage of the BCL2 homology 3 (BH3)-interacting domain death agonist (BID) and its subsequent activation can activate the intrinsic pathway leading to MOMP. The distinction between type I and II cells is dependent on the requirement of MOMP- dependent inhibition of XIAP in death receptor-mediated apoptosis[11,13].

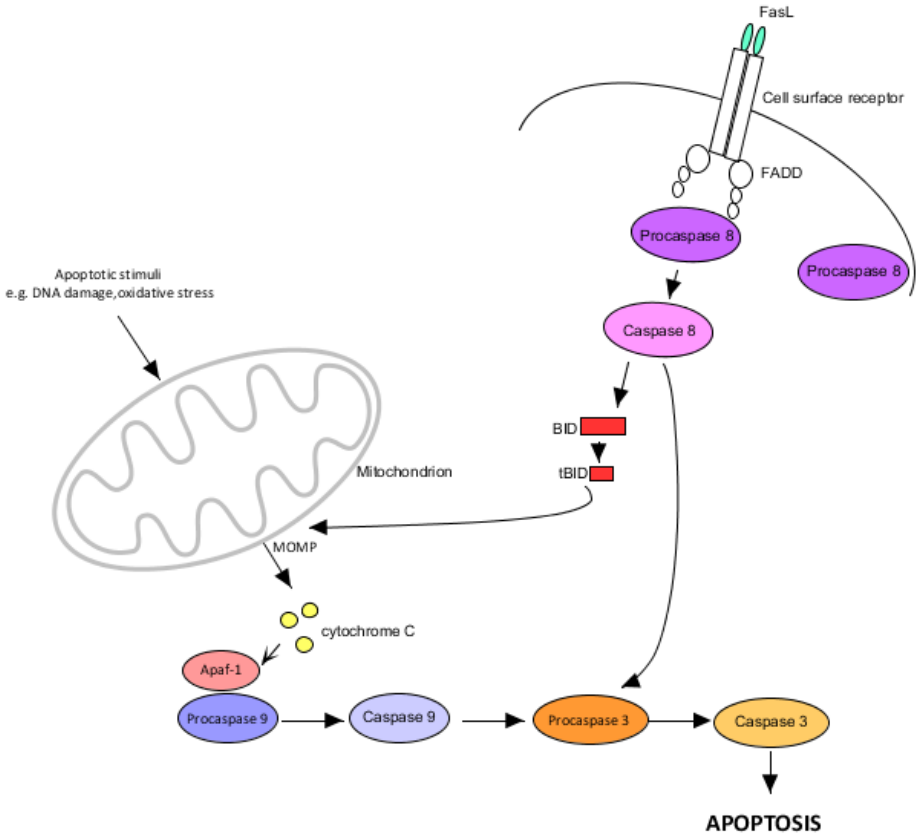

Figure 1.1. Extrinsic and Intrinsic Apoptotic Pathways

The extrinsic and instrinsic apoptotic pathways are activated by diverse stress stimuli. The binding of ligands to cell surface death receptors activates the extrinsic pathway. This involves the activation of caspase 8, which can directly activate caspase 3 leading to apoptosis or activate MOMP through the cleavage of BID. The intrinsic pathway is characterized by mitochondrial outer membrane permeabilization, release of cytochrome C and activation of a cytosolic apoptosome complex. This is turn leads to activation of downstream caspases 9 and 3 and cell death.

(iii) Alternate programmed cell death pathways

Apart from the above "classical" apoptotic pathways, other forms of programmed of cell death related to necrosis have been recently described. Necrosis is an autolytic form of cell death characterized loss of cell membrane integrity and release of cellular contents. Traditionally thought of as an unregulated process, it is now apparent that necrotic cell death can also occur in a programmed manner[14]. These programmed forms of necrosis include processes such as necroptosis, ferroptosis, mitochondrial permeability transition (MPT)-dependent necrosis, pyroptosis and pyronecrosis. Of these, pyroptosis and necroptosis are the best characterized forms. Pyroptosis is induced by inflammasome activation and has important functions in host defense and inflammation. Necroptosis is mediated by the receptor interacting protein kinase-3 (RIPK3) and its substrate, mixed lineage kinase like (MLKL) and its dysregulation is implicated in the pathogenesis of many diseases related to chronic inflammation[15,16].

BCL-2 Family of Proteins

(i) Classification of BCL-2 family proteins

In addition to its suppression by IAPs, the initiation of MOMP and release of cytochrome C is tightly regulated by the B cell CLL/lymphoma-2(BCL2) family of proteins. This family consists of closely related proteins possessing different combinations of four BCL2 homology (BH) domains and can be divided into three classes. The first class contains anti-apoptotic BCL-2 proteins (e.g. BCL2, BCLXL, and MCL1) that possess all four BH domains. The proteins interact with the BH3 domains of the pro-apoptotic BCL-2 effectors (e.g. BAK and BAX) which possess three BH domains, or with the pro-apoptotic BH3-only domain proteins (e.g. NOXA, BIM, PUMA, and BAD)[17,18].

BCL-2 family members also possess additional roles in non-apoptotic cells including maintenance of normal cell physiology, autophagy, calcium homeostasis, mitochondrial dynamics, and cellular energetics[19]. Both BCL2 and BCLXL interact with members of the mitochondrial fusion and fission machinery (MFN1/2 and DRP1, respectively) to regulate mitochondrial dynamics[20]. In addition, a relationship between mitochondrial fusion and BAX-dependent permeability transition pore formation has been described[21,22].

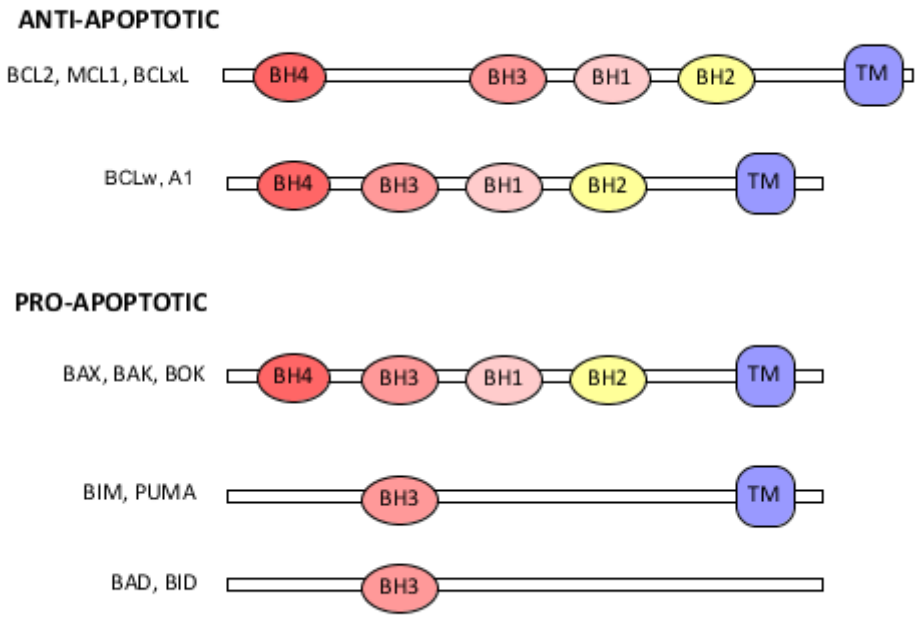

Figure 1.2. The BCL-2 Family of Proteins

Schematic representation of BCL-2 family members classified as anti- or pro-apoptotic, possessing different combinations of BH domains.

(ii) Interactions between BCL-2 family members

Many specific functional interactions between the BCL2 family members have been described. Broadly speaking, interactions between the anti- and pro- apoptotic members dictate whether a cell lives or dies. Under steady state conditions, the anti-apoptotic

members serve to inhibit the activity of the pro-apoptotic proteins. Upstream apoptotic stimuli induce conformational changes and alterations in the stoichiometry between pro- and anti- apoptotic proteins. The activated pro-death proteins such as BIM, PUMA, NOXA and BAD specifically interact with and inhibit BCL2, BCLXL and MCL1, to activate the downstream death signaling cascade[18,23,24].

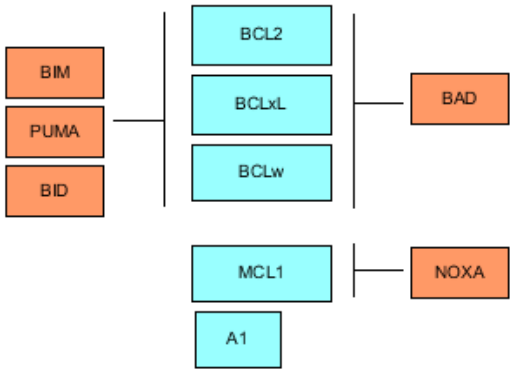

Figure 1.3. Specific interactions between pro- and anti- apoptotic proteins

In response to apoptotic stimuli, the BH3-only proteins BIM, PUMA, NOXA and BAD (shown in orange) specifically inhibit anti-apoptotic proteins (shown in blue), thereby inducing cell death.

Two models that explain regulation of the apoptotic switch have been described. First is the "director activation" model involves the BH3-only proteins such as BIM and PUMA, which directly engage and activate the pro-apoptotic effectors BAX and BAK. On the other hand, the indirect activator or "derepressor" model involves the binding of BH3-only proteins to pro-survival BCL-2 family members, which leads to the release of BH3-only activator proteins. In most cases, the apoptotic response is elicited by a combination of

events described in both models[25,26]. However, there remain many unanswered questions regarding the way in which diverse apoptotic and stress stimuli govern these interactions, and whether other mitochondrial proteins have prominent roles in coordinating the apoptotic response.

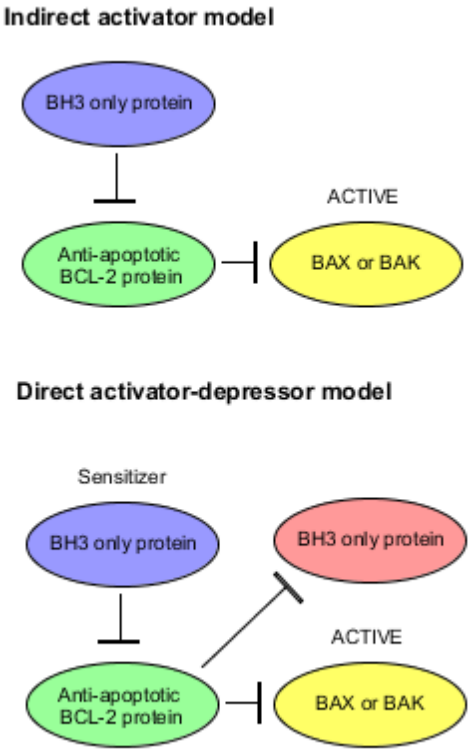

Figure 1.4. BCL-2 family interactions

Two models of BAX and BAK activation have been described- the indirect activator and the direct activator–derepressor models. The indirect activator model proposes that BAX and BAK are bound and inhibited by anti-apoptotic BCL-2 proteins, and that competitive interactions of activated BH3-only proteins with anti-apoptotic BCL-2 family members is required to activate BAX and BAK. In the direct activator–derepressor model, BAX and BAK are activated through interactions with BH3-only proteins. These interactions are inhibited by the anti-

apoptotic BCL-2 proteins, which sequester the activating BH3-only proteins or bind directly to BAX and BAK.

Since the present study is focused on select BCL-2 family members, including NOXA, MCL1 and BCLXL, these proteins will be discussed in detail in the following sections. For an in-depth discussion of other family members, see Youle, Strasser., 2008[27].

(iii) MCL1 anti-apoptotic protein

The myeloid cell leukemia 1 (MCL1) protein was initially discovered as an immediate early gene expressed during PMA-induced differentiation of a myeloid leukemia cell line (ML-1)[28]. In addition, MCL1 is essential for embryonic development, hematopoiesis and lymphopoiesis[29].

MCL1 exerts its anti-apoptotic function through the sequestration of pro-apoptotic BAX and BAK and also through interactions with BH3-only proteins, which in turn prevents BAX/BAK activation[26].

MCL1 has the same three BH domains as those present in BCL2 and BCLXL, but differs from its anti-apoptotic counterparts in that is possesses a much longer N-terminal region. This region contains critical residues responsible for MCL1 function and turnover, including sites for ubiquitination and N-terminal processing events. In addition this region also contains numerous proline (P), glutamic acid (E), serine (S) and threonine (T) residues that collectively form the PEST domain, which is characteristic of short-lived proteins. MCL1 protein indeed possesses a short half-life, as confirmed through pulse chase experiments. Its stability is regulated primarily through post-translational events such as phosphorylation and ubiquitination. The PEST domain contains phosphorylation sites for JNK, ERK-1, and p38 MAPK kinases. Phosphorylation by these kinases stabilizes MCL1, thus conferring anti-apoptotic activity. Conversely, phosphorylation by the GSK3 kinase

can serve as a "priming" event for further post-translational modifications, such as ubiquitination and degradation of MCL1. This in prevents interactions of MCL1 with pro-death proteins such as PUMA and BIM, thereby unleashing their apoptotic activity[30,31].

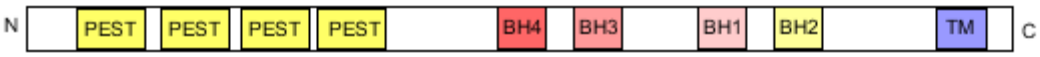

Figure 1.5. Anti-apoptotic MCL1

MCL1 possesses a long amino terminus consisting of numerous regulatory sites including residues important for phosphorylation (PEST), ubiquitination and N terminal processing.

Although MCL1 abundance can be regulated at the transcriptional level depending on the availability of growth factors and cytokines, its turnover is mainly regulated post-translationally through its ubiquitination. To date four E3 ubiquitin ligases have been identified that bind and target MCL1 for degradation. These are MULE, a HECT domain ubiquitin ligase, βTRCP and FBXW7, two SKP1-cullin-1-F-box (SCF) complex E3 ligases, and TRIM17, an E3 ligase implicated in the ubiquitination and degradation of MCL1 in neurons[32,33,34]. The ubiquitination by βTRCP, FBXW7, and TRIM17 relies on the phosphorylation sites present in the long unstructured N-terminal region of MCL1. This region contains the PEST-associated phosphodegron sites (i.e., the phosphorylation sites for the JNK, ERK and GSK3 kinases) that control the access of the E3 ligases to MCL1[31]. MCL1 stability is also controlled by the deubiquitinase, USP9X. After USP9X binds MCL1, USP9X removes the Lys 48-linked polyubiquitin chains that mark MCL1 for proteasomal degradation[35].

MCL1 expression is often dysregulated in cancer. For example, many solid and haematological malignancies harbor extra copies of the *MCL1* gene, with MCL1 being amplified in up to 10.9% of all samples analyzed. Amplification frequency was especially high in lung and breast cancers[36,37]. In addition, cancer cells also exploit the ubiquitin proteasome system responsible for MCL1 turnover. This occurs via MCL1 E3 ubiquitin ligases, increased levels of MCL1 deubiquitinases or through modification of MCL1 itself. Consequently, this leads to reduced turnover rate and increased stability of MCL1 protein[33,35].

Upregulation of MCL1 renders cancers refractory to chemotherapeutic-induced cell death. Apart from its anti-apoptotic role at the mitochondrial outer membrane, recent studies have shown that MCL1 can also localize to the mitochondrial matrix and regulate mitochondrial fusion and respiration[38]. Thus, it appears that MCL1 is a critical regulator of diverse mitochondrial signaling pathways. An in depth understanding of MCL1 function and the pathways that regulate its stability and activity would provide insight into targeting MCL1 for therapeutic purposes. In principle, MCL1 could be inhibited by accelerating its degradation or by functional antagonism that would relieve MCL1's inhibitory activity toward pro-apoptotic proteins.

(iv) NOXA

Intriguingly, as was the case for MCL1, NOXA or PMAIP1, was initially described as a PMA-induced gene[39]. It was later defined as a p53 target, as irradiation of mice lead to p53-dependent upregulation of NOXA[40]. NOXA belongs to the 'BH3-only' class of pro-apoptotic proteins. The ectopic expression of NOXA triggers cell death while NOXA depletion protects from diverse apoptotic stimuli[41].

NOXA acts as a "derepressor" protein by binding and specifically inhibiting MCL1 and A1 activity. The interaction between NOXA and MCL1 serves to displace BAK from MCL1, leading to cell death. In addition, the binding of NOXA and MCL1 serves to target MCL1 for proteasomal degradation[42]. Treatment of multiple myeloma cell lines with the proteasomal inhibitor, Bortezomib, caused concomitant upregulation of NOXA and MCL1, leading to the cleavage of MCL1 through the activation of caspases[43,44]. Thus the NOXA/MCL1 axis appears to be critical in mediating cell death in response to diverse stimuli. It is still unclear whether functional inhibition of MCL1 by NOXA absolutely requires NOXA-mediated MCL1 degradation.

The transcriptional regulation of NOXA expression itself is poorly understood, and both p53-dependent and -independent mechanisms have been described. As mentioned above, radiation-induced NOXA expression is p53-dependent. However, generation of reactive oxygen species by cisplatinum in chronic lymphocytic leukemia led to specific upregulation of NOXA in a p53-independent manner[45]. Regulation of NOXA at the post-translation level is also complex. For example, NOXA can be turned over by the proteasome in a ubiquitin-dependent and -independent manner[43,46]. Interestingly, the degradation of NOXA is blocked by MCL1, which interacts with the BH3 domain of NOXA and stabilizes it[46]. This further emphasizes the importance of the NOXA-MCL1 interactions in regulating the levels of both proteins.

(v) BCLXL

Similarly to MCL1, BCLXL is a key survival factor in numerous solid tumors. In particular, there is a high frequency of BCLXL amplification in colorectal cancers, and many of these tumors depend on this protein for survival[47]. BCLXL exerts its anti-apoptotic activity by binding to and inhibiting the activity of the effector proteins BAX and BAK as well as the BH3-only proteins BIM and PUMA[18]. BCLXL activity can be

regulated through phosphorylation by the JNK kinase[48]. This causes the release of BAX from BCLXL, leading to apoptosis. Targeting of BCLXL offers an attractive therapeutic strategy, and a number of specific inhibitors (e.g. WEHI-539) have been designed to specifically target this protein[49].

BH3 mimetics

Many cancer cells depend on the up-regulation of the anti-apoptotic arm of the BCL-2 pathway in order to evade cell death, thus acquiring unlimited proliferative capacity.

The dependency on BCL2, BCLXL, and MCL1 serves to inhibit cell death through the formation of heterodimers between the anti-apoptotic proteins and pro-death members. This heterodimer formation is mediated via binding of the BH3 domain of pro-apoptotic proteins with the hydrophobic clefts found in anti-apoptotic proteins[18].

The hydrophobic cleft has become an attractive target for molecules designed to disrupt binding between anti- and pro-apoptotic proteins. The canonical compounds of this class are the BH3 mimetics, which act as competitive inhibitors by binding to the hydrophobic cleft. This in turn allows for the activation of pro-apoptotic members of the family[50].

In addition to their therapeutic potential, BH3 mimetics facilitate the functional dissection of the BCL-2 pathway. Chemical and genetic studies using BH3 mimetics have also elucidated key regulators of apoptosis. For example, an RNAi screen has uncovered a role for the RNA/DNA helicase DHX9 in sensitizing Eμ-Myc/Bcl-2 lymphomas to the BH3 mimetic, ABT-737[51].

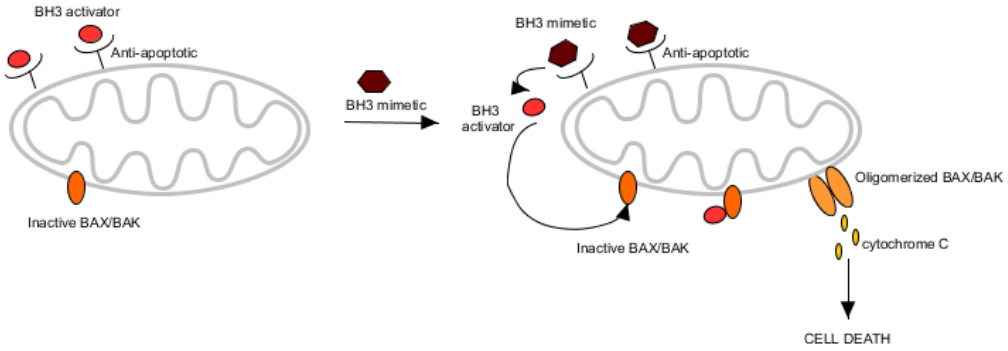

Figure 1.6. BH3 mimetics mechanism of action

BH3 mimetics are designed to "mimic" the BH3 domains of derepressor proteins such as BAD. By competitively binding to anti-apoptotic proteins, the activator proteins are released and can in turn activate the effector proteins BAX and BAK.

ABT-737, a specific inhibitor of BCL2, BCLXL and BCLW, is the most well characterized of these compounds, and an orally available form (Navitoclax) is currently in phase I/II clinical trials[52]. Although this compound has shown great promise in the treatment of certain hematological malignancies, its BCLXL-inhibitory activity is associated with occurrence of thrombocytopenia[53]. This condition, which is characterized by the loss of platelets, results in ineffective clotting of blood and can lead to internal bleeding. In order to overcome this side effect, the first orally available BCL2 selective inhibitor, ABT-199 has been developed. ABT-199 has shown promising anti-tumor activity in chronic lymphocytic leukemia (CLL), lymphomas and certain subsets of myelomas with reduced thrombocytopenia[54].

WEHI-539 was the first BCLXL specific inhibitor that was described to have on-target specificity in cell lines engineered to rely on BCLXL for survival[49]. However, WEHI-539 has poor efficacy in vivo due to a potentially toxic hydrazone moiety and poor

physiochemical properties. This has led to the design of a more stable compound, A-1155463, which has is a potent inducer of death in BCLXL-dependent colorectal cancer cell lines[55].

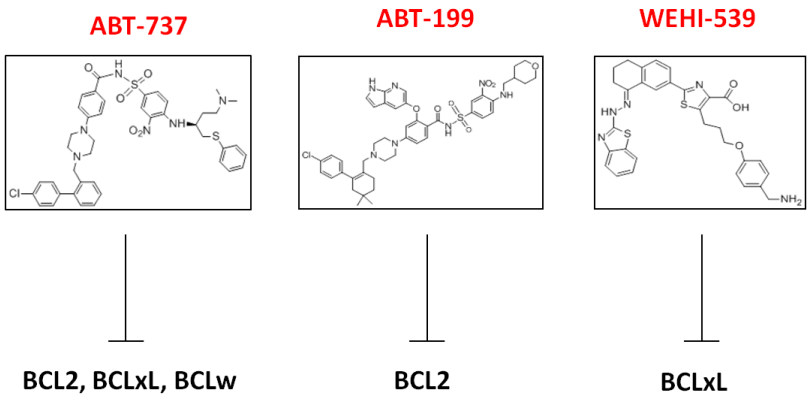

Figure 1.7. BH3 mimetics

Representation of BH3 mimetics that collectively target BCL2, BCLXL and BCLW, or exhibit selectivity for either BCL2 or BCLXL. (*Images adapted from http://www.chemietek.com/*)

Although these compounds are the most potent BCL2/BCLXL inhibitors to date, they have little or no effect in MCL1-dependent leukemias and solid tumors. This is since none of them bind effectively to the MCL1 hydrophobic cleft[56].

One of the strategies to overcome this resistance has been to employ ABT-737 in combination with proteasome inhibitors such as Bortezomib. Bortezomib neutralizes MCL1 function through up-regulation of NOXA[57]. Alternatively, CDK1 inhibitors such as roscovitine inhibit the transcription of short-lived proteins such as MCL1 and have been used in combination with ABT-737[58]. A number of pan-BCL-2 inhibitors have also been developed in order to inhibit all the anti-apoptotic BCL-2 proteins. Amongst these, Obatoclax (GX-15-070) was found to inhibit the binding of anti-apoptotic family members

to pro-apoptotic BAX and BAK[59]. However, further studies have shown that this compound also initiates apoptosis in a BCL-2 independent manner, and that it possesses non-specific toxic effects. Thus, enthusiasm for obatoclax as a BCL-2 targeted therapy is somewhat tempered[60]. Two other potential MCL-1inhibitors, Maritoclax and Dinaciclib, are able to induce BAX/BAK and caspase activation. However, these effects were also observed in cells lacking MCL1, suggesting some off-target activities. These observations underscore the difficulty in designing specific MCL1 inhibitors[61].

A recent study has demonstrated that an indole-2-carboxylic acid core-based MCL1 inhibitor, A1210477 shows increased binding affinity to MCL1 and is capable of specifically targeting MCL1 in various MCL1-dependent cell lines, including multiple myelomas and non small cell lung carcinoma lines. This leads to the disruption of MCL1:BIM complexes, thereby triggering activation of the intrinsic apoptotic pathway. A1210477 also synergizes with Navitoclax (ABT-263) to cause cell death in multiple cancer cell lines[62].

The efficacy of this MCL1-specific inhibitor *in vivo* and in clinical settings still remains to be seen. Thus, due to the lack of clinically relevant compounds specifically targeting MCL1, it is clear that further studies are required to fully elucidate MCL1 function and its regulation. This is turn would assist in specifically targeting this protein for therapeutic purposes.

p53-dependent signaling

One of the master regulators of apoptosis is the p53 tumor suppressor gene, which is activated in response to stress stimuli and induces apoptosis through both transcription-dependent and -independent mechanisms[63,64].

The death-inducing functions of p53 stem from its ability to regulate the transcription of the pro-apoptotic BCL-2 family members *BAX*, *PUMA* and *NOXA*[6540,65]. This transcriptional up regulation is thought to affect the ratio of pro to anti-apoptotic proteins, thereby allowing for the release of cytochrome C, caspase activation and cell death[63]. In addition, p53 can also regulate the transcription of *CDKN1A (p21)*, an inhibitor of cell cycle progression, leading to cell cycle arrest rather than apoptosis[66,67]. The ultimate outcome of p53 activation is likely determined by the relative stoichiometry between its downstream apoptotic and cell cycle arrest proteins. As an example, genetic screens have identified transcription factors such as TCF3/E2A, which induces the expression of *p21* and represses *PUMA*. The depletion of TCF3 impairs cell cycle arrest and promotes PUMA-dependent apoptosis upon p53 activation. This demonstrates that the p21:PUMA ratio determines cell fate upon the activation of p53[68].

Apart from its role as a nuclear transcription factor, p53 acts in the cytosol and at mitochondria to promote apoptosis through transcription-independent mechanisms[69]. This predominantly occurs through physical and functional interactions of p53 with the BCL-2 family of proteins. Notably, p53 interacts with and activates the effector proteins BAK and BAX, thus directly activating apoptosis. In addition, the upregulation of PUMA upon p53 activation also serves to activate BAX and BAK either directly, or through indirect means such as binding to BCLXL and BCL2. This allows for the release of sequestered pro-apoptotic effectors. The interaction of p53 with pro-survival BCL-2 family members such as BCL2 and BCLXL has also been demonstrated in biochemical studies[70,71,72,73].

The processes of mitochondrial fusion and division are important for maintenance of mitochondrial function and integrity. The balance between fusion and fission is essential for maintaining the mitochondrial network, for mitochondrial respiration, and for exchange of mitochondrial DNA. These two processes are therefore highly dynamic and serve to regulate mitochondrial morphology in response to different stimuli and cellular states, thereby dictating the mitochondrial signaling response[74].

(i) Regulation of fusion and fission

Extensive studies in *Drosophila melanogaster* and yeast have identified key regulators of the mitochondrial fission and fusion machinery. The *Drosophila* gene Fzo and its yeast homologue, Fzo1, promote mitochondrial fusion. Screens performed in order to identify repressors of the fusion machinery led to the identification of molecules involved in mitochondrial fission. It has also been discovered that much of the fusion and fission machinery is conserved in mammalian systems[75].

In mammals, two large GTPases localized in the mitochondrial outer membrane, Mitofusin 1 and 2 (MFN1, MFN2) form the key components of the outer membrane fusion machinery[76,77]. Mice lacking mitofusins display fragmented mitochondria and poor mitochondrial function and die during development[78]. Mutations in *Mfn2* have also been linked to the onset of Charcot-Marie-Tooth disease, a neurodegenerative disorder characterized by muscle and nerve atrophy[79]. The fusion of the inner membrane is in turn regulated by the optic atrophy protein 1 (OPA1), which is a dynamin family GTPase localized to the mitochondrial inner membrane. Similar to the effects observed in the absence of mitofusins, the depletion of OPA1 also leads to mitochondrial fragmentation in addition to abnormal cristae structure[75–77].

Mitochondrial fission in mammalian systems is mainly regulated by two proteins, dynamin-related protein 1 (DRP1) and FIS1. DRP1 is mainly localized in the cytosol but is recruited to fission sites on mitochondria. Inhibition of DRP1 leads to the formation of longer and interconnected mitochondrial networks. FIS1, the other key regulator of mitochondrial fission is distributed uniformly on the outer mitochondrial membrane and (like DRP1) its depletion results in elongated mitochondria[80–83].

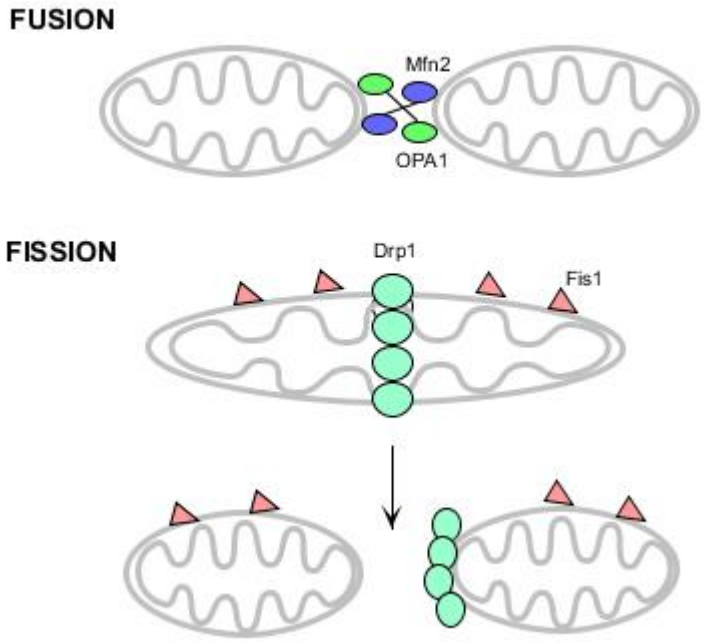

Figure 1.8. Mitochondrial Fusion and Fission

Mitochondrial fusion is regulated by the outer membrane protein Mitofusin 2 (MFN2) and the inner membrane protein Optic Atrophy protein 1 (OPA1). The mitochondrial fission or division process is mediated by the dynamin-related protein 1 (DRP1) and FIS1.

(ii) Fusion and fission in the control of cellular responses

A tight regulation of mitochondrial dynamics is required in order to prevent alterations in organelle function and consequently changes in mitochondrial signaling pathways related to programmed cell death and metabolism. The proteins that regulate fusion and fission have therefore been implicated in the regulation of cellular responses such as bioenergetics, cell division, and apoptosis.

Mitochondria undergo extensive fragmentation during apoptosis and this is predominantly regulated by the fission proteins, DRP1 and FIS1. The inner membrane fusion protein OPA1, which is required for maintaining cristae structure, can also prevent the release of cytochrome C[80,82,84,85]. In addition, the pro-apoptotic effector proteins BAX and BAK interact with members of the fusion and fission machinery in order to regulate mitochondrial morphology during the induction of apoptosis and are also required for the maintenance of normal mitochondrial networks[22,86–88]. Two anti-apoptotic BCL2 proteins, BCLXL and MCL1, can also localize to the inner membrane and mitochondrial matrix respectively, where they interact with and regulate components of the electron transport chain, thereby controlling ATP production[89,38].

The maintenance of an intact mitochondrial network is also crucial in regulating cell cycle progression. Over expression of MFN2 or inhibition of DRP1 with siRNA or a small molecule, mdivi-1, was sufficient to inhibit mitochondrial fission and induce cell cycle arrest and apoptosis[21,80,85,90,91]. Two major regulators of cell cycle progression, the cyclin B-CDK1 complex and Aurora A, can phosphorylate DRP1 enabling mitochondrial division during mitosis; this ensures the proper segregation of mitochondria into daughter cells[92].

The faithful division of mitochondria is essential for maintaining the integrity of the organelle during cell division. However, under conditions of stress such as that induced by the generation of excessive reactive oxygen species (ROS) or nutrient starvation,

mitochondria undergo hyperfusion. This prevents mitochondria from undergoing autophagosomal degradation and enhances energy production, thus enabling survival under non-optimal conditions. This stress-induced mitochondria hyperfusion precedes the fission that occurs when cells undergo apoptosis, and is also dependent on the mitofusins and OPA1. The rearrangement of the mitochondrial network thus represents a pro-survival mechanism in response to stress conditions[75,80,93–95].

Ubiquitin pathway

The ubiquitin system is responsible for post-translational modification of substrates in order to regulate their stability and function. Ubiquitin (Ub) is a highly conserved 8.5 kDa protein that is attached covalently to predominantly lysine residues of target proteins in a reversible manner. Target substrates can be modified by different types of Ub attachment: (i) attachment of a single ubiquitin molecule (monoubiquitination), (ii) single ubiquitin molecules at different sites on the protein (multiple monoubiquitination), or by ubiquitin chains (polyubiquitination).

The ubiquitinated proteins can in turn be deubiquitinated by specific enzymes called deubiquitinases (DUBS)[96,97].

The actual conjugation of ubiquitin onto the target protein occurs in a three-step process that involves three discrete enzyme classes. These are E1 activating enzyme, E2 conjugating enzyme, and an E3 ligase.

The ubiquitin reaction is initiated by the activation of the ubiquitin molecule in an ATP-dependent manner by the E1 activating enzyme and involves the formation of a thioester bond between the C-terminal carboxyl group of ubiquitin and an active Cys group of the E1 enzyme. The activated ubiquitin is then transferred from the Cys residue onto an E2

conjugating enzyme, again via formation of a thioester bond. The E3 ligases in turn recognize target substrates and recruit the E2 enzymes loaded with ubiquitin. The two major E3 ligase classes differ in regard to whether ubiquitin is directly conjugated to them (HECT E3 ligases) or not (RING E3 ligases) prior to its transfer to the substrate[96,98–100].

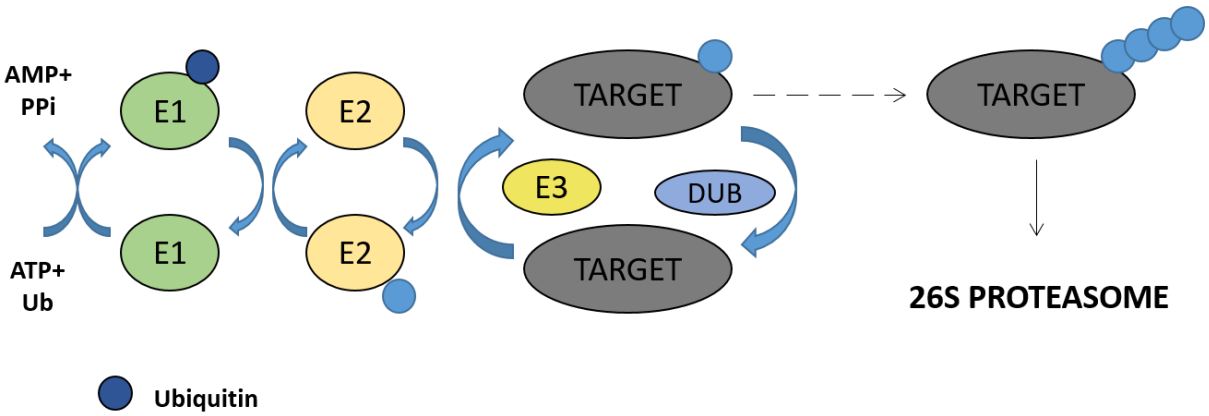

Figure 1.9. Ubiquitin Pathway

The E1 activating enzyme binds to ubiquitin in an ATP-dependent process. The ubiquitin conjugating enzyme E2 accepts ubiquitin from the E1 and transfers it to a protein substrate that is bound to the E3 ubiquitin ligase. The ubiquitin chain can then be extended. The ubiquitinated protein is then targeted to the 26 S proteasome in order to be degraded. This is a reversible process, since ubiquitin can be removed by a deubiquitinating enzyme.

The formation of different ubiquitin chains dictates the fate of the targeted protein and in turn, of downstream signaling responses. Lysine 48-linked chains generally target the modified substrate to the proteasome for degradation. A specific example is that of the MDM2 E3 ligase, which targets the tumor suppressor p53 for degradation[101]. On the other hand, lysine 63-conjugated ubiquitin chains mediate signaling events, such as that observed following ubiquitination of the NF-κB pathway components NEMO by the TRAF6 ubiquitin ligase. This leads to activation of downstream signaling cascades

including those that lead to the activation of IKK and JNK kinases[102]. Monoubiquitination can regulate protein-protein interactions, and also regulates processes such as endocytosis. An example of the latter is monoubiquitination of the EGFR receptor, which is required for the receptor to be internalized[103,104]. Other atypical ubiquitin chain types, such as those conjugated through lysine 27, are involved in processes such as PINK1/PARKIN-dependent mitophagy. PARKIN mediates the formation of lysine 27-conjugated ubiquitin chains on mitochondrial proteins such as MIRO[105]. In addition, the cullin 3 ubiquitin ligase can catalyze K33-linked ubiquitination of CRN7 in order to regulate protein trafficking[106]. Recent studies have also identified a novel linkage mediated by methionine 1 of ubiquitin to form linear chains that are responsible for NF-κB activation[107,108].

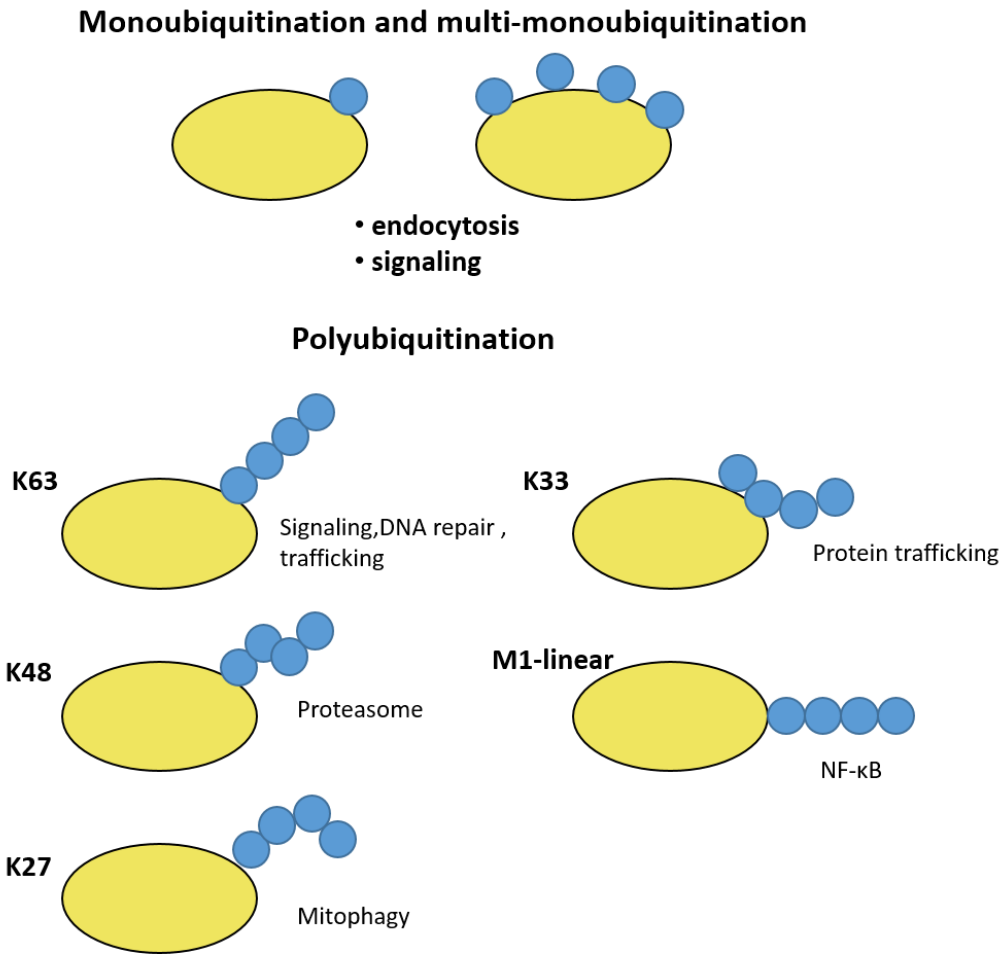

Figure 1.10. Types of ubiquitin linkages

The ubiquitin molecule can be attached to the substrate in different manners. This in turn can target proteins for degradation or activate downstream signaling pathways.

(i) E3 ubiquitin ligases

The specificity of the ubiquitination reaction is dictated by the E3 ligases, which recognize the substrate and mediate the transfer of ubiquitin onto these proteins. The E3 ligases themselves are themselves regulated by phosphorylation and/or ubiquitination. In addition, acetylation of lysine residues also dictates protein stability by preventing proteasome-mediated degradation of proteins. Different families of E3 ligases regulate the final steps of the ubiquitination cascade[109].

(a) HECT family of E3 ligases

The *h*omologous to *E*6-AP *c*arboxyl *t*erminus (HECT) E3 ligases are characterized by the presence of a C-terminal HECT domain, which was first identified in the E6-associated protein. This protein was originally identified as an ancillary factor required for degradation of p53 by the human papillomavirus E6 oncoprotein. The HECT domain ligases possess intrinsic catalytic activity and mediate ubiquitination by binding to an ubiquitin-charged E2. This is followed by direct conjugation of ubiquitin onto the E3 ligase itself through the formation of a thioester bond with a catalytic Cys residue located in the C-terminus of the HECT domain. The ubiquitin molecule is then transferred directly onto the target protein. This category of E3 ligases includes the NEDD4 family members. This family of ligases mediate the ubiquitination and degradation of membrane proteins such as ion channels and receptors via endocytosis[100,110].

(b) RING finger E3 ligases

Most E3 ubiquitin ligases belong to the family of Really Interesting New Gene (RING) domain containing family of E3 ligases. In contrast to HECT ligases, RING E3s catalyze the transfer of ubiquitin directly from the E2 conjugating enzyme onto the substrate without forming an E2-E3 intermediate. Over 600 RING domain ligases have been identified in mammals. The RING domains can coordinate two Zn^{2+} ions in a cross-braced arrangement which creates a platform for binding of E2 enzymes. The RING domains can adopt different conformations, which are summarized in the table below[99,111].

RING Type	**Sequence**	**Example**
RING-HC	C2H2C4	MDM2
RING-HC	C3HC4	c-CBL, BRCA1/BARD1, cIAP-1, -2, PML
RING-CH	C4HC3	MARCH5 MULAN
RING-H2	C3H2C3	PIRH1, RBX2

Figure 1.11. Tabulated summary of RING domain conformations

Different E3 ligases possessing different conformations within their RING domain. MARCH5 possesses the C4HC3 conformation i.e. four cysteine residues, a histidine and three cysteines within the eight Zn^{2+} coordinating residues.

Some RING E3 ligases can dimerize through their RING domains to form homodimers (e.g., cIAP and TRAF2)[112] or heterodimers (MDM2/MDMX and BRCA1/BARD1). This dimerization is thought to be required for functional regulation of E3 ligase activity. For example the formation of a heterodimer between MDM2 and MDMX allows for the stabilization of MDM2, thereby leading to more effective degradation of its target substrate, p53[113].

RING domain ligases can also exist in multisubunit complexes. Examples are the Cullin-RING E3 ubiquitin ligases (CRLs), which are the most abundant class of E3 ligases. They are multi-subunit complexes composed of RING proteins coupled to cullins. The cullins act as scaffold proteins for their cognate E3 ubiquitin ligase. This complex also consists of diverse adaptor proteins that recruit substrates for ubiquitination. Examples of CRLs include the Skp, Cullin, F-box containing complex or SCF complex, which regulates cell cycle progression[99,111,114].

The dysfunction or abnormal expression of these E3 ligases can contribute to various disease states, including cancer. Several RING E3 ligases have been described as tumor suppressors or as oncoproteins. These include IAP family members, which inhibit caspase-dependent cell death, and the SCF E3 ligases whose dysregulation leads to uncontrolled proliferation and genomic instability. In the case of IAPs, their molecular interactions are well characterized, which had greatly facilitated their validation as therapeutic targets. Several Smac mimetic agents, that inhibit IAPs are being tested in clinical trials e.g. birinapanet 12. It is likely many other ligases will be added to the list of therapeutic targets once the molecular mechanisms associated with their biological activity are more thoroughly delineated[33,100,101,115,116].

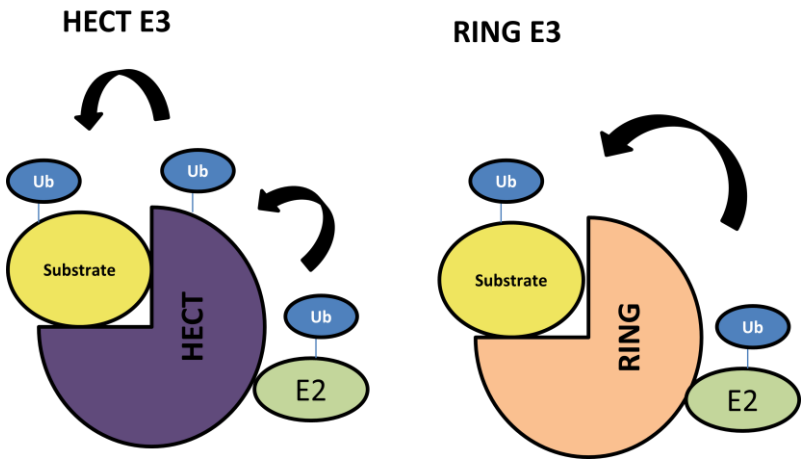

Figure 1.12. HECT and RING domain E3 ligases

HECT and RING domain E3 ligases differ in the transfer of ubiquitin onto target substrates. HECT ligases form a E3 ubiquitin intermediate while the RING E3 ligases mediate direct transfer of ubiquitin onto substrates.

(ii) Deubiquitinases (DUBs)

The removal of ubiquitin from proteins is an equally important process that regulates protein stability and function. Around 100 DUBs have been identified in mammals, and they can be divided into five families based on their catalytic domains. These include the USP, OTU, UCH, Josephin, or JAMM/MPN+ domains[117]. DUBs have important roles in diverse cellular processes such as the cell cycle (CYLD and USP13)[118], chromatin remodeling (USP21 and USP22)[119] and regulation of signaling pathways (A20 modulates the NF-κB pathway and USP7 regulates the MDM2-p53 pathway)[120,121]. Given that DUBs regulate key growth and survival pathways, it is not surprising that some have oncogenic (e.g. USP28) or tumor suppressor (e.g. CYLD) properties.

Mitochondria-dependent ubiquitin signaling

Ubiquitination is a critical regulator of mitochondrial signaling pathways and mitochondrial quality control. Several E3 ligases are either localized to mitochondrial membranes, or are recruited to mitochondria in response to specific stimuli. These include mitochondrial ligases such MULAN, which regulates NF-κB signaling at the mitochondria and PARKIN, an E3 ligase that is recruited to mitochondria upon the induction of mitophagy[122].

(i) Mitochondrial apoptotic signaling

The mitochondrial or intrinsic apoptotic pathway is regulated by a group of RING E3 ligases called inhibitors of apoptosis proteins (IAPs). These proteins inhibit apoptosis by preventing the activation of caspases. The X-chromosome-linked IAP (XIAP) and cellular IAP1 (c-IAP1) bind to caspases 3, 7 and 9, block their catalytic activity and regulate their levels through ubiquitin-dependent targeting for proteasomal degradation[123].

RNF144B, an E3 ligase with an 'in between RING' (IBR) domain is recruited to mitochondria where it interacts with activated BAX and regulates its ubiquitination and stability[124].

In addition, the levels and functions of other BCL-2 family members are also regulated through ubiquitination. For example the unphosphorylated form of BCL2 is targeted for ubiquitination and subsequent degradation[125]. The E3 ligases in this process however, have not been identified. In addition, the MCL1 protein is ubiquitinated by MULE and other E3 ligases and this depends on MCL1 phosphorylation status[32,34]. However, most of these ubiquitin ligases are localized to the cytosol and are recruited to mitochondria in a stimulus-specific manner. Whether additional E3 ligases located in the mitochondrial outer

membrane can directly regulate the BCL2 family of proteins to co-ordinate the apoptotic response remains unclear.

(ii) Innate immune signaling

Another mitochondrial signaling pathway that is ubiquitin-dependent is the NF-κB pathway. The mitochondrial associated viral sensor (MAVS), is located on the mitochondrial outer membrane, and acts as an adaptor for E3 ligases such as TRAF3 and TRAF6. These ligases bind and mediate ubiquitination of the NF-κB essential modifier (NEMO), which in turn activates downstream IKK and promotes transcription of target genes. The mitochondrial RING domain E3 ligase MULAN also regulates NF-κB activation through the ubiquitination of TRAF2 under stress conditions. This in turn leads to increased transcription of pro-inflammatory cytokines and anti-apoptotic proteins, thereby enabling cell survival[102,122,126,127].

(iii) Mitochondrial quality control

It is essential that quality control systems are present to maintain optimal mitochondrial function. The most well studied quality control system is mitophagy, which is regulated by PINK1 (PTEN-induced kinase 1) and PARKIN[128,129].

The IBR E3 ligase, PARKIN, co-operates with PINK1 to remove damaged or dysfunctional mitochondria. The activation and stabilization of PINK1 leads to recruitment of PARKIN from the cytosol to the mitochondria, where it is responsible for ubiquitinating many outer mitochondrial membrane proteins. The ubiquitination of substrates, which include TOMM20, MFN1/2, and VDAC1, serves as a signal to recruit autophagosomes to the mitochondria. Mutations in PINK1 or PARKIN prevent autophagosome formation, and

thus engender the accumulation of damaged mitochondria[130,131]. This has direct clinical relevance, since mutations in both PINK1 and PARKIN are associated with mitochondrial dysfunction that accompanies the symptoms of Parkinsons' disease[132]. Intriguingly, PINK1/PARKIN mutations have also been found in cancer tissue, suggesting aberrations in these proteins may also contribute to the transformed phenotype[133]. Whether this is due to increased mitochondrial dysfunction, or because of improper regulation of other targets of PINK1/PARKIN remains unclear. Further studies of PINK1/PARKIN and their functional interactions with other mitochondrial outer membrane and cytosolic proteins are clearly warranted in this regard.

MARCH5 Ubiquitin Ligase

MARCH5 is a RING domain E3 ligase that is localized to the mitochondrial outer membrane. The protein contains an N-terminal RING domain and four transmembrane domains[134].

Figure 1.13. MARCH5 ubiquitin ligase

MARCH5 possesses an amino terminus RING domain and four mitochondrial membrane spanning domains. The RING domain possesses the critical catalytic residues important for transfer of ubiquitin onto the target substrate.

MARCH5 belongs to the group of *M*embrane-*a*ssociated *R*ING-*CH* (MARCH) proteins. RING-CH proteins have a cysteine residue in the fourth position and a histidine in the fifth position of the RING domain. This conformation is also characteristic of membrane associated E3 ligases. The MARCH family of proteins were originally described as homologs of K3 and K5, which are E3 encoded by Kaposi's sarcoma-associated herpesvirus (KSHV). There are eleven members in this family, each of which possesses a RING-CH domain, at least one transmembrane domain, and E3 ubiquitin ligase activity. The specific functions of each MARCH5 member are tabulated below[135].

MARCH Family Member	**Function**	**Subcellular Localization**
MARCH1	Ubiquitination of MHC II and antigen presentation	Plasma membrane, endosomes
MARCH2	Endosomal trafficking	Plasma membrane, endosomes
MARCH3	Endosomal trafficking	Endosomes
MARCH4	Regulation of MHC I	Golgi apparatus
MARCH5	Mitochondrial dynamics, innate immune signaling	Mitochondria
MARCH6	ER protein degradation	Endoplasmic reticulum
MARCH7	Regulation of lymphocytes, general proliferation	Nucleus, cytosol and plasma membrane
MARCH8	Downregulation of MHC I, transferrin receptor and ubiquitination of MHC II	Endosomes
MARCH9	Ubiquitination of MHC I and ICAM	Lysosomes
MARCH10	Unknown	Spermatids-association with microtubules
MARCH11	Ubiquitin dependent endosomal protein sorting	Multi-vesicular bodies

Figure 1.14. Table summarizing the functions of MARCH family members

MARCH family members are localized to diverse cellular compartments and mainly involved in protein turnover.

MARCH5 is the only family member localized to the mitochondria, and is therefore perfectly situated to regulate neighboring mitochondrial proteins and/or signaling events that occur on the mitochondrial outer membrane[136].

MARCH5 plays a role in mitochondrial dynamics by interacting with proteins that control fusion and fission, thereby regulating mitochondrial morphology and function. Mitofusin 2 (MFN2) has been identified as a MARCH5 substrate, and this interaction is important in mediating mitochondrial fusion as well as mitochondrial-endoplasmic reticulum interactions. This interaction is critical for the maintenance of calcium homeostasis[137]. Another fusion protein, mitofusin 1 (MFN1) is also ubiquitinated by MARCH5, and this interaction increases in response to mitochondrial stress. The MARCH5-dependent ubiquitination of acetylated MFN1 serves to modulate levels of MFN1 protein under stress conditions[138].

MARCH5 depletion leads to hyperfusion of mitochondria, which is followed by an increase in intracellular ROS and induction of cellular senescence[139]. In addition, MARCH5 can also regulate the levels of misfolded proteins within the mitochondria, thereby exhibiting a quality control function. Specifically, MARCH5 can ubiquitinate manganese superoxide dismutase and S-nitrosylated LC1, leading to their degradation[140–142]. This has clinical implications, as loss of function of these proteins leads to mitochondrial stress associated with Parkinson's disease.

In addition, MARCH5 also has a role in the innate immune response as it ubiquitinates and TANK, a negative regulator of TRAF6, following initiation of Toll-like Receptor 7 (TLR7) signaling. This enhances TLR7 signaling, as the resulting derepression of TRAF6 in turn activates the NF-κB pathway[143]. An opposing role for MARCH5 in innate immune signaling has been demonstrated by recent reports that show a negative regulation of the mitochondrial anti-viral signaling (MAVS) by MARCH5 thereby preventing excessive host immune response[144]. Thus, the role of MARCH5 in this context remains unclear and may be dependent on the type of upstream immunogenic stimulus.

Strikingly MARCH5 is also implicated in the maintenance of pluripotency in embryonic stem cells. Mechanistically, this is via catalyzing K63-linked polyubiquitination of PRKAR1a, a negative regulatory subunit of PKA. The subsequent activation of PKA leads to inhibition of RAF/MEK/ERK signaling; inhibition of ERK signaling is required for maintenance of pluripotency[145].

Anecdotal reports suggest that MARCH5 knockout mice display degenerative phenotypes similar to those found in murine Alzheimer models (unpublished data), indicating that prolonged depletion of MARCH5 is deleterious, at least in a neurological context[146]. Studies on the role of MARCH5 in the regulation of MAVS also described the homozygous deletion of MARCH5 as being embryonic lethal[144]. Taken together, these studies suggest MARCH5 plays a protective role in cells.

However, the role of MARCH5 in the regulation of other mitochondrial signaling pathways is virtually unexplored. Given that MARCH5 appears to be critical for the maintenance of mitochondrial homeostasis, we hypothesized that it might directly or indirectly regulate cell death signaling, as many events in both the intrinsic and extrinsic apoptotic pathways converge at the mitochondria.

Through chemical and genetic approaches introduced in the following chapters, we demonstrate that MARCH5 has a direct functional interaction with the intrinsic apoptotic pathway. This is due to MARCH5-dependent regulation of the MCL1/NOXA axis, which dictates the threshold for sensitivity to specific BH3 mimetics. The significance of this in a biological context, as well as from a clinical perspective, will be discussed.

CHAPTER 2. MATERIALS AND METHODS

Cell culture

Cells were grown in McCoy's 5A (HCT116), DMEM (U2OS, MDA-MB-231, and HeLa), or DMEM/HAM's F12 (MDA-MB-468) media supplemented with 10% fetal bovine serum, 4 mM L-glutamine, 100 U/ml penicillin, and 100 U/ml of streptomycin, in a humidified atmosphere of 5% CO_2 at 37°C. Cells were passaged prior to reaching full confluency for general maintenance. DMEM, L-glutamine, penicillin and streptomycin were purchased from Lonza (Basel, Switzerland). McCoy's 5A and HAM's F12 were purchased from Gibco (ThermoFisher Scientific, MA, USA). Cells were purchased from ATCC (Manassas, VA). HCT116 p53-/-, BAX-/-, BAK-/- and BAX/BAK-/- were a kind gift from Dr. Bert Vogelstein, Johns Hopkins University. HeLa $NOXA^{WT}$ and $NOXA^{L29E}$ inducible cell lines were a kind gift from Dr. Andreas Villunger, Biocenter - Innsbruck Medical University.

Compound treatments

For compound treatments, cells were allowed to attach overnight and then treated with the indicated concentrations of compounds. All the solutions were adjusted to have an equivalent amount of DMSO (final DMSO not more than 0.1% in all experiments). Nutlin-3a was purchased from Sigma-Aldrich (St. Louis, MO, USA), ABT-737 was from Santa Cruz (Dallas, TX, USA), ABT-199 from Selleckchem (Houston, Texas, USA), and WEHI-539 (BCLXL inhibitor) and A1210477 (MCL1 inhibitor) were purchased from Chemietek (Indianapolis, IN, USA). MG-132 was purchased from Enzo Life Sciences (Farmingdale, NY, USA) and doxycycline, cycloheximide, CCCP,

and mdivi-1 from Sigma Aldrich (St. Louis, MO, USA). For cycloheximide pulse chase assays, cells were then treated with cycloheximide (100 μg/ml) for the given time points before being subjected to western blot analysis.

Colony formation assay and quantification

U2OS osteosarcoma cell lines transfected with either siRLUC or siMARCH5 were plated at a density of 100 cells/well on black clear-bottom optical 96-well plates. Cells were treated the following day with ABT-737 at the indicated doses. Colony formation was monitored for 6–7 days. The colonies were then fixed and stained with DAPI and HCS CellMask Red Stain (Life Technologies). The 96-well assay plates were scanned using a Nikon Ti-Eclipse widefield microscope (Ti-Eclipse; Nikon) with a 4× objective in order to acquire a large area of the well. Image processing and analysis pipelines are further described in Ricci et al., 2015[147].

Plasmids, expression constructs and mutagenesis

Wild type human MARCH5 with a 3× N-terminal FLAG tag (a kind gift of Professor Shigehisa Hirose, Tokyo Institute of Technology) was subcloned into pLi196, a Dox-responsive entry vector for RMCE[148]. Using this plasmid as a template, the MARCH5 mutants were generated by site-directed mutagenesis (Stratagene). The primers used for the mutagenesis were as follows:

Mutants	Forward (5'-3')	Reverse (5'-3')
H43W	tgtagacaggcctgccaaacccattttgtagatcctct Gcacc	ggtgcagaggatctacaaaatgggtttggcaggcctgt ctaca
C65SC68S	attcagcattgctctgaggacttgccactctggctgtac	attcagcattgctctgaggacttgccactctggctgtac
V16A	catcagtagcaaaacaagcccagcaacttctgtcc	ggacagaagttgctgggcttgttttgctactgatg
V51A	ctctttgcttttcatccgcccagcgttgtagacag	ctgtctacaacgctgggcggatgaaaagcaaagag
P66A	cagcattgcactgagcacatgccactctggc	gccagagtggcatgtgctcagtgcaatgctg
D202Y	gagtagcagagacatgatatgctaaaggattggcctc	gaggccaatcctttagcatatcatgtctctgctactc
D202G	gagtagcagagacatgacctgctaaaggattggcc	ggccaatcctttagcaggtcatgtctctgctactc

For transfection, U2OS cells were plated on 100-mm plates and transfected with 5 μg of empty vector or HA-ubiquitin (a kind gift from Dr. Simona Polo) with Lipofectamine 3000 reagent (Life Technologies). Media was changed 6 h post-transfection and cells were harvested after 48 h.

Generation of cell lines

All Dox-inducible FLAG-MARCH5 cell lines were created by recombination mediated cassette exchange (RMCE) of Doxycyline-responsive FLAG-MARCH5 plasmids into a master parental U2OS cell line as previously described[149]. Cells were induced with Dox (50 ng/ml) for 24 h to induce expression of the various FLAG-MARCH5 constructs before harvesting for western blot analysis. For RNAi experiments, cells were transfected with siRNA for 24 h and then induced with Dox for a further 24 h.

RNAi experiments

siGENOME SMARTpool siRNAs for MARCH5, *Renilla* luciferase negative control, PLK1 positive control, MCL1, BIM, NOXA, and RNF144B were purchased from GE Life Sciences/Dharmacon (Lafayette, CO, USA) and used at a final concentration of 25 nM. Cells were seeded on 6-well plates for forward transfection. U2OS cells were transfected with 3 μl DharmaFECT 1 (Dharmacon); HCT116, MDA-MB-231, MDA-MB-468 and HeLa cells were transfected with 3 μl RNAiMAX (Life Technologies). Cells were harvested 48 h post-transfection for protein and RNA extraction or seeded on 96-well plates 24 h post-transfection and treated with compounds the following day for viability assays. Deconvolution experiments were performed with siGENOME individual siRNAs as well as C911 controls. siRNA sequences are tabulated below.

Gene Symbol	Gene ID	Catalog Number	Sequences
MARCH5	54708	M-007001-01	UCAAACAGCAGCAAUAUUU GGACAGCUGUGACUUAUGG GUAAAUUGAUGUUCAGUAG GACAGAAGUUGCUGGGUUU
MARCH5 C911 Controls	n/a	Custom	GUAAAUUGAUGUUCAGUAG GCUGAAUACCUAAUAGUUU GCGCAAAUACUCGAAUAAA GAAUAAUGGUCGGCUCUAU
MCL1	4170	M-004501-008	CGAAGGAAGUAUCGAAUUU AGAACGAAUUGAUGUGUAA GGACCAACUACAAAUUAAU GCUACGUAGUUCGGGCAAA
BIM	10018	M-004383-02	CCGAGAAGGUAGACAAUUG UGAUGUAAGUUCUGAGUGU AUGUAAGUUCUGAGUGUGA GUUCUGAGUGUGACCGAGA
NOXA	5366	M-005725-03	AAACUGAACUUCCGGCAGA AAUCUGAUAUCCAAACUCU CUGGAAGUCGAGUGUGCUA GCAAGAACGCUCAACCGAG
PLK1	5347	M-003290-01	CAACCAAAGUCGAAUAUGA CAAGAAGAAUGAAUACAGU GAAGAUGUCCAUGGAAAUA CAACACGCCUCAUCCUCUA
RNF144B	255488	M-025119-01	CAGCUUGCCUGAAACAGUA AAGCUGAGAUUGCCUGUUU GUAGAGACAGUCAGCCUAU GGGUUUAUAUCGAACGCAA

Western blots and antibodies

Cells were lyzed in 0.5% NP-40 lysis buffer (50 mM Tris, pH 8.0, 5 mM EDTA, 150 mM NaCl, 0.5% NP-40, 1 mM phenylmethylsulfonyl fluoride, 1 mM Na_3VO_4, 10 mM NaF and Complete Mini Protease Inhibitors (Roche, Nutley, NJ, USA), at 4 °C for 30 min. Following SDS-PAGE electrophoresis, proteins were transferred onto nitrocellulose membranes. Membranes were incubated with the following antibodies: anti-MARCH5 (a gift of Dr. Nobuhiro Nakamura, Tokyo Institute of Technology), anti-PARP (BD Biosciences), anti-MCL1 (Santa Cruz Biotechnologies), anti-PUMA (Santa Cruz Biotechnologies), anti-Actin (Sigma-Aldrich), anti-Vinculin (Sigma-Aldrich) anti-NOXA (Calbiochem), anti-p53 (Santa Cruz Biotechnologies), anti-BCL2 (BD Biosciences), anti-BCL-XL (Cell Signaling Technologies), anti-cleaved caspase 3 (Cell Signaling Technologies) and anti-FLAG (Sigma-Aldrich). Rabbit and mouse secondary antibodies were purchased from Bio-Rad Laboratories. Blots were developed using Clarity Western ECL Substrate (Bio-Rad Laboratories).

Immunoprecipitation

Cells were lysed in IP lysis buffer consisting of 50 mM Tris, pH 8.0, 5 mM EDTA, 150 mM NaCl, 0.5% NP-40, 1 mM phenylmethylsulfonyl fluoride, 1 mM Na_3VO_4, 10 mM NaF, Complete Mini Protease Inhibitors (Roche, Nutley, NJ, USA) and 25 μM PR-619 DUB inhibitor (Calbiochem), at 4°C for 30 min. Supernatants were then incubated for 4 h with HA Epitope Tag Antibody, Agarose conjugate (2-2.2.14) under constant rotation at 4°C. Beads were washed five times in ice-cold lysis buffer and eluted protein was subjected to SDS-PAGE and immunoblotted with the indicated antibodies.

Viability assay

Cell viability was assessed 24 h after drug treatment using the CellTiterGlo Luminescent Cell Viability Assay (Promega, Fitchburg, WI, USA) per the manufacturer's instructions. Following compound treatments, CellTiterGlo reagent was added to the cells; after a 10-min incubation period to allow for stabilization of luminescence, samples were transferred to solid white multiwell plates and luminescence was read on a PHERAstar FS microplate reader (BMG LABTECH, Ortenberg, Germany).

qRT-PCR

Total RNA was extracted using RNeasy Mini Kit (Qiagen) and complementary DNA (cDNA) was synthesized using the ImProm-II Reverse Transcription System (Promega). Ten nanograms cDNA was used per PCR reaction with SYBR Green PCR Master Mix (Applied Biosystems, ABI) and quantified on the BIORAD CFX96 Real Time System. Fold changes in mRNA expression was quantified using the Δ-ΔCt algorithm with *18S* ribosomal RNA as loading control. qPCR primers are tabulated below.

	Forward (5'-3')	Reverse (5'-3')
18S	GATTAAGTCCCTGCCCTTTGTACA	GATCCGAGGGCCTCACTAAAC
MARCH5	GATGCTGGACAGAAGTTGCTGG	CCACTCTGGCTGTACTGTTTCC
MCL-1	GGTGCCTTTGTGGCCAAACACTTA	ACCCATCCCAGCCTCTTTGTTTGA
PUMA	ACGACCTCAACGCACAGTACG	TCCCATGATGAGATTGTACAGGAC
p21	CTGGAGACTCTCAGGGTCGAAA	GATTAGGGCTTCCTCTTGGAGAA
NOXA	CAGGACTGTTCGTGTTCAGC	TTCTGCCGGAAGTTCAGTTT
RNF144B	CATTATGACAAAGGGCCATGC	CATACATTTTGCTGGTACTGCC
BIM	TGGCAAAGCAACCTTCTGATG	GCAGGCTGCAATTGTCTACCT

Immunofluorescence

U2OS were seeded onto coverslips pre-coated with gelatin. Following RNAi, compound treatments or transfections with FLAG-MARCH5 constructs, cells were fixed in 4% paraformaldehyde. Cells were permeabilized with 0.05% Triton X-100 and coverslips were blocked in 10% bovine serum albumin/PBS for 20 min. Cells were incubated with anti-TOMM20 (Santa Cruz Biotechnology) at 1:100 dilution for 1 h to stain mitochondria and/or anti-FLAG M2 (Sigma-Aldrich) at a dilution of 1:1000. Following three washes with PBS, cells were incubated with Alexa-488 (Life Technologies) at a dilution of 1:400, Alexa-647 at a dilution of 1:400 and DAPI (1:3000) for 1 h. Coverslips were washed and mounted with glycerol on glass slides. Imaging was performed on the Leica TCS SP2 AOBS laser confocal scanner mounted on a Leica DM-IRE2 inverted microscope with a 63× oil immersion objective.

Quantification of perinuclear mitochondria

For the quantification of perinuclear mitochondria, U2OS cells were transfected on 96 multi-well black optical clear plates for 72 h, fixed and stained for TOMM20 and DAPI. Images were acquired by a 20× objective on a Nikon Ti-Eclipse widefield microscope (Ti-Eclipse; Nikon). Segmentation of nuclei was performed and the cytoplasm was defined based on the nuclear region. A region of interest (ROI) was applied around the nucleus and mitochondria staining was quantified in this ring region. Analysis and quantification was performed on the Columbus Image Data Storage and Analysis System (PerkinElmer).

Measurement of mitochondrial membrane potential

U2OS cells transfected with siRLUC or siMARCH5 on 96 multi-well black optical clear plates for 72 h were stained with TMRE. TMRE is a cell permeable, positively-charged, red-orange dye that readily accumulates in active mitochondria due to their relative negative charge. Depolarized or inactive mitochondria have decreased membrane potential and fail to sequester TMRE. Nuclei were stained with Hoechst and live cell imaging was performed with a 20× objective on a Nikon Ti-Eclipse widefield microscope (Ti-Eclipse; Nikon). Nuclear and cytoplasmic regions were defined during image segmentation and the intensity of the TMRE signal within the cytoplasmic compartment was quantified. Analysis and quantification was performed on the Columbus Image Data Storage and Analysis System (PerkinElmer).

Gene expression and multivariate analysis

We used a classical statistical modeling approach (Multiple Linear Regression with multiple variables[150]) to relate drug sensitivity to the expression profiles of 8 selected genes. Data for sensitivity to ABT-263 were downloaded from the Wellcome 'Genomics of Drug Sensitivity in Cancer' database (http://www.cancerrxgene.org/translation/Drug/1011) and RNA expression data for the corresponding cell lines were retrieved from the 'Whole Genome Project' section of the COSMIC public database (http://cancer.sanger.ac.uk/cosmic) of the Welcome Trust Sanger Institute.

For 648 of the 971 cell lines in the database, both ABT sensitivity and mRNA expression data (for *MARCH5*, *MCL1*, *BIM*, *BAX*, *HUWE1*, *BAK1*, *NOXA*, and *BCLXL*) were available. The RNA expression levels are all normalized (z-score) in order to standardize gene expression estimates obtained different platforms used for sequencing the samples (IlluminaHiSeq_RNASeqV2, IlluminaGA_RNASeqV2, AgilentG4502A_07_3). For the sensitivity parameter in our models, we used IC50 values for ABT-263 for each cell line.

For some analyses, we further subdivided thedataset into cell lines with wild type p53 (221 samples) and those with mutant/deleted p53 (427 samples). For optimization of the model, we used the Akaike Information Criterion (AIC). The model optimization was done in a backward selection fashion, starting from the full linear model specification, (i.e., mRNA expression levels for each individual gene, and for all possible pairwise combinations were provided prior to optimization). Optimization was run separately for each individual subset (all wild type p53 samples, all mutant samples, or blood wild type p53 samples).

Statistical analysis

Statistical analysis was performed using an unpaired Student's t-test. Data were calculated as mean and standard deviation. Statistical significance is represented in figures by asterisks as follows: (*) $p < 0.05$, (**) $p < 0.01$, (***) $p < 0.001$.

CHAPTER 3. RESULTS

(I) INTERACTION OF MARCH5 WITH THE BCL-2 PATHWAY

MARCH5 depletion sensitizes to BH3 mimetic induced apoptosis

Given that MARCH5 is localized to the mitochondrial outer membrane and appears to promote cell survival, we hypothesized that MARCH5 might have functional interactions with the mitochondrial apoptotic pathway. In order to investigate this, clonogenic analysis was performed by transfecting the U2OS osteosarcoma cell line with siRNA targeting MARCH5 or siRLUC control, seeding cells at low density and assessing the colony forming potential upon treatment with the BH3 mimetic, ABT-737. ABT-737 is an efficient tool to dissect the mitochondrial apoptotic pathway as it is a specific inhibitor of BCL2, BCLXL, and BCLW[52].

The depletion of MARCH5 in combination with the drug led to the formation of smaller and fewer colonies quantified as percentage area covered by colonies (Fig. 3.1a). This experiment was also repeated at high cell density in U2OS and HCT116 (human colorectal carcinoma cells). The depletion of MARCH5 sensitized cells to ABT-737, while little or no effects were observed with administration of the drug alone (Fig. 3.1b). The mode of cell death was confirmed as mitochondrial apoptosis, indicated by the cleavage of the caspase 3 and its downstream substrate, PARP (Fig. 3.1c).

a

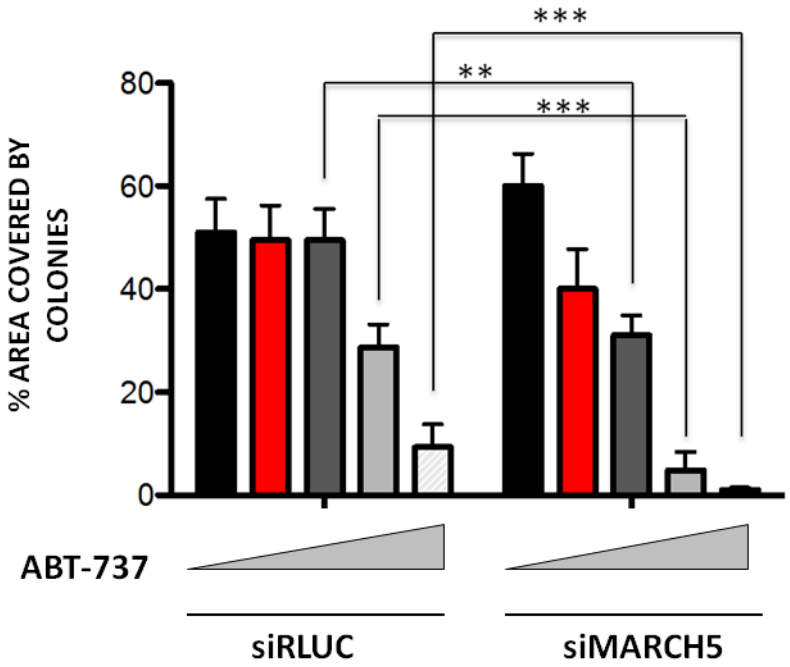
***
**
***
80
60
40
20
0
% AREA COVERED BY COLONIES
ABT-737
siRLUC
siMARCH5

b

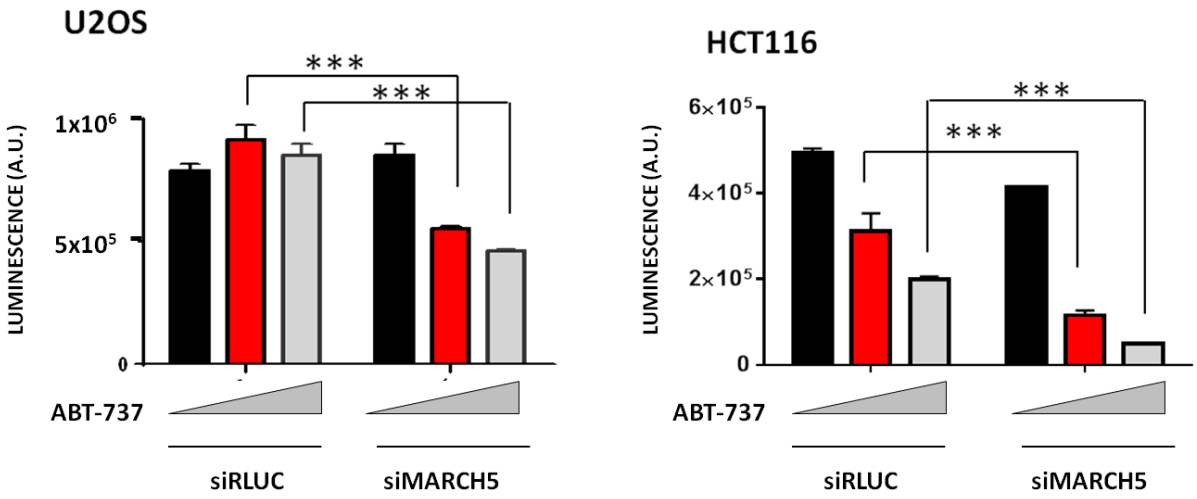
U2OS
***
***
1x10^6
5x10^5
0
LUMINESCENCE (A.U.)
ABT-737
siRLUC
siMARCH5
HCT116
***
***
6×10^5
4×10^5
2×10^5
0
LUMINESCENCE (A.U.)
ABT-737
siRLUC
siMARCH5

c

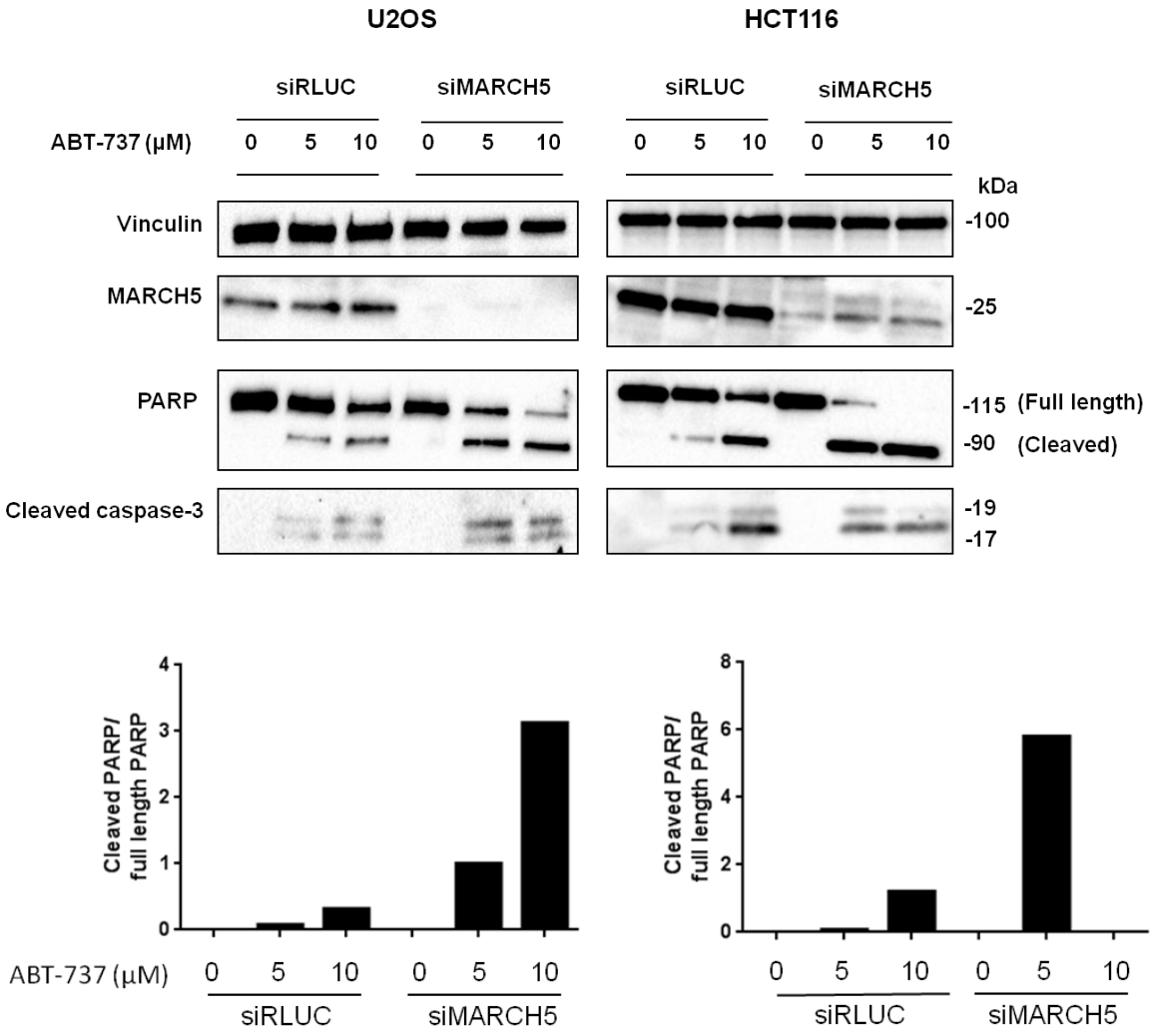

Figure 3.1. MARCH5 depletion sensitizes solid tumor cell lines to BH3-mimetic induced apoptosis

(a) U2OS osteosarcoma cell lines were transfected with siRNA targeting MARCH5 or a control siRNA. Cells were then plated on 96-well plates at low density and treated with ABT-737 (Black bar: DMSO, red: 0.5 μM, dark grey: 1 μM, light grey: 5 μM, white: 10 μM) and colony formation was monitored for 7 d. After 7 d, cells were fixed and stained with DAPI and HCS CellMask red stain and percentage area covered by colonies was then calculated.

(b) U2OS and HCT116 colorectal cancer cell lines transfected with siRNA targeting MARCH5 as well as a control siRNA targeting luciferase (RLUC) were treated with ABT-737 (Black bar: DMSO, red: 5 μM, grey: 10 μM). The cell viability was measured using CellTiter-Glo. The error bars represent the SD from triplicate experiments. The asterisks (***) indicate a p value of < 0.001 compared to the respective controls using Student's t-test.

(c) Whole cell lysates from U2OS and HCT116 cells transfected with siRLUC or siMARCH5 and treated with ABT-737 (10 μM) were subjected to SDS-PAGE and immunoblotted with the indicated antibodies. The extent of PARP cleavage was quantified as the ratio of cleaved to full length PARP.

In order to validate that this sensitization was on-target, several independent siRNAs targeting MARCH5 were used. In addition, C911 control siRNAs were also included in the validation experiment. These siRNAs possess the same "seed" region as the biologically active siRNA but have bases 9-11 scrambled. These sequences therefore provide information about potential seed-based off-target effects. The sensitization to ABT-737 was phenocopied by the additional siRNAs (Fig. 3.2a) while three of four C911 controls failed to knockdown MARCH5 mRNA (Fig.3.2b) and "rescued" this phenotype (Fig. 3.3a). C911 control-1 did not rescue this phenotype. This could be attributed to some residual ability to knock down *MARCH5* mRNA (Fig. 3.2b). In addition, the knockdown of another mitochondrial ubiquitin ligase, RNF144B, did not sensitize cells to ABT-737, indicating that this effect was specific to MARCH5 (Fig. 3.2b).

a

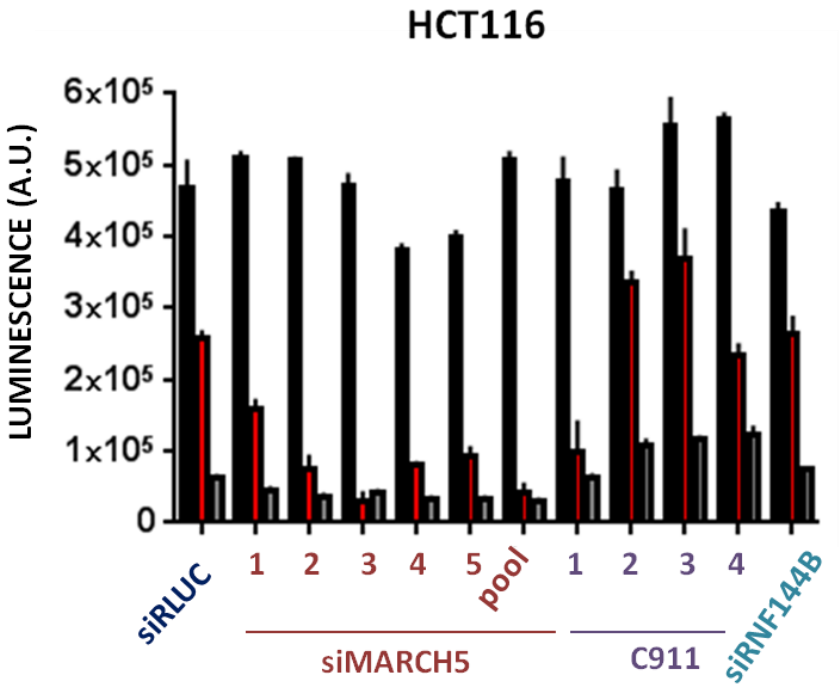
HCT116
LUMINESCENCE (A.U.)
6x10⁵
5x10⁵
4x10⁵
3x10⁵
2x10⁵
1x10⁵
0
siRLUC
1
2
3
4
5
pool
1
2
3
4
siRNF144B
siMARCH5
C911

b

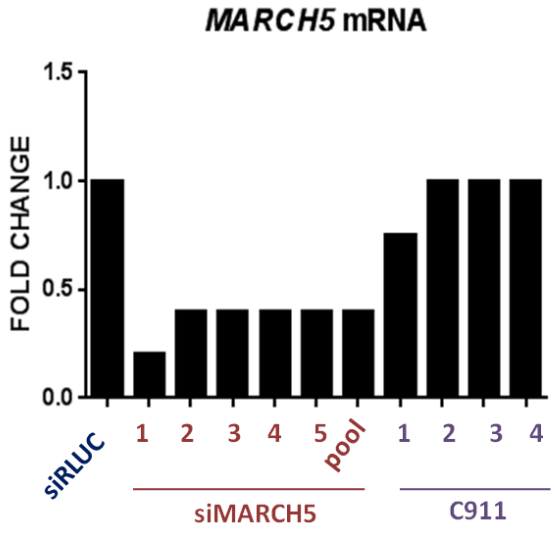
MARCH5 mRNA
FOLD CHANGE
1.5
1.0
0.5
0.0
siRLUC
1
2
3
4
5
pool
1
2
3
4
siMARCH5
C911

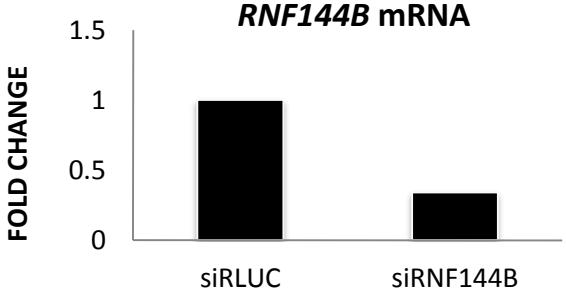
RNF144B mRNA
FOLD CHANGE
1.5
1
0.5
0
siRLUC
siRNF144B

Figure 3.2. Sensitization to ABT-737 upon MARCH5 loss is on-target

(a) HCT116 cells were transfected with the given siRNAs and treated with ABT-737 (Black bar: DMSO, red: 5 µM, grey: 10 µM). Cell viability was measured using CellTiter-Glo. The error bars represent the SD from triplicate measurements for each condition.

(b) Knockdown of *MARCH5* and *RNF144B* mRNA was validated by quantitative RT-PCR. Values were normalized to *18S* mRNA used as loading control.

Sensitization to apoptosis upon MARCH5 depletion is dependent on the BH3 effector protein, BAX

The two terminal effector proteins involved in the release of cytochrome C from mitochondria upon membrane permeabilization are BAX and BAK. The requirement for each of these proteins for induction of cell death depends on the precise apoptotic stimulus and cellular context[11]. The use of single or double knockout isogenic cell lines for these proteins revealed that MARCH5-dependent sensitization was BAX-dependent but BAK-independent (Fig. 3.3).

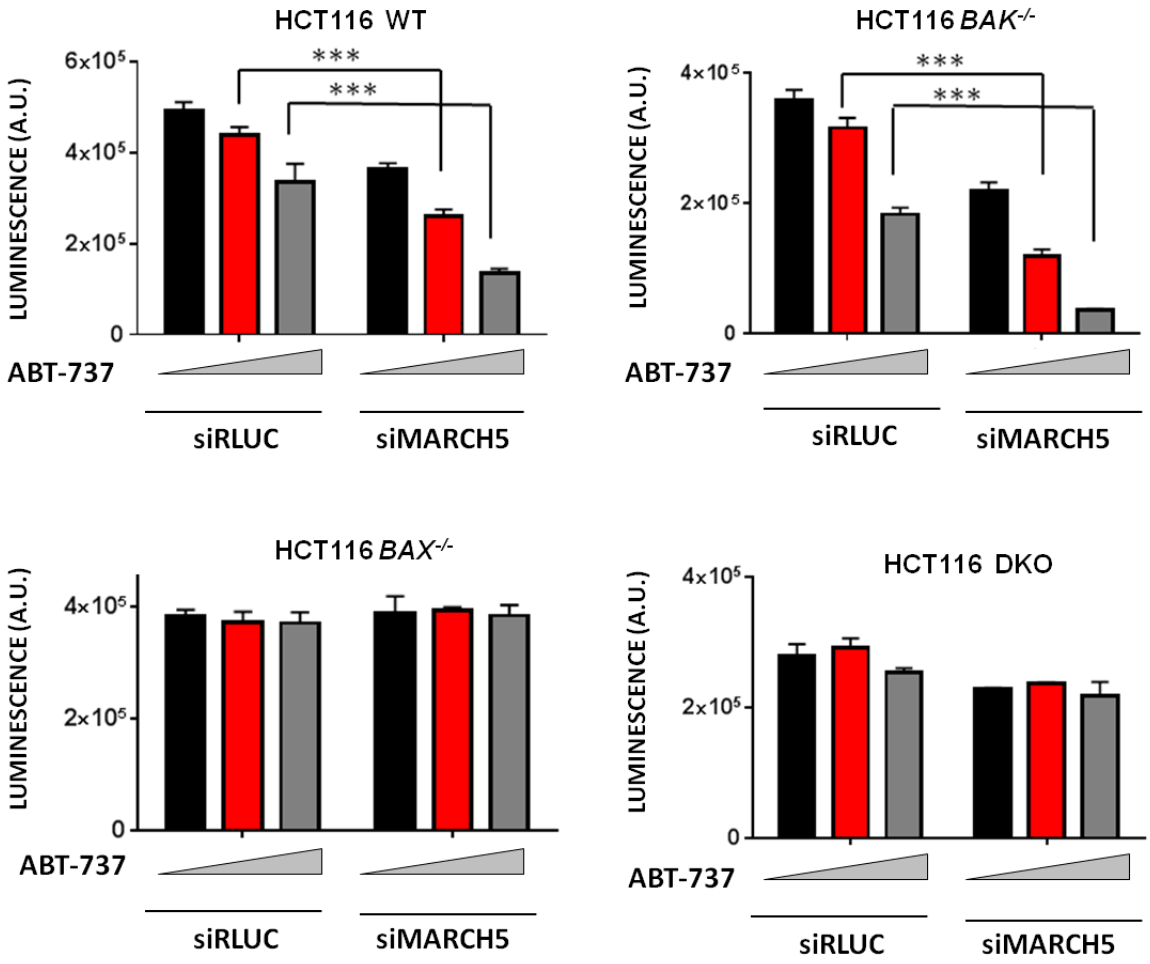

Figure 3.3. MARCH5-dependent sensitization to ABT-737 requires the presence of BAX

WT, *BAK*$^{-/-}$, *BAX*$^{-/-}$ and *BAK/BAX* DKO HCT116 cells were depleted of MARCH5 and treated with ABT-737 (Black bar: DMSO, red: 5 µM, grey: 10 µM). Error bars represent the SD of triplicate measurements for each condition. Asterisks (***) indicate p values < 0.001 compared to the respective controls using Student's t-test.

MARCH5 regulates the stability of MCL1

ABT-737 can antagonize BCL2, BCLXL, and BCLW, but not MCL1. Thus many tumors are refractory to ABT-737 treatment as they express high levels of MCL1. *In vitro* studies have shown that such tumors can be re-sensitized to ABT-737 following siRNA-mediated MCL1 knockdown[151]. Given that MARCH5 also sensitizes to ABT-737, we speculated that MARCH5 and MCL1 might exhibit a functional interaction. Since MARCH5 loss sensitized to ABT-737, which is blocked by high MCL1 expression, we initially hypothesized that MARCH5 depletion would engender a reduction of MCL1 level. Strikingly, however, loss of MARCH5 led to a robust stabilization of MCL1 (Fig. 3.4a). This effect was specific, as the levels of other anti-apoptotic proteins did not change upon depletion of MARCH5 (Fig. 3.4a). The stabilization of MCL1 was post-translational, as *MCL1* mRNA was unchanged following MARCH5 loss (Fig. 3.4b).

To further characterize the stabilization of MCL1, cycloheximide pulse chase experiments were performed on U2OS and HCT116 cell lines following transfections with siRLUC or siMARCH5. The depletion of MARCH5 led to prolonged stabilization of MCL1 in contrast to its normal turnover rate as observed in the control (Fig. 3.4c).

In line with these observations, the overexpression of MARCH5 led to the destabilization of MCL1 protein and this effect could be rescued through the addition of a proteasomal inhibitor, MG132 (Fig. 3.4d). Together, these data suggest that MARCH5 controls MCL1 levels by regulating its proteasome-dependent degradation.

a

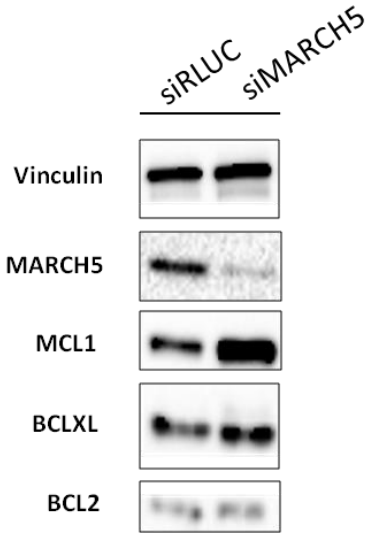
siRLUC
siMARCH5
Vinculin
MARCH5
MCL1
BCLXL
BCL2

b

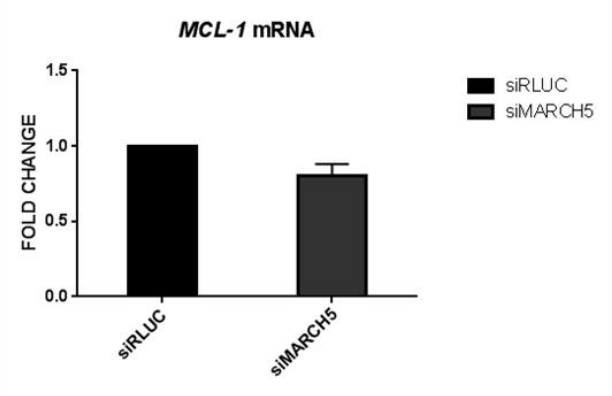
MCL-1 mRNA
FOLD CHANGE
1.5
1.0
0.5
0.0
siRLUC
siMARCH5
siRLUC
siMARCH5

c

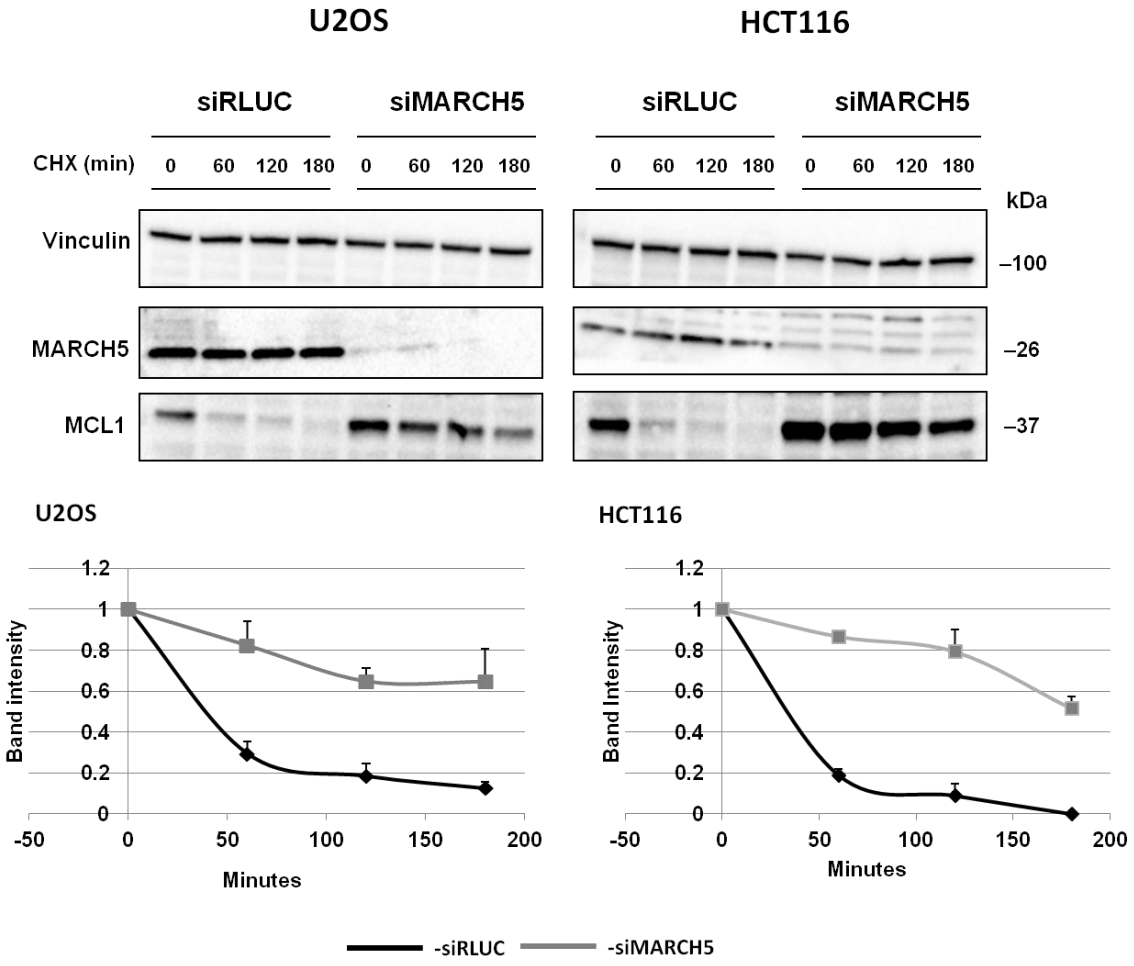
U2OS
HCT116
siRLUC
siMARCH5
siRLUC
siMARCH5
CHX (min)
0 60 120 180 0 60 120 180
0 60 120 180 0 60 120 180
kDa
Vinculin
MARCH5
MCL1
–100
–26
–37
U2OS
HCT116
Band intensity
Band Intensity
1.2
1
0.8
0.6
0.4
0.2
0
-50 0 50 100 150 200
Minutes
-siRLUC
-siMARCH5

d

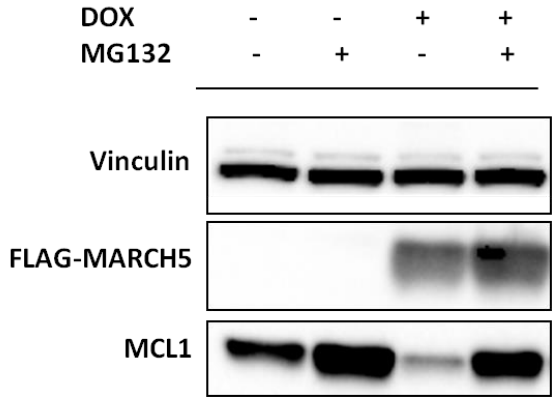

Figure 3.4. MARCH5 regulates MCL1 stability

(a) Lysates from HCT116 cells transfected with control siRNA or siRNA targeting MARCH5 were subjected to SDS-PAGE and western blotting.

(b) *MCL1* mRNA levels were measured following MARCH5 knockdown using quantitative RT-PCR and were normalized to *18S* mRNA. Error bars indicate the SD of triplicate measurements.

(c) Cycloheximide pulse-chase experiments were performed by treating transfected cells with cycloheximide for the given time points. Lysates were subjected to SDS-PAGE and immunoblot analysis to observe MCL1 stability. Graphs show MCL1 protein band intensities normalized to the loading control.

(d) U2OS cells expressing doxycycline-inducible FLAG-MARCH5 were treated with 50 ng/ml doxycycline for 24 h and with 10 μM MG132 for 3 h. Whole cell lysates were subjected to SDS-PAGE and immunoblotted with the indicated antibodies.

MARCH5 regulates MCL1 ubiquitination

In order to assess whether MARCH5 regulates MCL1 ubiquitination, doxycycline-inducible MARCH5^{WT} and MARCH5^{C65SC68S} (ligase defective mutant) expressing cells were transfected with HA-ubiquitin. MARCH5^{WT} expressing cells were also treated with MG132 in order to block the degradation of MCL1 upon the overexpression of MARCH5. Less MCL1 was co-immunoprecipitated with HA-ubiquitin following overexpression of MARCH5^{C65SC68S} as compared to MARCH5^{WT} treated with proteasome inhibitor (Fig. 3.5). These data indicate that MCL1 ubiquitination is controlled by MARCH5 ligase activity and that the MARCH5^{C65SC68S} mutant stabilizes MCL1 by preventing its ubiquitination. The MARCH5^{C65SC68S} appears to function as a dominant-negative (i.e., it likely inhibits the function of the endogenous wild-type MARCH5).

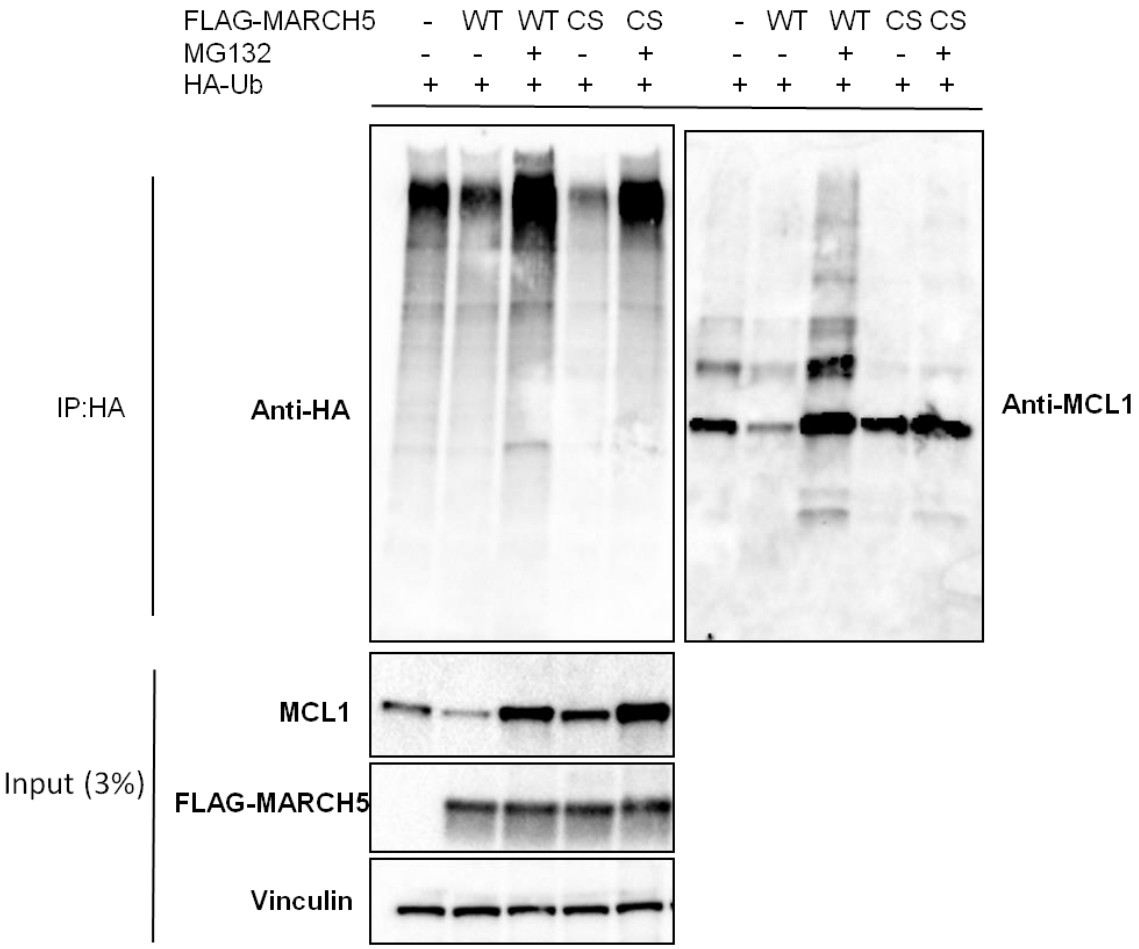

Figure 3.5. MARCH5 regulates MCL1 ubiquitination

Whole cell lysates from U2OS cells stably expressing doxycycline-inducible FLAG-MARCH5^{WT} or FLAG- MARCH5^{C65SC68S} transfected with the indicated plasmids and treated with Doxycyline (50 ng/ml) and/or MG132 (10 μM) as shown were subjected to immunoprecipitation using anti-HA antibody. Immunoprecipitated complexes were then subjected to SDS-PAGE and immunoblotted with the indicated antibodies. Input blots represent levels of indicated proteins in the whole cell lysate.

Loss of MARCH5 promotes transcriptional upregulation of p53 targets

Having observed a paradoxical stabilization of the anti-apoptotic protein, MCL1, we reasoned that MARCH5 loss might also promote up-regulation of pro-apoptotic proteins. This would counter the increase in MCL1 levels, and would reconcile our findings of increased sensitivity to ABT-737 under these conditions. Since the p53 tumor suppressor can modulate ABT-737-induced cell death[152], we therefore examined the levels of p53 and its downstream transcriptional targets. Quantitative PCR and western blotting showed that p53 and several of its targets are upregulated in MARCH5 knockdown cells compared to control (Fig. 3.6 a, b).

a

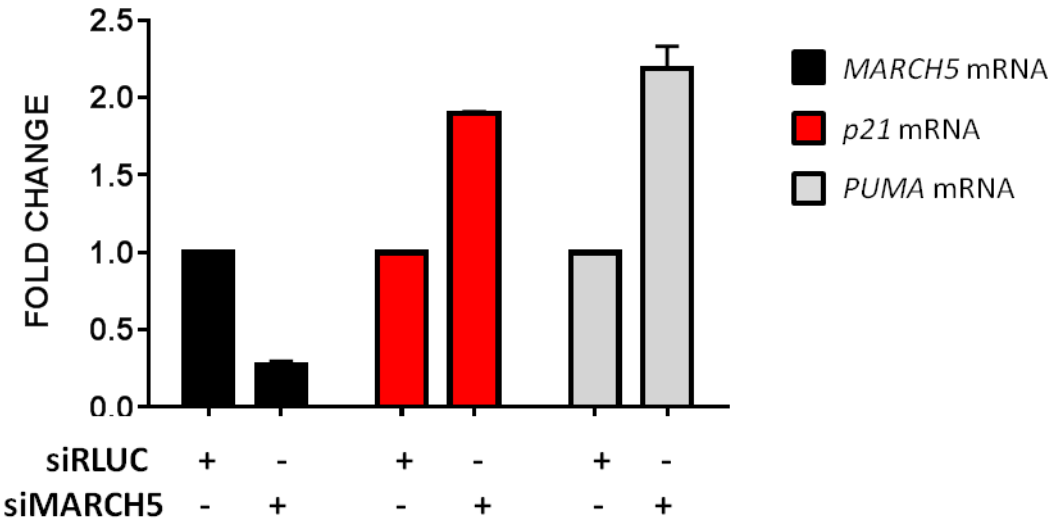
2.5
2.0
1.5
1.0
0.5
0.0
FOLD CHANGE
MARCH5 mRNA
p21 mRNA
PUMA mRNA
siRLUC + - + - + -
siMARCH5 - + - + - +

b

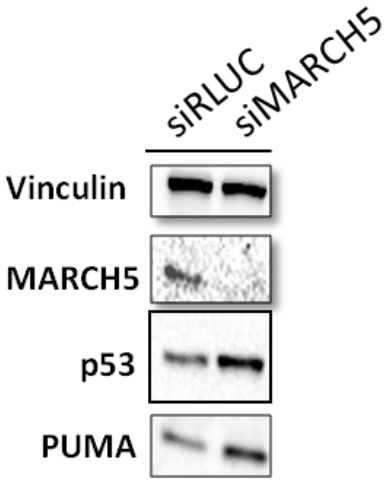
siRLUC
siMARCH5
Vinculin
MARCH5
p53
PUMA

Figure 3.6. MARCH5 loss leads to increased expression of p53 targets

(a) The expression of p53 targets-*PUMA* and *p21* following MARCH5 knockdown in HCT116 cells were assessed by quantitative RT-PCR. Error bars indicate the SD of triplicate measurements.

(b) Whole cell lysates from control or MARCH5-depleted HCT116 cells were subjected to SDS-PAGE and immunoblotted with the indicated antibodies.

Sensitization to apoptosis upon MARCH5 loss is partially p53-dependent

Given that p53 targets were upregulated upon MARCH5 loss, experiments were performed to assess whether the sensitization to ABT-737 in the absence of MARCH5 was p53-dependent. Isogenic HCT116 $p53^{WT}$ and HCT116 $p53^{-/-}$ cell lines were transfected with siMARCH5 and treated with ABT-737. The absence of p53 ameliorated the enhanced cell death observed upon MARCH5 loss and ABT-737 treatment although some sensitization was observed at higher concentrations of the compound (Fig. 3.7a, b).

a

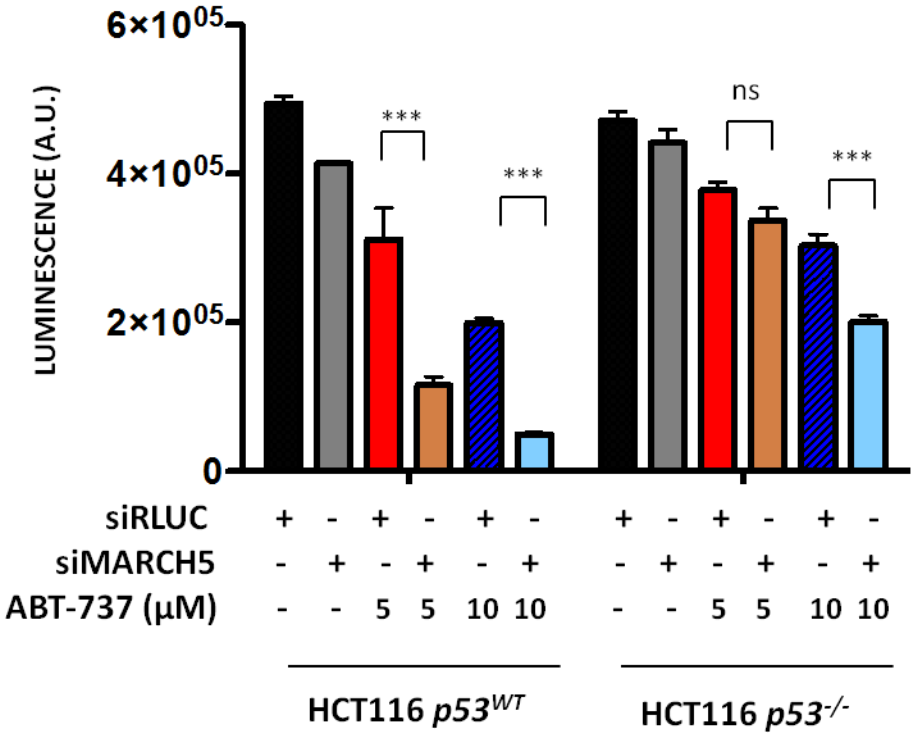
LUMINESCENCE (A.U.)
6×10^05
4×10^05
2×10^05
0
***
***
ns
***
siRLUC + - + - + - + - + - + -
siMARCH5 - + - + - + - + - + - +
ABT-737 (μM) - - 5 5 10 10 - - 5 5 10 10
HCT116 p53^WT
HCT116 p53^-/-

b

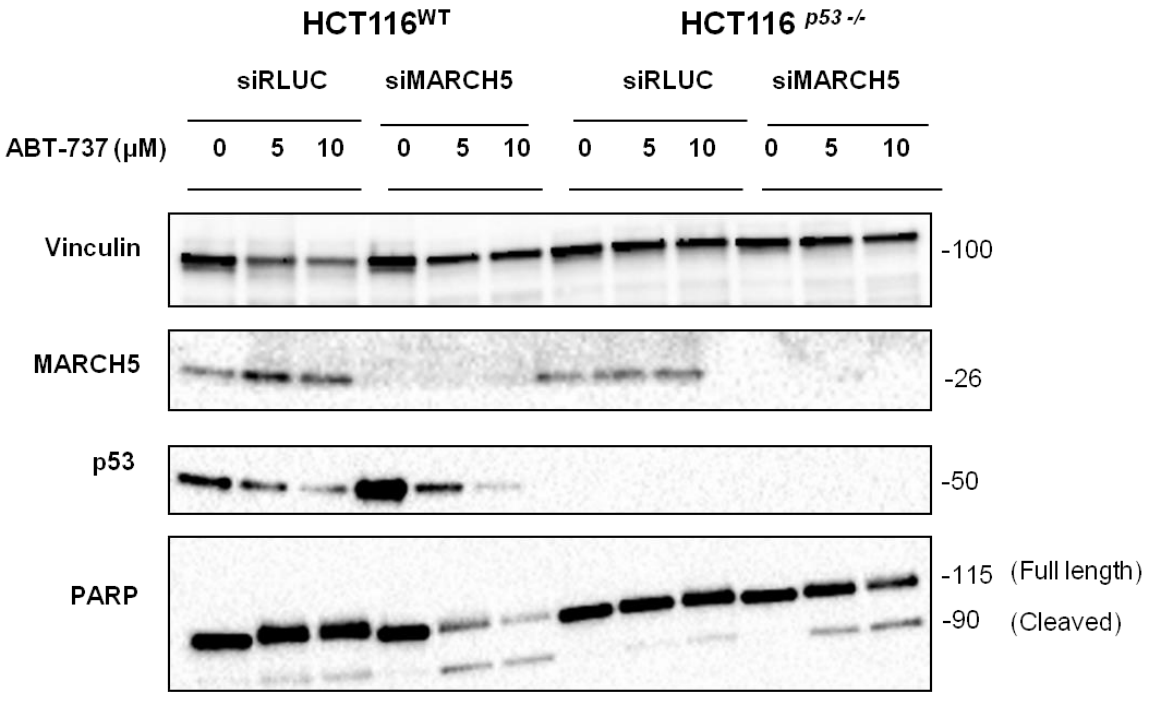
HCT116^WT
HCT116 p53 -/-
siRLUC
siMARCH5
siRLUC
siMARCH5
ABT-737 (μM) 0 5 10 0 5 10 0 5 10 0 5 10
Vinculin
MARCH5
p53
PARP
-100
-26
-50
-115 (Full length)
-90 (Cleaved)

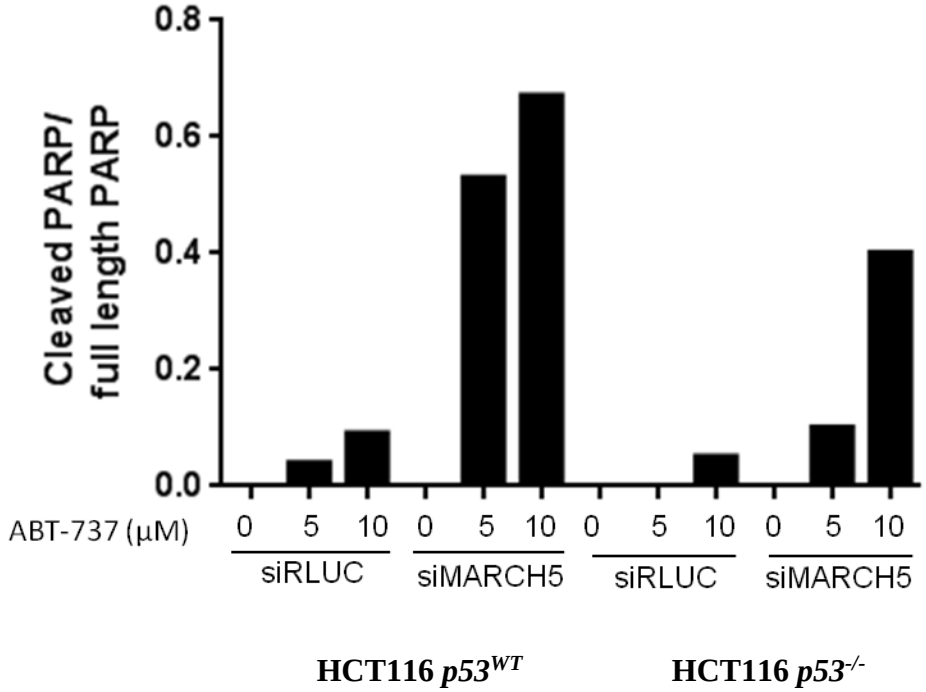

Figure 3.7. MARCH5 depletion sensitizes cells to apoptosis in a largely p53-dependent manner

(a) Isogenic HCT116 $p53^{WT}$ and HCT116 $p53^{-/-}$ cells were transfected with control siRNA or siRNA targeting MARCH5 and treated with ABT-737 at the indicated concentrations. Cell viability was measured using CellTiter-Glo. Error bars represent the SD of triplicate experiments. Asterisks (***) indicate p values <0.001 compared to the respective controls using Student's t-test. No significant difference represented by (ns).

(b) Isogenic HCT116 $p53^{WT}$ and HCT116 $p53^{-/-}$ cells were transfected with control siRNA or siRNA targeting MARCH5 and treated with ABT-737 at the indicated concentrations. Whole cell lysates were harvested and subjected to SDS-PAGE and immunoblotted with the indicated antibodies. PARP cleavage was quantified as the ratio of cleaved to full length PARP.

BH3 profiling reveals that NOXA is an essential mediator of apoptosis following MARCH5 loss

In order to functionally dissect the BCL-2 pathway downstream of MARCH5, BH3 profiling was performed through genetic studies using isogenic cell lines or RNAi. PUMA, BIM, and NOXA are BH3-only "de-repressor" pro-apoptotic proteins that are responsible for the inhibition of the anti-apoptotic BCL-2 family members or for the direct activation of BAX and BAK[26]. Experiments with the isogenic cell lines HCT116 *PUMA*^{WT} and HCT116 *PUMA*$^{-/-}$ revealed that PUMA was dispensable for the sensitization to apoptosis upon MARCH5 loss (Fig. 3.8a). Similar experiments were performed using siRNA to target BIM and NOXA in order to determine which of these proteins was required for cell death following MARCH5 knockdown. The loss of NOXA (but not BIM) specifically abrogated sensitization to ABT-737 (Fig. 3.8b, c).

a

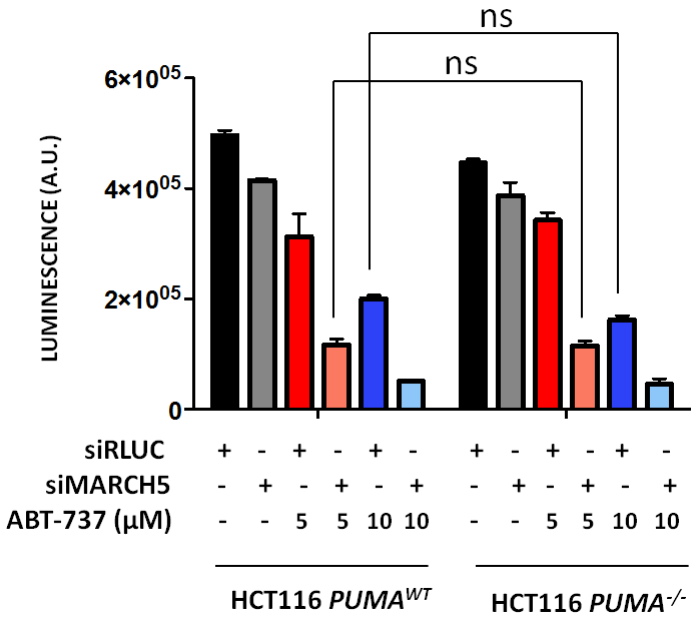

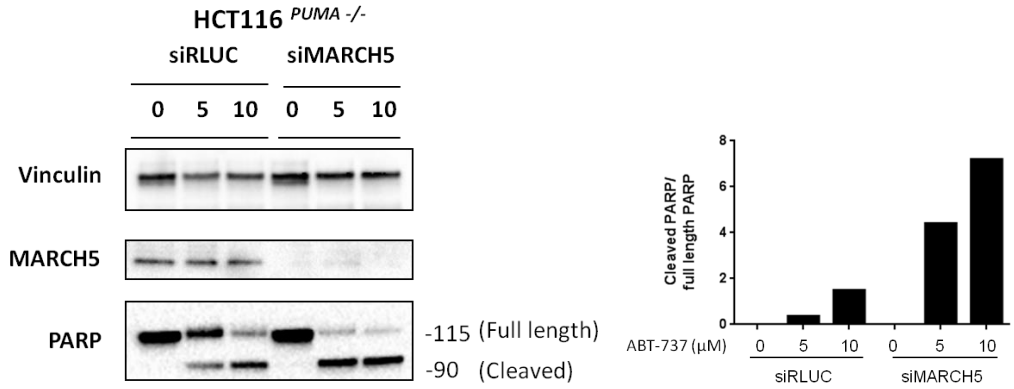
HCT116 PUMA -/-
siRLUC
siMARCH5
0 5 10 0 5 10
Vinculin
MARCH5
PARP
-115 (Full length)
-90 (Cleaved)
Cleaved PARP/ full length PARP
ABT-737 (μM)
0 5 10 0 5 10
siRLUC
siMARCH5

b

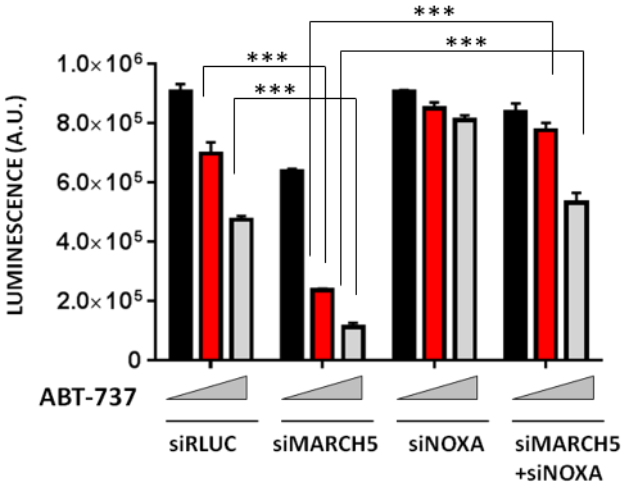
***
***
***
***
LUMINESCENCE (A.U.)
1.0×10⁶
8.0×10⁵
6.0×10⁵
4.0×10⁵
2.0×10⁵
0
ABT-737
siRLUC
siMARCH5
siNOXA
siMARCH5 +siNOXA

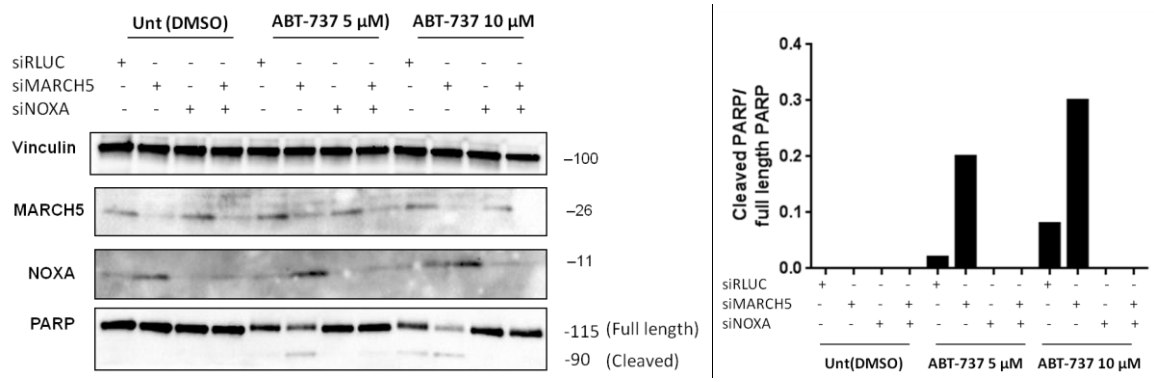
Unt (DMSO)
ABT-737 5 μM)
ABT-737 10 μM
siRLUC
siMARCH5
siNOXA
Vinculin
MARCH5
NOXA
PARP
–100
–26
–11
-115 (Full length)
-90 (Cleaved)
Cleaved PARP/ full length PARP
Unt(DMSO)
ABT-737 5 μM
ABT-737 10 μM

c

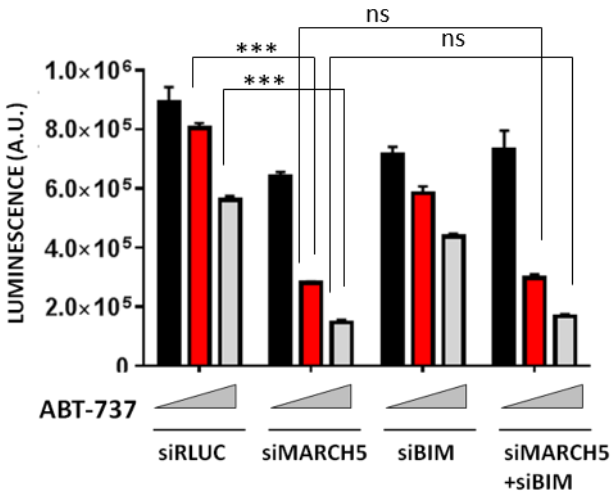
ns
ns
***
***
1.0×10⁶
8.0×10⁵
6.0×10⁵
4.0×10⁵
2.0×10⁵
0
LUMINESCENCE (A.U.)
ABT-737
siRLUC
siMARCH5
siBIM
siMARCH5 +siBIM

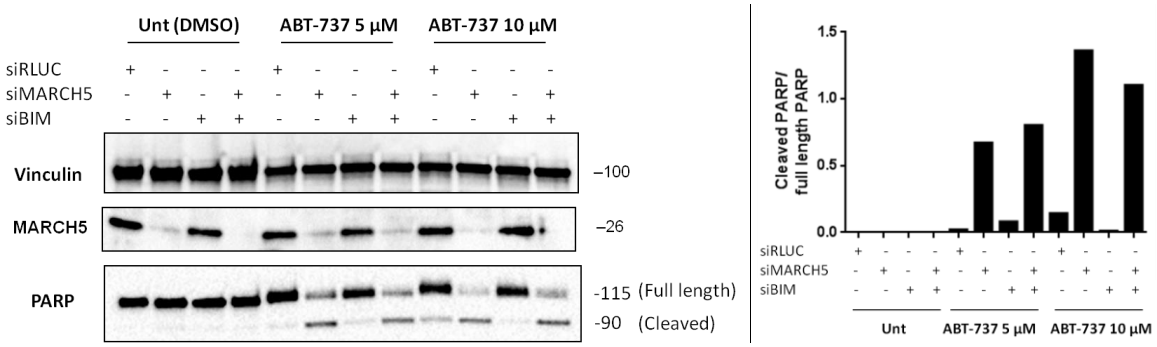
Unt (DMSO)
ABT-737 5 µM
ABT-737 10 µM
siRLUC
siMARCH5
siBIM
Vinculin
MARCH5
PARP
–100
–26
-115 (Full length)
-90 (Cleaved)
Cleaved PARP/ full length PARP
1.5
1.0
0.5
0.0
Unt
ABT-737 5 µM
ABT-737 10 µM

d

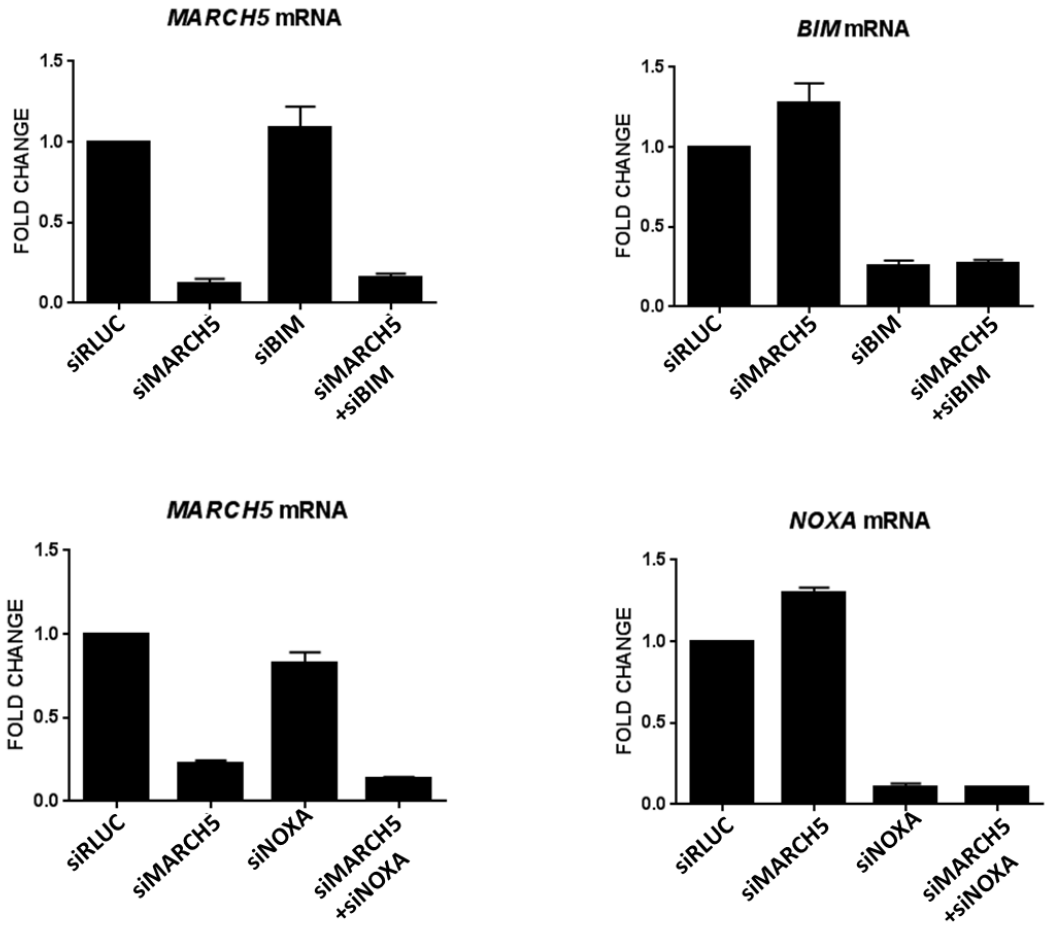

Figure 3.8. Sensitization to apoptosis upon MARCH5 loss is dependent on the BH3-only protein NOXA

(c) Isogenic HCT116 *PUMA*^{WT} and HCT116 *PUMA*$^{-/-}$ cells were transfected with control siRNA or siRNA targeting MARCH5 and treated with ABT-737 at the indicated concentrations. Cell viability was measured using CellTiter-Glo. Error bars represent the SD of triplicate experiments. 'ns' represents no significant difference between the levels of sensitization through combined MARCH5 loss and ABT-737 treatment in the two cell lines. Isogenic HCT116 *PUMA*^{WT} and HCT116 *PUMA*$^{-/-}$ cells were transfected with control siRNA or siRNA targeting MARCH5 and treated with ABT-737 at the indicated concentrations. Whole cell lysates were

harvested and subjected to SDS-PAGE and immunoblotted with the indicated antibodies. PARP cleavage was quantified as the ratio of cleaved to full length PARP.

(d) HCT116 cells transfected with siRLUC, siMARCH5, siNOXA or co-transfected with siMARCH5/siNOXA were treated with ABT-737 (Black bar: DMSO, red: 5 μM, grey: 10 μM). Cell viability was assessed using CellTiter-Glo. Error bars represent the SD of triplicate experiments. Asterisks (***) indicate p values <0.001 compared to the respective controls using Student's t-test. No significant difference represented by (ns). Whole cell lysates were harvested and subjected to SDS-PAGE and immunoblotted with the indicated antibodies. PARP cleavage was quantified as the ratio of cleaved to full length PARP.

(e) HCT116 cells transfected with siRLUC, siMARCH5, siBIM or co-transfected with siMARCH5/siBIM were treated with ABT-737 (Black bar: DMSO, red: 5 μM, grey: 10 μM). Cell viability was assessed using CellTiter-Glo. Error bars represent the SD of triplicate experiments. Asterisks (***) indicate p values <0.001 compared to the respective controls using Student's t-test. No significant difference represented by (ns). Whole cell lysates were harvested and subjected to SDS-PAGE and immunoblotted with the indicated antibodies. PARP cleavage was quantified as the ratio of cleaved to full length PARP.

(f) Validation of knockdown was performed by quantitative RT-PCR and mRNA levels were normalized to *18S* mRNA

MARCH5 loss leads to stabilization of MCL1 in a NOXA-dependent manner

Since the loss of MARCH5 led to stabilization of MCL-1 and still sensitized cells to BH3 mimetics, we reasoned that one of the BH3- only proteins might be responsible for neutralizing MCL1's anti-apoptotic activity. Two BH3-only proteins BIM and NOXA have been reported to bind to and inhibit MCL1[153,43]. To determine which of these proteins was required for stabilization, we knocked down MARCH5 in the presence and absence of siRNA to BIM or NOXA. Following MARCH5 loss, the knockdown of BIM had no effects on MCL1 levels (Fig. 3.9). The loss of NOXA alone led to a slight stabilization of MCL1, as reported in prior studies[154]. However, the concomitant loss of NOXA and MARCH5 attenuated the induction of MCL1 that we observed upon MARCH5 knockdown (Fig. 3.9). Validation of knockdown was performed using qRT-PCR (Fig. 3.8d)

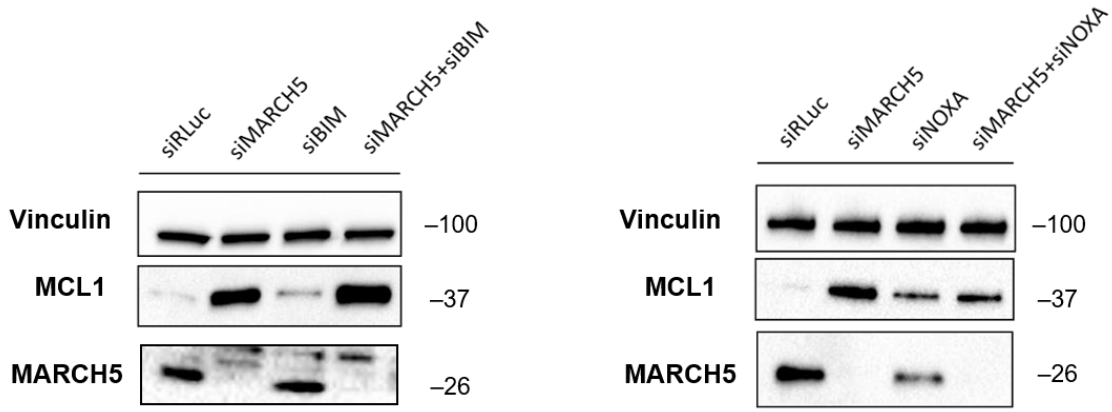

Figure 3.9. MARCH5-dependent stabilization of MCL1 requires NOXA

Whole cell lysates from HCT116 cells transfected with siRLUC, siMARCH5, siBIM, siNOXA, or co-transfected with siMARCH5/siBIM and siMARCH5/siNOXA were subjected to SDS-PAGE and immunoblotted with the indicated antibodies.

Depletion of MARCH5 leads to stabilization of NOXA in a p53-independent manner

Having observed a NOXA-dependent induction of apoptosis and the stabilization of MCL1 upon MARCH5 loss, we surmised that the loss of MARCH5 promotes up regulation of NOXA. Quantitative real-time PCR revealed that MARCH5 depletion did not affect *NOXA* at the transcriptional level (Fig. 3.8d). However, a robust stabilization of NOXA protein was observed in the absence of MARCH5 (Fig. 3.10a and Fig. 3.8b). Interestingly, the loss of NOXA promoted a destabilization of MARCH5 protein, indicating some level of co-regulation between these two proteins (Fig. 3.10a). This will be further addressed in the Discussion.

Since NOXA is a p53 transcriptional target, we formally excluded a role for induction of *NOXA* mRNA by using isogenic HCT116 $p53^{WT}$ and HCT116 $p53^{-/-}$ cell lines. This demonstrated that both NOXA and MCL-1 were stabilized in both genetic backgrounds upon MARCH5 loss. However, the absolute level was lower in the HCT116 $p53^{-/-}$ cells than that observed in HCT116 $p53^{WT}$ (Fig. 3.10b).

a

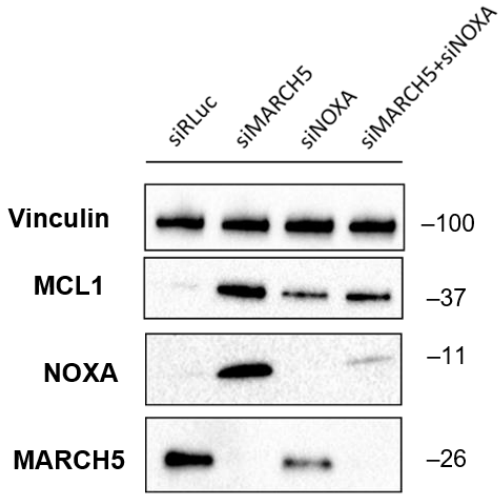

b

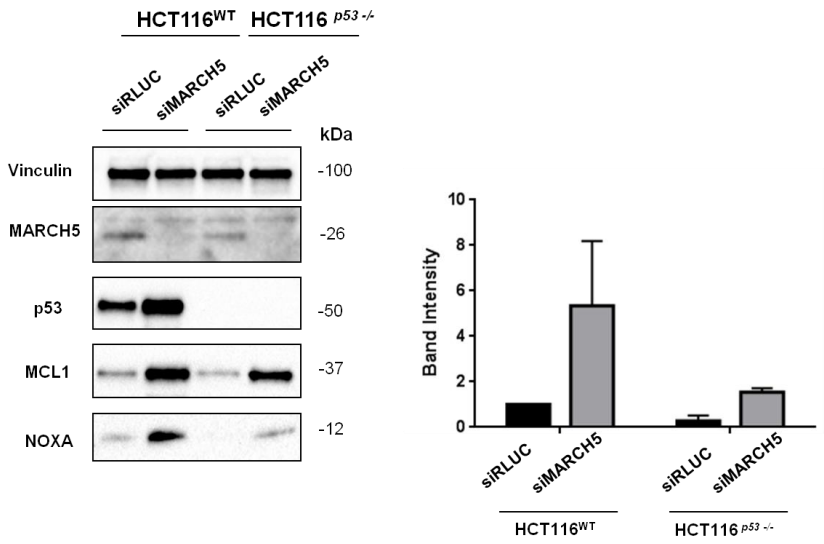

Figure 3.10. MARCH5 loss stabilizes NOXA

(a) Whole cell lysates from HCT116 cells transfected with siRLUC, siMARCH5, siNOXA, or co-transfected with siMARCH5/siNOXA were subjected to SDS-PAGE and immunoblotted with the indicated antibodies.

(b) HCT116 $p53^{WT}$ and HCT116 $p53^{-/-}$ cells were transfected with control siRNA or siRNA targeting MARCH5. Lysates were then subjected to SDS-PAGE and immunoblotted with the indicated antibodies. NOXA band intensities were quantified in HCT116 $p53^{WT}$ and HCT116 $p53^{-/-}$ cells. Error bars are SD of three independent experiments.

A MARCH5 ligase-deficient mutant promotes concomitant upregulation of MCL1 and NOXA

MARCH5 depletion led to the stabilization of MCL1 and NOXA; it was therefore surmised that loss of MARCH5 E3 ubiquitin ligase activity underpinned this observation. In order to test this, cell-based assays were also performed using doxycycline inducible $MARCH5^{WT}$ and a ligase-deficient $MARCH5^{C65SC68S}$ (CS). As shown in Fig. 3.11a, the overexpression of $MARCH5^{WT}$ reduced endogenous MCL1 levels, whereas $MARCH5^{CS}$ stabilized both MCL1 and NOXA (Fig. 3.11a). Interestingly, overexpression of this mutant also stabilized endogenous MARCH5 (Fig. 3.11a). This could be since it interacts with the endogenous form, thereby not only preventing its degradation, but also rendering it functionally inactive.

In order to assess the importance of NOXA in the MARCH5-dependent degradation of MCL1, U2OS cells expressing doxycycline-inducible $MARCH5^{WT}$ and $MARCH5^{CS}$ were transfected with control siRNA (siRLUC) or siRNA targeting NOXA. The expression of FLAG- MARCH5 was induced and the levels of MCL1 were assessed in the presence and absence of NOXA. The depletion of NOXA abrogated the MARCH5-dependent degradation of MCL1 (compare lanes 2 and 7). Interestingly, the loss of NOXA also inhibited the stabilization of MCL1 observed with the expression of $MARCH5^{CS}$ (Fig. 3.11b). This recapitulated the earlier results in the RNAi experiments where concomitant depletion of MARCH5 and NOXA abrogated MCL1 stabilization.

a

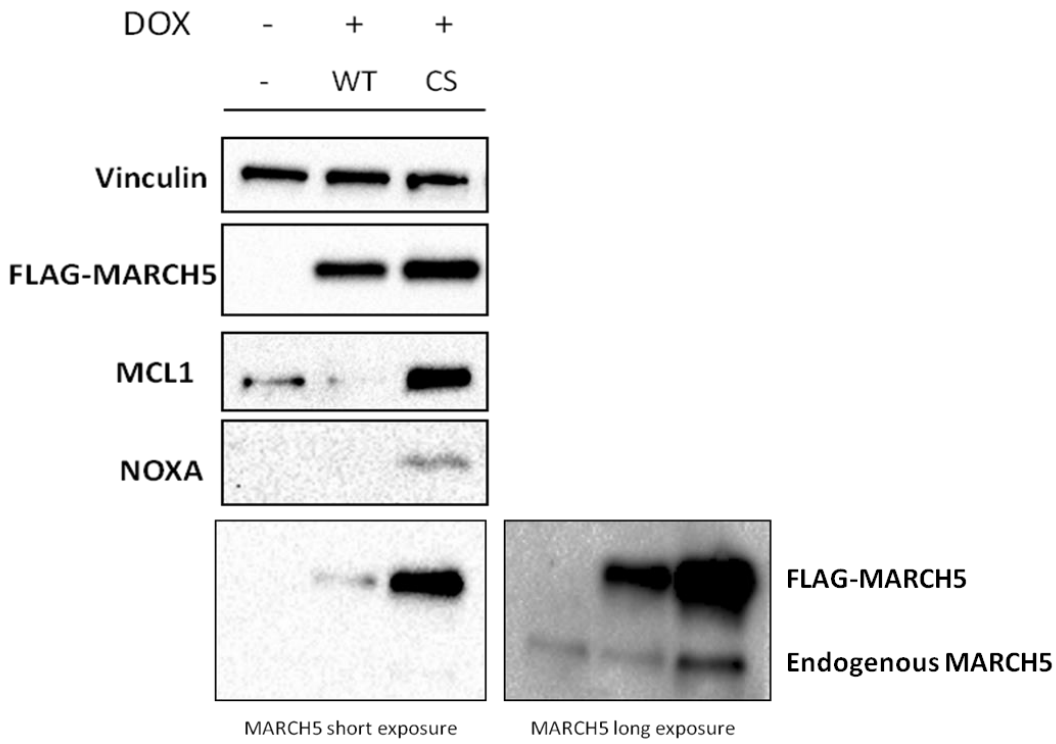
DOX
-
+
+
-
WT
CS
Vinculin
FLAG-MARCH5
MCL1
NOXA
FLAG-MARCH5
Endogenous MARCH5
MARCH5 short exposure
MARCH5 long exposure

b

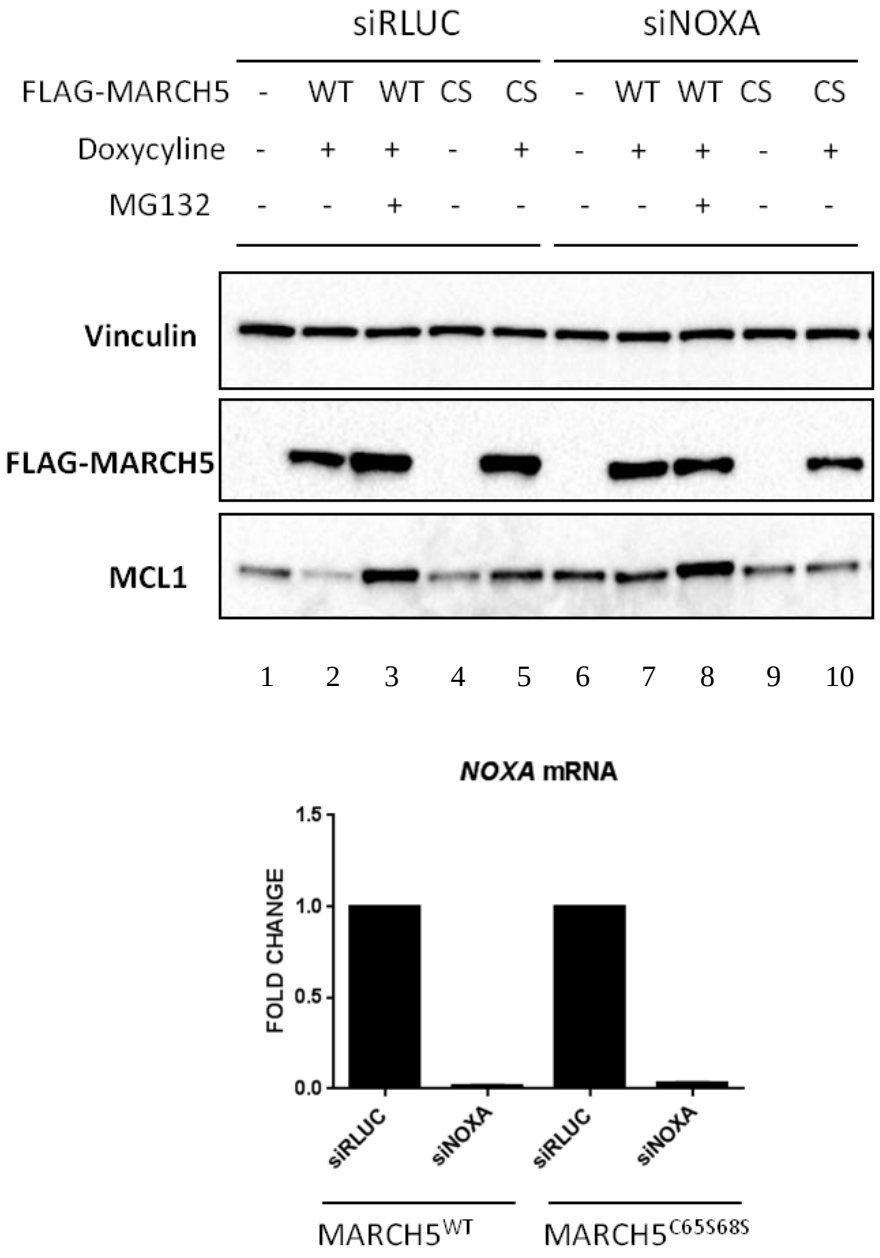

Figure 3.11. NOXA is required for the regulation of MCL1 by MARCH5

(a) U2OS cells stably expressing doxycycline-inducible FLAG-MARCH5^{WT} or FLAG-MARCH5^{C65SC68S} were induced with 50 ng/ml doxycyline for 24 h. Whole cell lysates were then subjected to SDS-PAGE and immunoblotted with the indicated antibodies.

(b) U2OS cells stably expressing doxycycline-inducible FLAG-MARCH5^{WT} or FLAG-MARCH5^{CS} were transfected with control siRNA or siRNA targeting NOXA. Twenty-four hours post transfection, the cells were treated with 50 ng/ml doxycycline for a further 24 h to induce the expression of FLAG-MARCH5. Cells expressing FLAG-MARCH5^{WT} were also treated with MG132 for 3 h to block the proteasomal degradation of MCL-1. Whole cell lysates were harvested, subjected to SDS-PAGE, and immunoblotted with the indicated antibodies.

Knockdown of *NOXA* mRNA in U2OS FLAG-MARCH5^{WT} and FLAG-MARCH5^{CS} was assessed by quantitative RT-PCR. Error bars indicate the SD of triplicate measurements.

MARCH5 RING domain mutant sensitizes cells to ABT-737 in a NOXA-dependent manner

The expression of MARCH5^{CS} promoted concomitant stabilization of MCL1 and NOXA, which recapitulates the phenotype observed with MARCH5 siRNA. Since the co-stabilization was critical for mediating sensitivity to ABT-737, we thus hypothesized that expression of MARCH5^{CS} should also sensitize to ABT-737. U2OS cells expressing doxycycline-inducible MARCH5^{WT} and MARCH5^{CS} were transfected with control siRNA (siRLUC) or siRNA targeting NOXA. When compared to the non-induced (-DOX) control, the expression of MARCH5^{CS} sensitized cells to the BH3 mimetic. In contrast, the absence of NOXA completely ameliorated this effect (Fig. 3.12). The overexpression of MARCH5^{WT} had no significant effect on ABT-737-induced cell death, and was similar to the –DOX control. The lack of protection by the wild-type MARCH5 may be attributed to the absence of NOXA stabilization (), which appears critical for response to ABT-737.

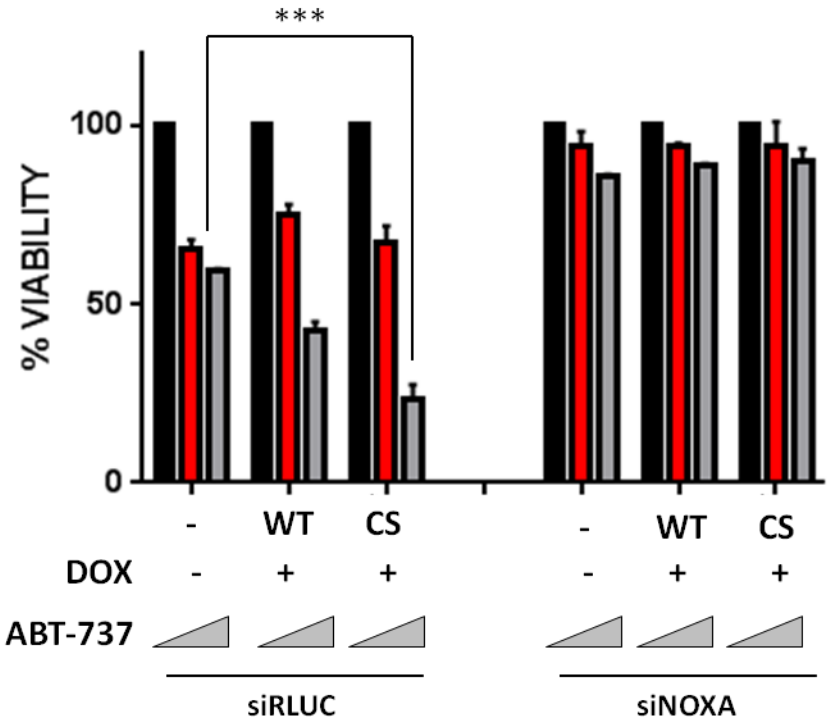

Figure 3.12. Sensitization to ABT-737 via a RING domain mutant of MARCH5 is abrogated upon depletion of NOXA

U2OS cells stably expressing doxycycline-inducible FLAG-MARCH5^{WT} or FLAG- MARCH5^{CS} were transfected with control siRNA or siRNA targeting NOXA. Twenty-four hours post transfection, the cells were treated with 50 ng/ml doxycycline to induce the expression of FLAG-MARCH5 and with ABT-737 (Black bar: DMSO, red: 5 µM, grey: 10 µM). Cell viability was assessed using CellTiter-Glo. Error bars represent the SD of triplicate measurements. Asterisks (***) represent a p value < 0.001 compared to the respective controls using Student's t-test.

MARCH5-dependent regulation of MCL1 stability and sensitivity to ABT-737 relies on direct MCL1-NOXA interaction

We observed a dependency on NOXA for MARCH5-mediated regulation of MCL1 stability and sensitization to ABT-737. However, it was unclear whether these effects required direct interactions between NOXA and MCL1.

In order to assess this question, HeLa cells expressing doxycycline-inducible $NOXA^{WT}$ or $NOXA^{L29E}$ (a NOXA BH3 domain mutant that cannot interact with MCL1)[154] were transfected with siRLUC, siMARCH5. This was followed by induction of ectopic expression of $NOXA^{WT}$ or $NOXA^{L29E}$.

The induction of $NOXA^{WT}$ following MARCH5 depletion elicited robust stabilization of MCL1. This is in line with our results that increased NOXA expression in required for the MARCH5-dependent stabilization of MCL1. In contrast, the expression of $NOXA^{L29E}$ significantly attenuated the stabilization of MCL1 upon MARCH5 loss (Fig. 3.13b). This suggests that direct interaction between the NOXA BH3 domain and MCL1 is required for MARCH5-dependent regulation of MCL1 (see model Figure in Discussion). $NOXA^{L29E}$ itself appeared to be more stable than $NOXA^{WT}$. This indicates that, in addition to mediating interactions between NOXA and MCL1, the BH3 domain is also required for the normal turnover of NOXA.

Interestingly, the exprssion of $NOXA^{WT}$ was not toxic in the absence of ABT, but became so when MARCH5 was concomitantly knocked down (Fig. 3.13a), and this correlated with increased levels of NOXA (Fig. 3.13b). Furthermore, MARCH5-dependent sensitization to ABT-737 was enhanced following induction of $NOXA^{WT}$, but was completely abrogated in the presence of $NOXA^{L29E}$ (Fig. 3.13a). Importantly, the MCL1 stabilization accompanying MARCH5 loss was also attenuated in the presence of $NOXA^{L29E}$.This phenocopies the

results of the NOXA siRNA experiments described above. Together, these data reveal a direct role for NOXA in the inactivation of MCL1 following loss of MARCH5.

a **b**

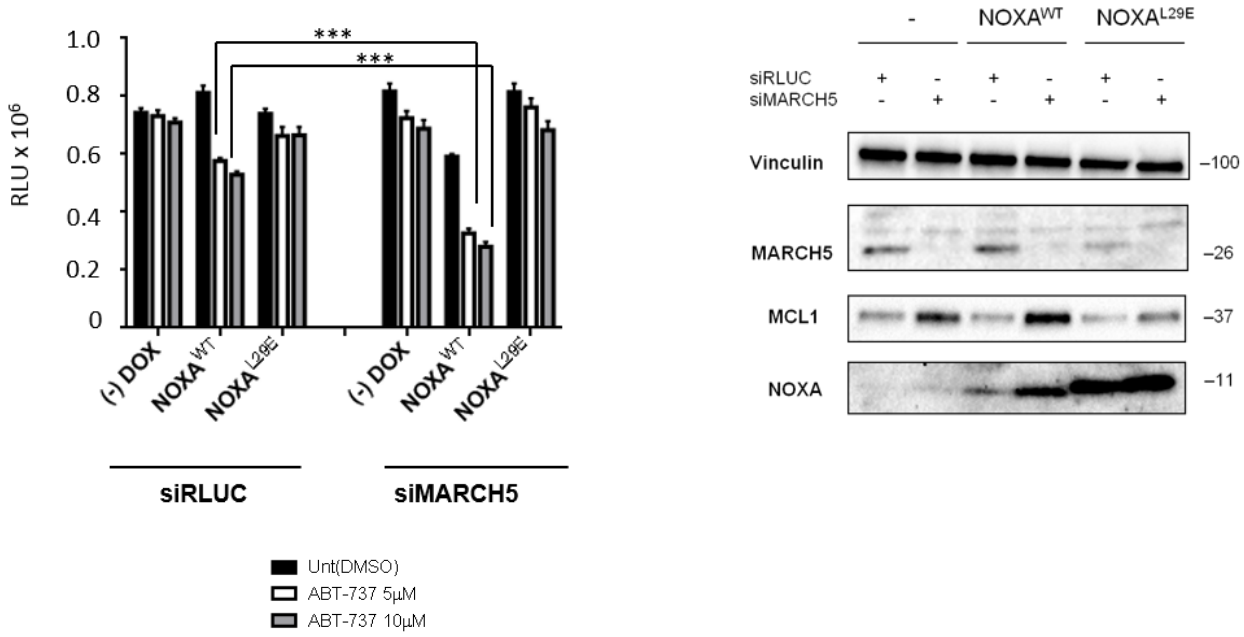

Figure 3.13. MARCH5-dependent regulation of MCL1 and sensitivity to ABT-737 requires direct MCL1/ NOXA interactions

(a) Doxycycline-inducible HeLa cells expressing either NOXA^{WT} or NOXA^{L29E} were transfected with the indicated siRNAs. Ectopic expression of NOXA or its mutant form was induced for 48 h. Cells were then harvested and plated on 96-well plates. Cells were treated with ABT-737 at the indicated concentrations for 24 h. Cell viability was assessed using CellTiter-Glo. Error bars represent the SD of triplicate measurements. Asterisks (***) represent a p value < 0.001 compared to the respective controls using Student's t-test.

(b) Whole cell lysates were subjected to SDS-PAGE and immunoblotted with the indicated antibodies.

Dissection of MARCH5-dependent synthetic lethal interactions using selective BH3 mimetics

Our observations thus far with ABT-737 demonstrate a MARCH5-dependent chemical-genetic lethal interaction with the BCL2 pathway. Since ABT-737 inhibits BCL2, BCLXL, and BCLW, this compound cannot be used to determine the relative contribution of each anti-apoptotic protein to the sensitization observed. To address this, we used specific BCL-2 antagonists that were developed during the course of our studies[49,155].

Synthetic lethality was observed with MARCH5 knockdown in the presence of the BCLXL-selective antagonist, WEHI-539, but not with ABT-199, a BCL2-selective antagonist (Fig. 3.14a, b). This result was further validated by concomitantly knocking down MARCH5 and BCL2 through RNAi (data not shown). Cumulatively, these data therefore indicate that although the loss of MARCH5 leads to the functional inactivation of MCL1 by NOXA, BCLXL can act as a "backup" and enable the survival of HCT116 cells.

a

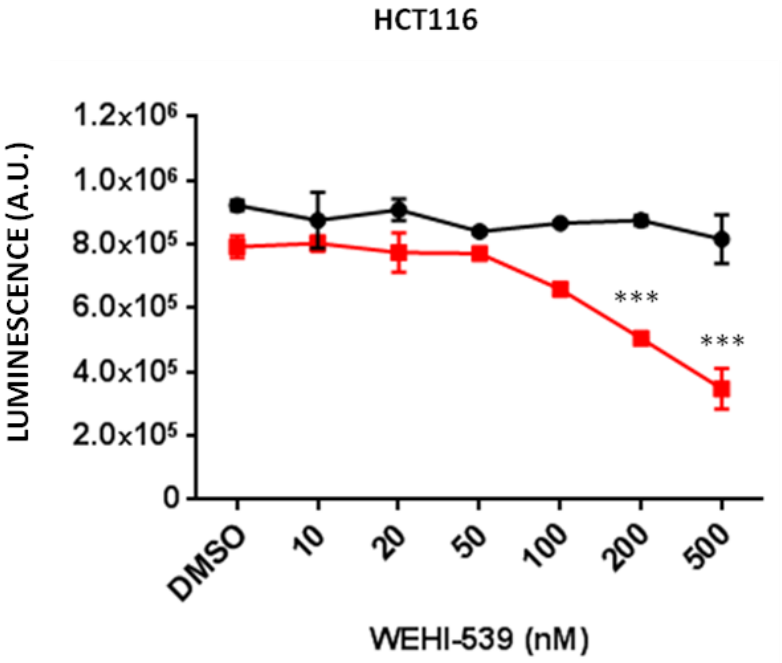
HCT116
LUMINESCENCE (A.U.)
1.2x10⁶
1.0x10⁶
8.0x10⁵
6.0x10⁵
4.0x10⁵
2.0x10⁵
0
***
***
DMSO
10
20
50
100
200
500
WEHI-539 (nM)

b

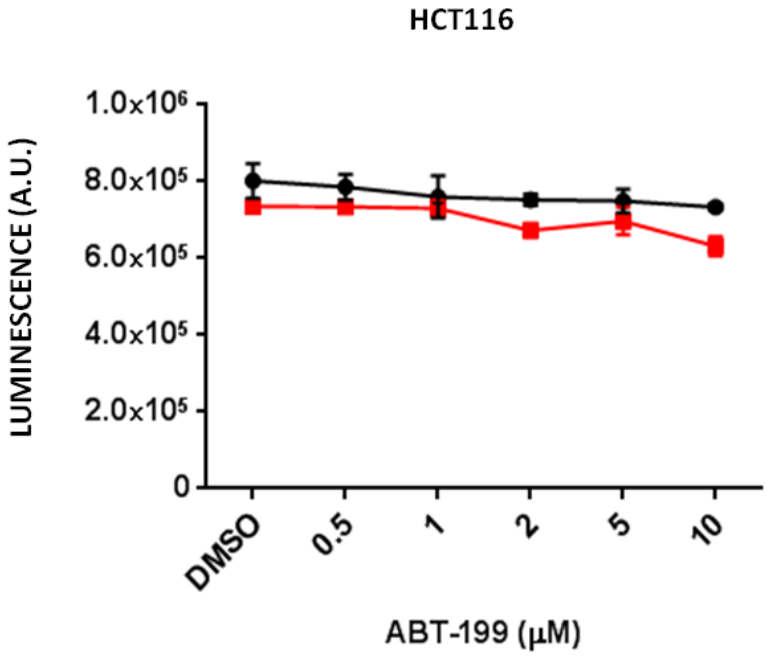
HCT116
LUMINESCENCE (A.U.)
1.0x10⁶
8.0x10⁵
6.0x10⁵
4.0x10⁵
2.0x10⁵
0
DMSO
0.5
1
2
5
10
ABT-199 (μM)

Figure 3.14. MARCH5 loss displays synthetic lethality with the BCLXL-specific antagonist, WEHI-539

(a) HCT116 cells transfected with siRNAs targeting luciferase or MARCH5 were treated with WEHI-539 at the indicated concentrations. Cell viability was measured using CellTiter-Glo. The error bars represent the SD from triplicate measurements for each condition. The asterisks (***) indicate a p value of < 0.001 compared to the respective controls using Student's t-test.

(b) HCT116 cells transfected with the indicated siRNAs were treated with ABT-199 at the given concentrations. Cell viability was measured using CellTiter-Glo. The error bars represent the SD from triplicate experiments.

Synthetic lethality of MARCH5 and MCL1 in MCL1-dependent breast cancer

Given our observations of a MARCH5/MCL1 link, we asked whether (independently of the chemical genetic interactions) a synthetic lethal relationship might exist between these two genes. This was not observed in HCT116 cells (Fig. 3.15b); however, chemical and genetic inhibition of MCL1 in HCT116 revealed that they are not dependent on MCL1, at least in these short-term assays (Fig. 3.15a, b). It was therefore hypothesized that MARCH5 loss would exhibit synthetic lethality in cell lines that are known to be MCL1-dependent. To this end, two triple negative breast cancer lines, MDA-MB-231 and MDA-MB-468 that differ with regard to their dependence on MCL1 were selected[156]. Using the MCL1 specific inhibitor A1210477, it was confirmed that the MDA-MB-468 cells were indeed MCL1-dependent, whereas the MDA-MB-231 line was not dependent on MCL1 for survival (Fig. 3.15a). This is consistent with previous studies, and was further validated using MCL1 RNAi (Fig. 3.15c).

Strikingly, concomitant loss of MARCH5 and MCL1 was synthetic lethal in the MCL1 dependent MDA-MB-468 cell line, but not in the MCL1 independent line MDA-MB-231 (Fig. 3.15c).

Interestingly, both these cells lines harbor inactive p53 mutant proteins (http://p53.free.fr/Database/p53_database.html). Consistent with their p53 status and with prior results in the isogenic HCT116^{WT} and HCT116$^{p53-/-}$ cells (Fig. 3.7), the loss of MARCH5 did not sensitize these cells to ABT-737 (Fig. 3.15d). These results validate our earlier observations and emphasize the importance of p53 in the MARCH5-dependent sensitization to ABT-737.

a

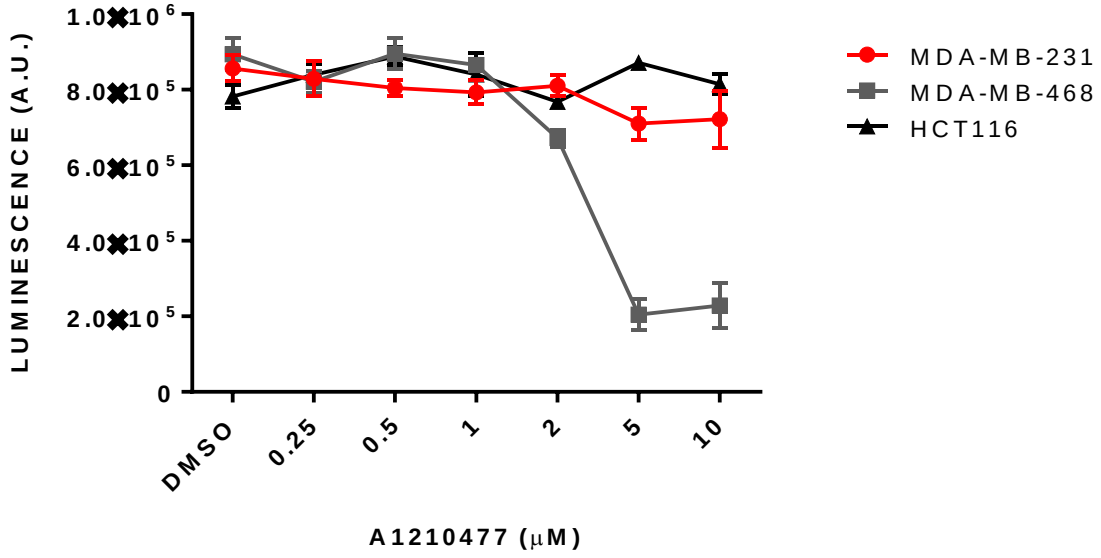

b

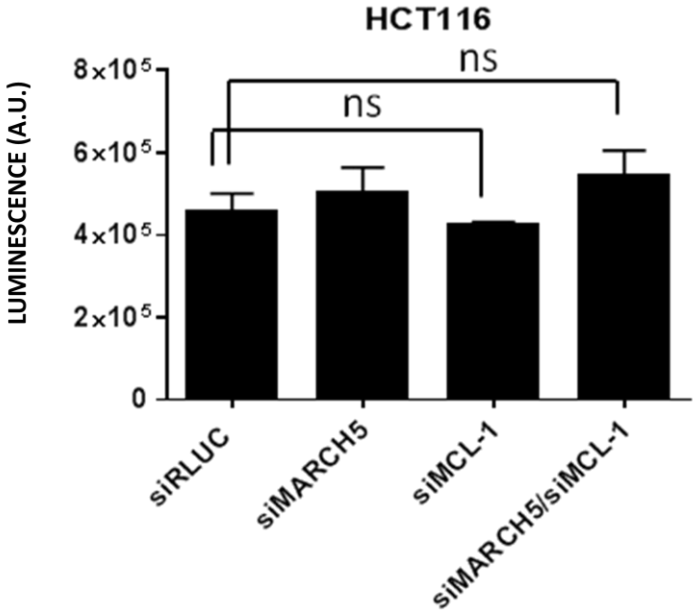
HCT116
LUMINESCENCE (A.U.)
8x10⁵
6x10⁵
4x10⁵
2x10⁵
0
ns
ns
siRLUC
siMARCH5
siMCL-1
siMARCH5/siMCL-1

c

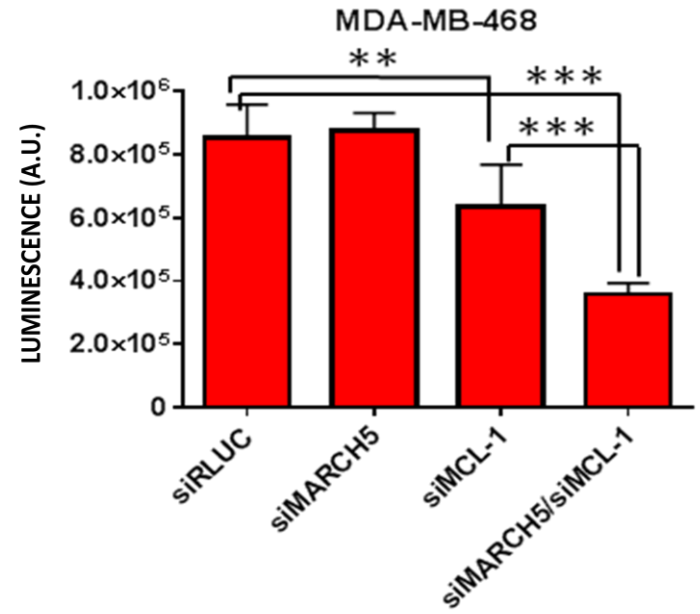
MDA-MB-468
**
***
***
LUMINESCENCE (A.U.)
1.0×10⁶
8.0×10⁵
6.0×10⁵
4.0×10⁵
2.0×10⁵
0
siRLUC
siMARCH5
siMCL-1
siMARCH5/siMCL-1

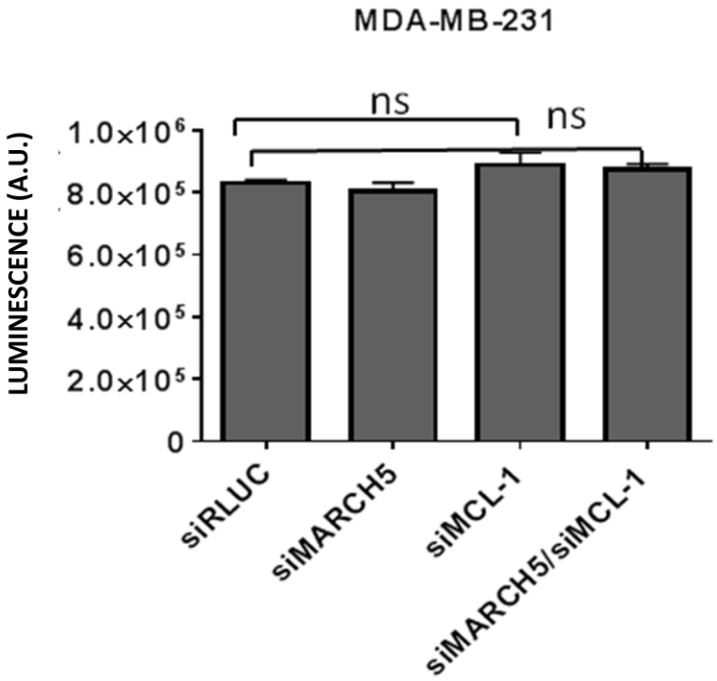
MDA-MB-231
ns
ns
LUMINESCENCE (A.U.)
1.0×10⁶
8.0×10⁵
6.0×10⁵
4.0×10⁵
2.0×10⁵
0
siRLUC
siMARCH5
siMCL-1
siMARCH5/siMCL-1

d

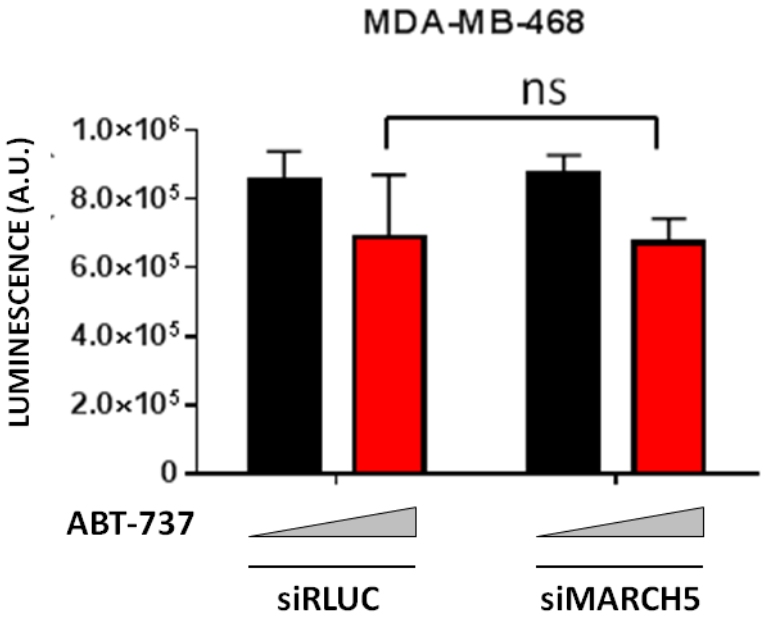
MDA-MB-468
ns
LUMINESCENCE (A.U.)
1.0×10⁶
8.0×10⁵
6.0×10⁵
4.0×10⁵
2.0×10⁵
0
ABT-737
siRLUC
siMARCH5

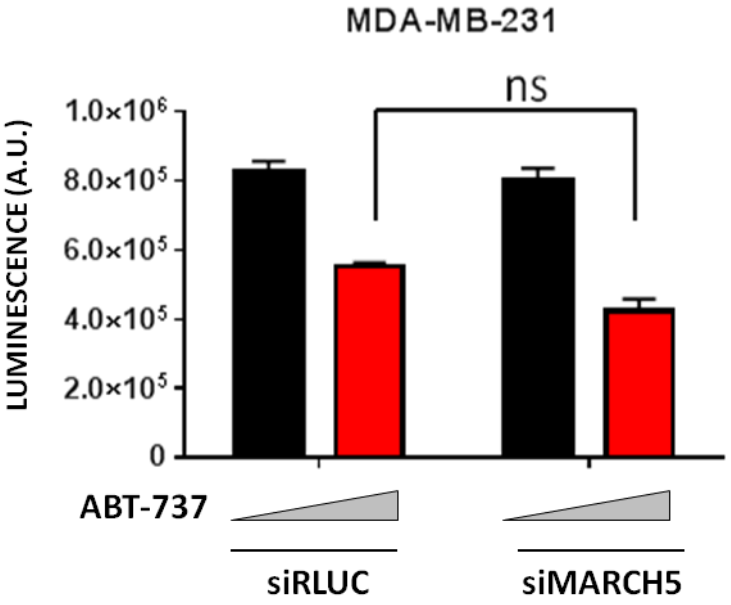
MDA-MB-231
ns
LUMINESCENCE (A.U.)
1.0×10⁶
8.0×10⁵
6.0×10⁵
4.0×10⁵
2.0×10⁵
0
ABT-737
siRLUC
siMARCH5

e

MDA-MB-231

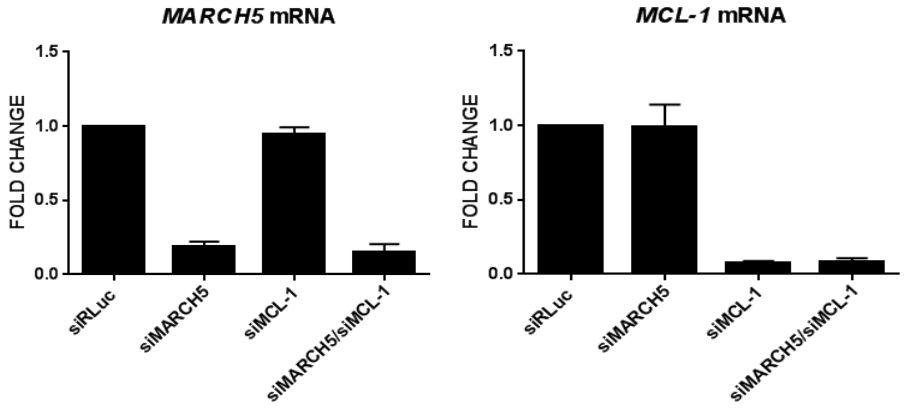

MDA-MB-468

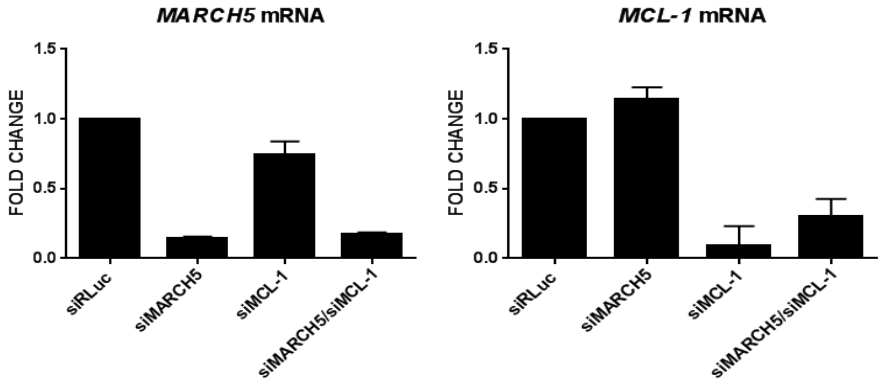

Figure 3.15. Concomitant loss of MARCH5 and MCL1 is synthetic lethal in MCL1 driven breast cancer lines.

(a) HCT116, MDA-MB-231 and MDA-MB-468 were treated with the MCL1-specific inhibitor, A1210477 at the indicated concentrations. Cell viability was measured using CellTiter-Glo. Error bars represent the SD from triplicate measurements.

(b) HCT116 cells were depleted of MARCH5 or MCL1 or co-depleted of MARCH5 and MCL1. Cell viability was measured using CellTiter-Glo. Error bars represent the SD of triplicate experiments. Ns represents no significant difference.

(c) MDA-MB-231 and MDA-MB-468 cells were depleted of MARCH5 or MCL1 or co-depleted of MARCH5 and MCL1. Cell viability was measured using CellTiter-Glo. Error bars represent the SD of triplicate experiments. The asterisks (**) and (***) indicate p values of <0.01 and <0.001 respectively compared to respective controls using Student's t-test. No significant difference is represented by ns.

(d) MDA-MB-231 and MDA-MB-468 cells were transfected with control siRNA or siRNA targeting MARCH5 and treated with ABT-737 (Black bar: DMSO, red: 5 μM, grey: 10 μM). Cell viability was assessed using CellTiter-Glo. Error bars represent the SD of triplicate experiments. No significant difference compared to respective controls is represented as 'ns' and was derived by using Student's t-test.

(e) Validation of knockdown was performed by quantitative RT-PCR and mRNA levels were normalized to *18S* mRNA.

Sensitization to ABT-737 upon MARCH5 loss is similar to that achieved with a direct chemical inhibitor of MCL1

During the course of this study, breakthroughs in the design of MCL1-specific inhibitors have been made. One specific compound, A1210477 has shown great promise in targeting MCL1-dependent tumors as a single agent or in combination with ABT-263 (Navitoclax) in other cell lines[157]. Since we observed similar effects upon loss of MARCH5, we wanted to compare the effect of MCL1 functional inhibition achieved by MARCH5 loss with that obtained using a direct chemical inhibitor of MCL1.

In line with this, (Fig. 3.15a) shows that treatment with A1210477 alone induced death in MCL1-dependent breast cancer cell lines but not in HCT116 cells, which are not dependent on MCL1. Combined treatment with high doses of ABT-737 and A1210477

induced cell death in HCT116 cells (Fig. 3.16a). This, however, was no more effective than a combination of ABT-737 and MARCH5 depletion (Fig. 3.16b). Therefore, the functional inhibition of MCL1 achieved by depleting MARCH5 is sufficient to induce the same response as through direct targeting of MCL1.

a

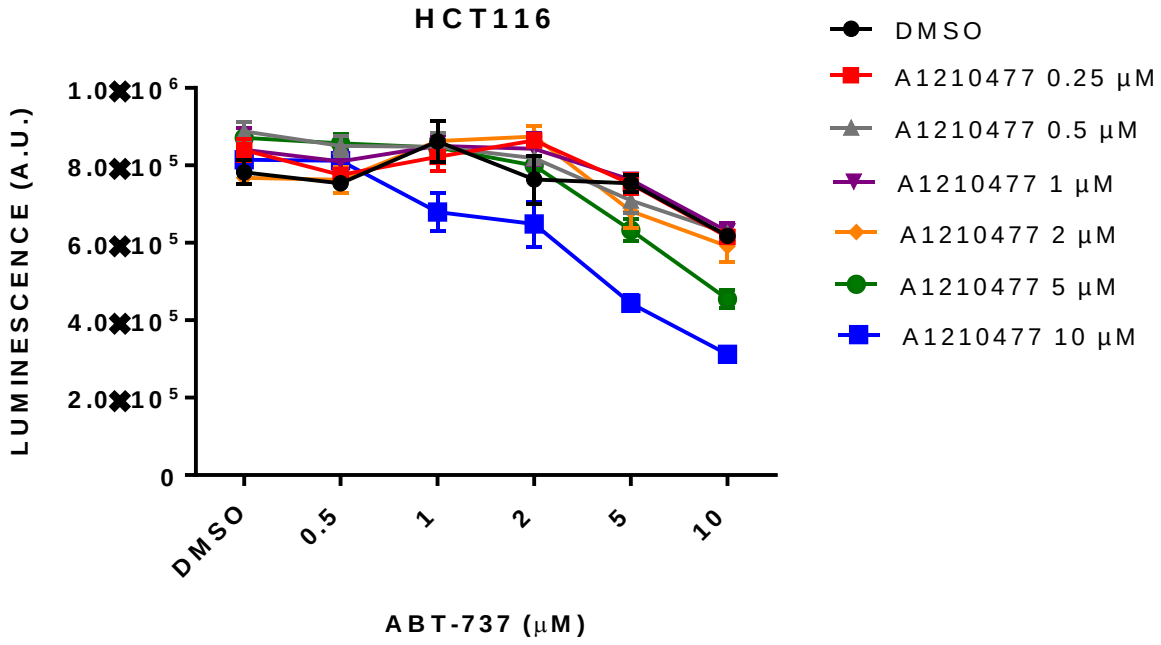

b

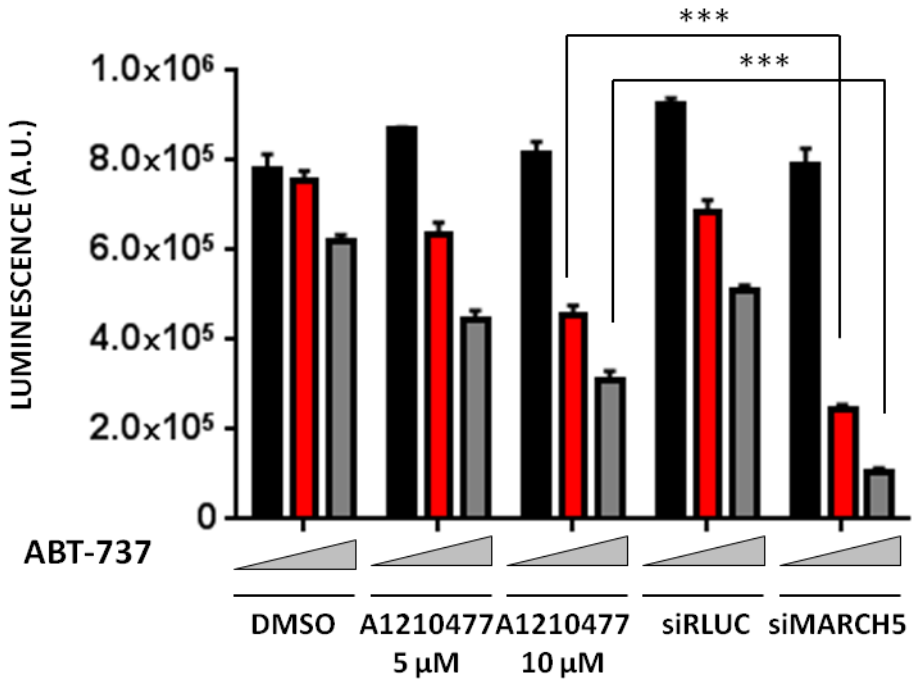

Figure 3.16. MARCH5-dependent sensitization to ABT-737 is comparable to combined treatment with ABT-737 and A1210477

(a) HCT116 cells were treated with ABT-737 and A1210477 either alone or in combination at the indicated concentrations. Cell viability was measured using CellTiter-Glo. Error bars represent the SD of triplicate measurements.

(b) HCT116 cells were transfected with control siRNA or siRNA targeting MARCH5 and treated with ABT-737 (Black bar: DMSO, red: 5 µM, grey: 10 µM) or treated with a combination of ABT-737 and A1210477. Cell viability was measured using CellTiter-Glo. Error bars represent the SD of triplicate measurements. The asterisks (***) indicate p values of < 0.001 compared to combination treatment of ABT-737 and A1210477 using Student's t-test.

MARCH5 contributes to a gene signature associated with ABT-263 sensitivity

Several factors in addition to MCL1 are associated with sensitivity to BH3 mimetics[158,156]. A strong prediction from the biological data in this study is that MARCH5 expression may also contribute to the response to ABT-737.

Using a publicly available dataset, multiple linear regression analyses were performed in order to determine whether expression of *MARCH5* mRNA (alone or in combination with selected other factors) was predictive of ABT-737 sensitivity. Together with MARCH5, other proteins such as BAX and BAK (since they are terminal effectors of the response to ABT-737), NOXA and BCL2L1/BCLXL (based on our current data), BCL2L11/BIM (as it is implicated in the response to ABT-737), and MCL1 (a well-documented determinant of sensitivity to ABT-737) were selected. HUWE1, an MCL1 ubiquitin ligase that can accelerate BH3-dependent apoptosis was also selected[32]. The stratification of the groups based on p53 status was also performed, since p53 can contribute to BH3 mimetic-induced death.

Fig. 3.17a shows the results of an optimized multiple linear regression model. Consistent with their known influence on ABT-737 sensitivity, expression of BAX, HUWE1, and NOXA were significant contributors to the gene signature in cells expressing either wild type or nonfunctional p53 (this latter group includes both p53 mutations and deletions).

Interestingly, MCL1 expression was a strong determinant of the ABT-737 sensitivity of cells expressing mutant p53. By contrast, the effect of MCL1 in cells with wild type p53 was much weaker. This underscores the finding that the level of MCL1 expression alone is not always sufficient to predict ABT-737 sensitivity , and also suggests that other p53-induced factors can to some extent attenuate the anti-apoptotic function of MCL1[159].

Although the biological data in this study show that MARCH5 is a clear modulator of the ABT-737 response, its expression was not identified as a significant determinant of sensitivity in the multiple regression analysis. However, since the analysis was performed on a large cohort of cell lines from diverse tumor types, it was reasoned that re-analysis based on tissue of origin might provide further insight. Therefore, data from all wild type p53 cell lines was compared to the data from the hematological malignancies (blood) subset.

This choice was based on evidence from both cell-based and preclinical animal models that individuals with liquid tumors comprise a suitable target population for BH3 mimetic treatment. As expected, the pro-apoptotic effectors BAX and BAK were associated with increased ABT-737 sensitivity in these malignancies (Fig. 3.17b). Strikingly, both MARCH5 and MCL1 were significantly associated with the ABT-737 sensitivity of the blood subset (Fig. 3.17b). Fig. 3.17c is a graphical representation of the contribution of these four genes to ABT-737 sensitivity, clearly indicating that MARCH5 and MCL1 expression were inversely correlated with ABT-737 sensitivity, whereas BAX and BAK were associated with increased sensitivity. Together with the experimental data, this analysis suggests that MARCH5 is a context-dependent modulator of the sensitivity to BH3 mimetics.

Intriguingly, the optimized model also identified pairwise combinations among these genes that contribute to sensitivity. For example, co-regulation of MARCH5/NOXA and MARCH5/BAX were significant factors that may contribute to the BH3 mimetics response (refer to Appendix I).

a

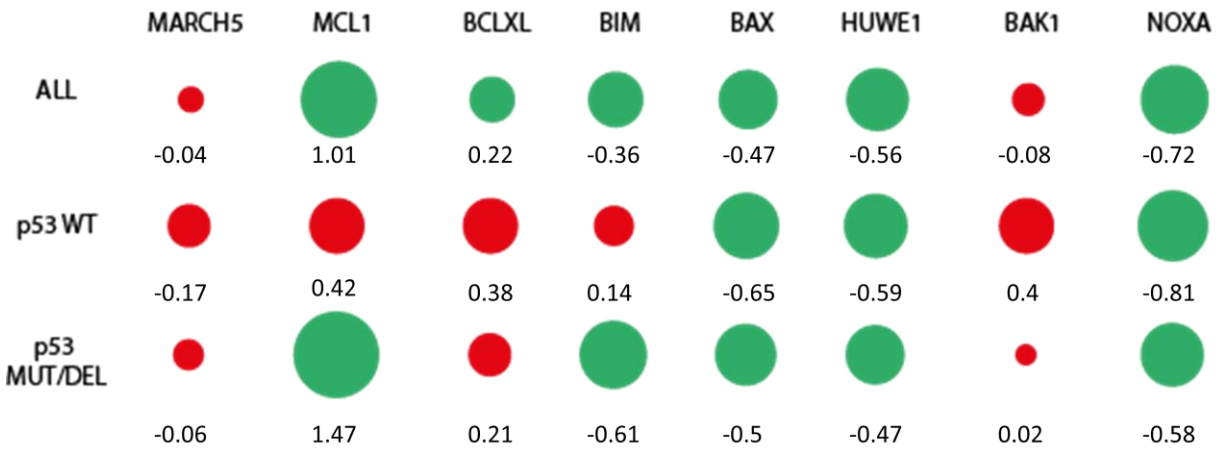
MARCH5
MCL1
BCLXL
BIM
BAX
HUWE1
BAK1
NOXA
ALL
-0.04
1.01
0.22
-0.36
-0.47
-0.56
-0.08
-0.72
p53 WT
-0.17
0.42
0.38
0.14
-0.65
-0.59
0.4
-0.81
p53 MUT/DEL
-0.06
1.47
0.21
-0.61
-0.5
-0.47
0.02
-0.58

b

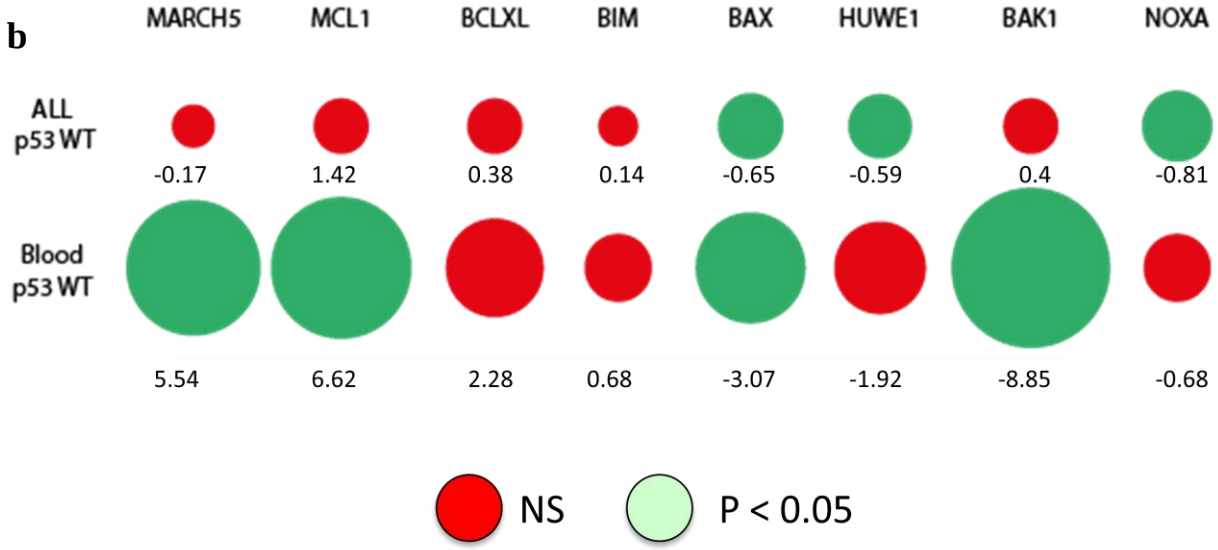
MARCH5
MCL1
BCLXL
BIM
BAX
HUWE1
BAK1
NOXA
ALL p53 WT
-0.17
1.42
0.38
0.14
-0.65
-0.59
0.4
-0.81
Blood p53 WT
5.54
6.62
2.28
0.68
-3.07
-1.92
-8.85
-0.68
NS
P < 0.05

c

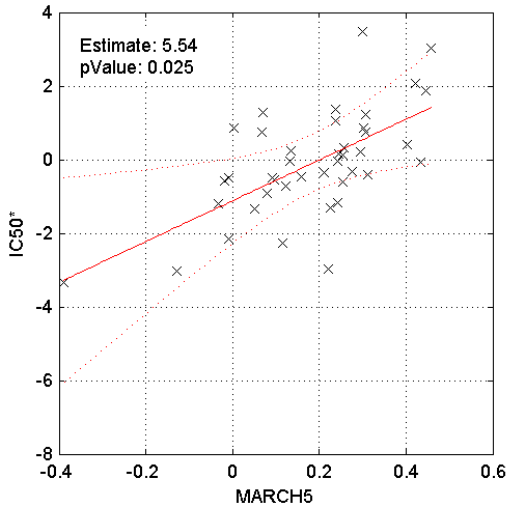
Estimate: 5.54
pValue: 0.025
IC50*
MARCH5

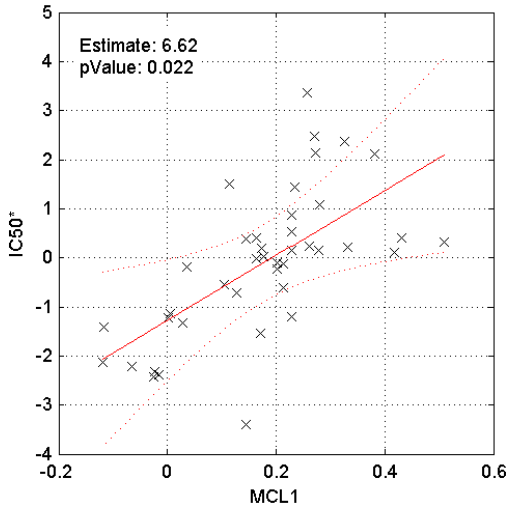
Estimate: 6.62
pValue: 0.022
IC50*
MCL1

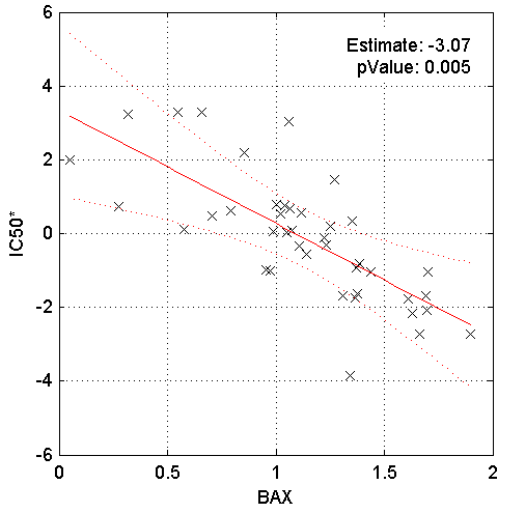
Estimate: -3.07
pValue: 0.005
IC50*
BAX

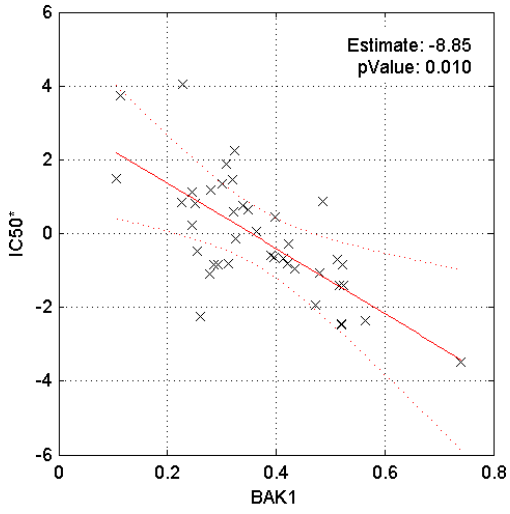
Estimate: -8.85
pValue: 0.010
IC50*
BAK1

Figure 3.17. Expression of MARCH5 and MCL1 are significant contributors to a gene signature predicting sensitivity to navitoclax

(a) Contribution of each gene to the multiple linear regression analysis of an 8-gene expression profile and navitoclax sensitivity across a panel of 648 cell lines (221 wild type p53, 427 non-functional p53). Green circles $p < 0.05$; Red circles, ns. The size of the circle is proportional to the effect size and the estimated effect size is enumerated below the circles. For example, MCL1 expression had the greatest influence on navitoclax sensitivity in the p53 MUT/DEL cell lines, whereas its effect was smaller and not significant in p53 WT cell lines.

(b) Comparison of the contribution of each gene to the sensitivity profiles of all tumor lines with wild type p53 versus the 'blood only' subset. Green circles $p < 0.05$; Red circles, ns. The size of the circle is proportional to the effect size.

(c) Relationship between navitoclax sensitivity and expression of the four genes that significantly contribute to the sensitivity profile of the 'Blood p53 WT' subset (corresponding to green circles in panel B). Each datapoint represents one cell line. Values on the y-axis ($IC50^{*}$) are regression-adjusted IC50 values. Values on the x-axis are regression-adjusted mRNA expression levels. Estimate values are derived from slope of the regression line and reflect the effect size.

(II) MARCH5 REGULATES MITOCHONDRIAL MORPHOLOGY

Loss of MARCH5 promotes accumulation of perinuclear mitochondria

MARCH5 has been previously identified as a regulator of mitochondrial dynamics through the modulation of the levels or activity of the pro-fusion GTPases, MFN1/2 and the pro-fission DRP1 GTPase[134,137,139,160]. Changes in mitochondrial morphology also dictate the response to chemotherapeutics[161]. Thus, we wanted to assess if changes in mitochondrial morphology due to loss of MARCH5 might contribute to the results described above (i.e., namely MCL1 stabilization and sensitization to apoptosis).

In order to assess whether MARCH5 loss led to changes in mitochondrial morphology, U2OS cells were depleted of MARCH5 and mitochondria were stained with an antibody against TOMM20, a marker of the mitochondrial outer membrane. The loss of MARCH5 led to the collapse of the mitochondrial network and accumulation of perinuclear mitochondria (Fig. 3.18a). These changes in morphology were quantified by segmenting for cell possessing perinuclear mitochondria; samples depleted of MARCH5 showed a significantly higher percentage of cells possessing perinuclear mitochondria as compared to control (Fig. 3.18b).

The collapse of the mitochondrial network and accumulation of perinuclear mitochondria has been associated with the presence of damaged and dysfunctional mitochondria that have reduced or altered mitochondrial membrane potential[162]. In order to assess whether MARCH5 loss led to reduction in mitochondrial membrane potential, cells depleted of MARCH5 were stained with the mitochondrial dye, TMRE. Depolarized or inactive mitochondria have decreased membrane potential and fail to sequester TMRE. Cells

transfected with siMARCH5 displayed lower levels of TMRE accumulation compared to RLUC controls suggesting that MARCH5 depletion leads to loss of mitochondrial membrane potential (Fig. 3.18c).

Increased production of ROS and disrupted calcium homeostasis often accompany alterations in mitochondrial membrane potential. This in turn has important implications in stress-related signaling pathways including apoptosis[163]. Therefore the loss of mitochondrial membrane potential upon MARCH5 depletion could induce a cellular stress response that "primes" cells to undergo apoptosis.

a

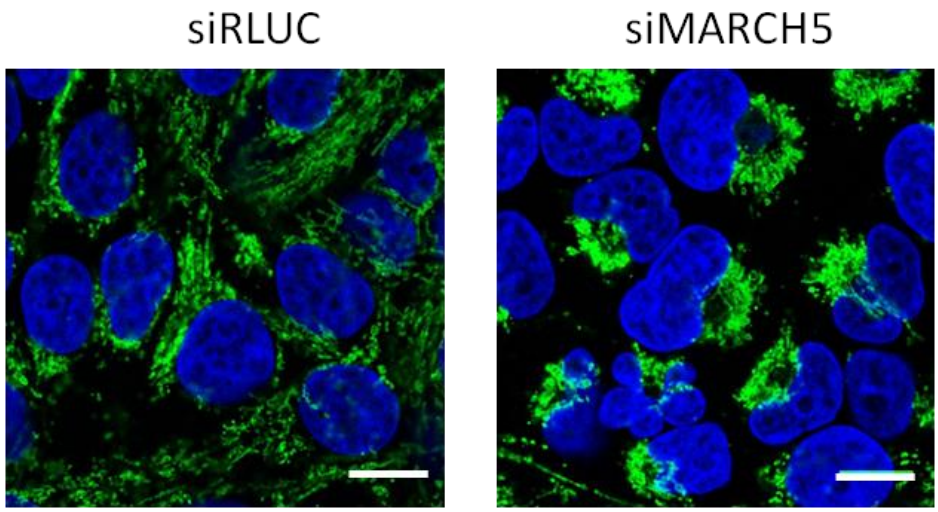

b

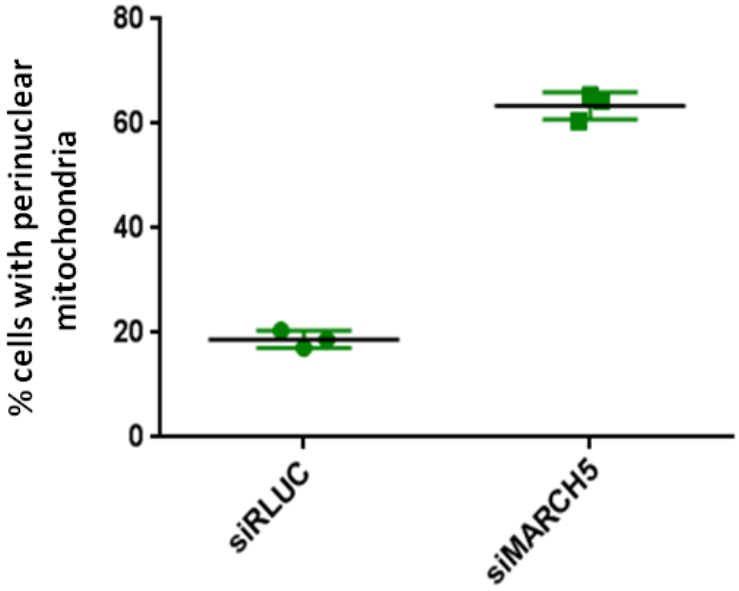
% cells with perinuclear mitochondria
80
60
40
20
0
siRLUC
siMARCH5

c

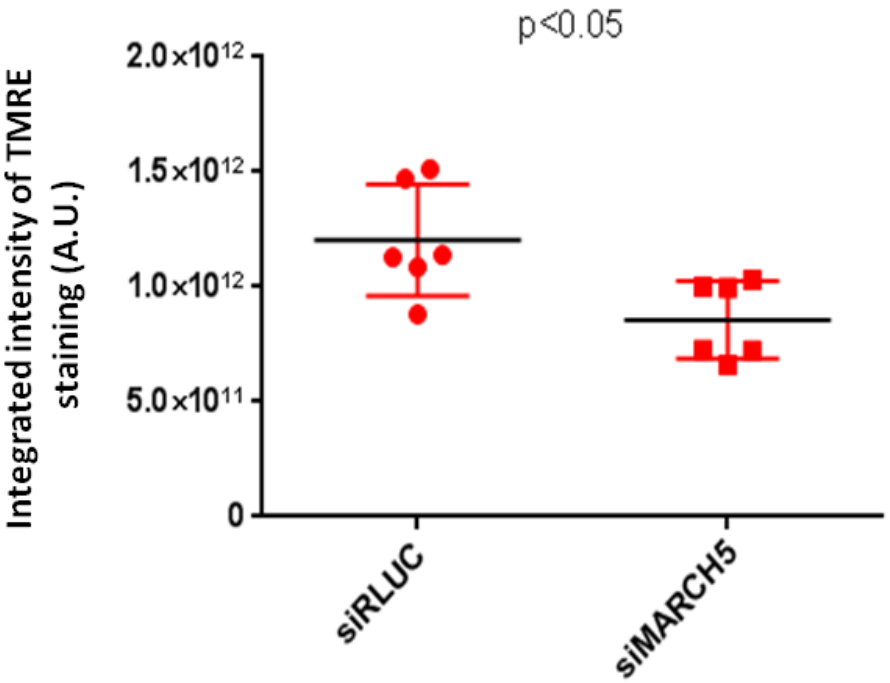
p<0.05
Integrated intensity of TMRE staining (A.U.)
2.0×10^12
1.5×10^12
1.0×10^12
5.0×10^11
0
siRLUC
siMARCH5

Figure 3.18. Loss of MARCH5 promotes accumulation of perinuclear mitochondria and loss of mitochondrial membrane potential

(a) U2OS cells were plated on coverslips and transfected with siRLUC or siMARCH5 for 72 h. Cells were then fixed in 4% paraformaldehyde and immunostained with anti-TOMM20 to stain mitochondria and DAPI for nuclear staining. Scale bars represent 10 μm.

(b) U2OS were plated on 96-well plates following transfection with siRLUC or siMARCH5. Cells were then fixed in 4% paraformaldehyde and immunostained with anti-TOMM20 to stain mitochondria and DAPI for nuclear staining. Segmentation was performed for both nuclei and perinuclear mitochondria. Number of cells scored per well >300 for triplicate wells per condition.

(c) U2OS cells were plated on 96-well plates following transfection with siRLUC or siMARCH5 and stained with TMRE. Nuclei were stained with Hoechst and live cell imaging was performed. Nuclear and cytoplasmic regions were defined during image segmentation and TMRE intensity was quantified. Number of cells scored per well >300 for six wells per condition.

MARCH5 mutants alter mitochondrial morphology

Given the importance of MARCH5 in the regulation of mitochondrial morphology, it was predicted that mutations in critical functional residues of MARCH5 could contribute to altered mitochondrial morphology. To this end, a panel of MARCH5 mutants were generated through site-directed mutagenesis. These mutants included two RING domain mutants- MARCH5^{H43W} and MARCH5^{CS} (Fig. 3.19a), and three ligase-defective constructs with mutations on hydrophobic patch residues suggested to be critical for E2 enzyme binding (MARCH5^{V16A}, MARCH5^{V51A}, and MARCH5^{P66A}) (Fig. 3.19a). In addition, a

survey of the COSMIC database revealed a number of somatic mutations associated with several solid tumors. Of note, the D202 residue (which is located within a cytoplasmic-facing loop) was mutated in independent patient samples, suggesting it may have functional relevance (ref). Thus, we generated MARCH5^{D202Y} and MARCH5^{D202G} mutants in order to understand their contribution to mitochondrial morphology.

As seen in Fig. 3.19b, the expression of all MARCH5 mutants except MARCH5^{V51A} elicited dramatic changes in mitochondrial morphology. Specifically, these mutants engendered high levels of fused mitochondria as compared to expression of MARCH5^{WT} (Fig. 3.19b). Although the mutant forms of MARCH5 predominantly localized to the mitochondrial outer membrane as seen by co-localization with TOMM20, some submitochondrial species were observed. This is consistent with prior studies reported by Karbowski and colleagues (2007)[134]. This in part could be explained by the increased stability of the mutants compared to MARCH5^{WT} and formation of higher order oligomers, which are indicative of defective turnover of the mutant proteins (Fig. 3.19c).

a

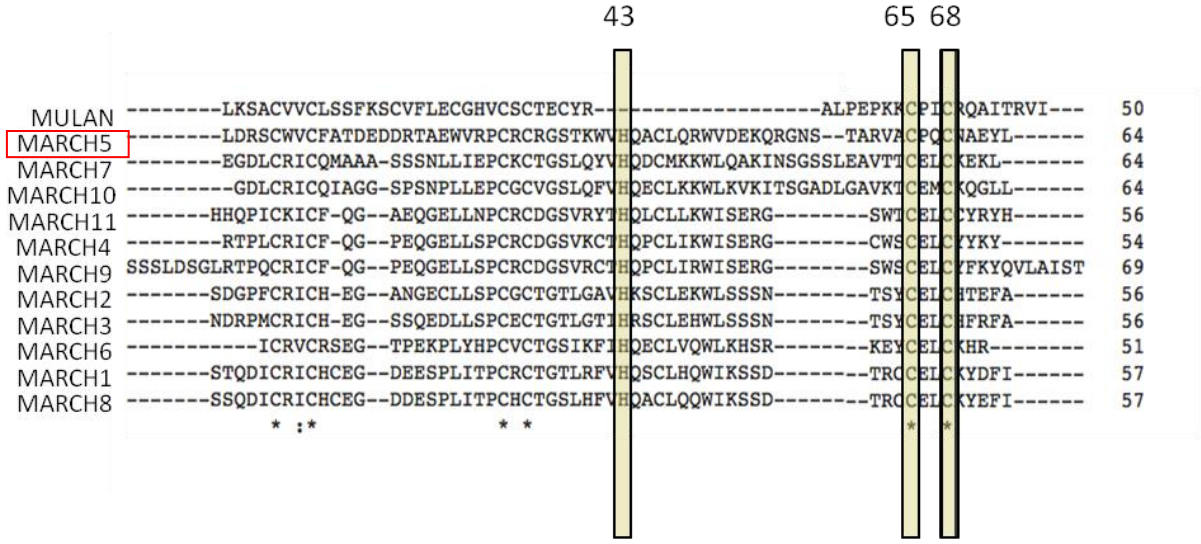

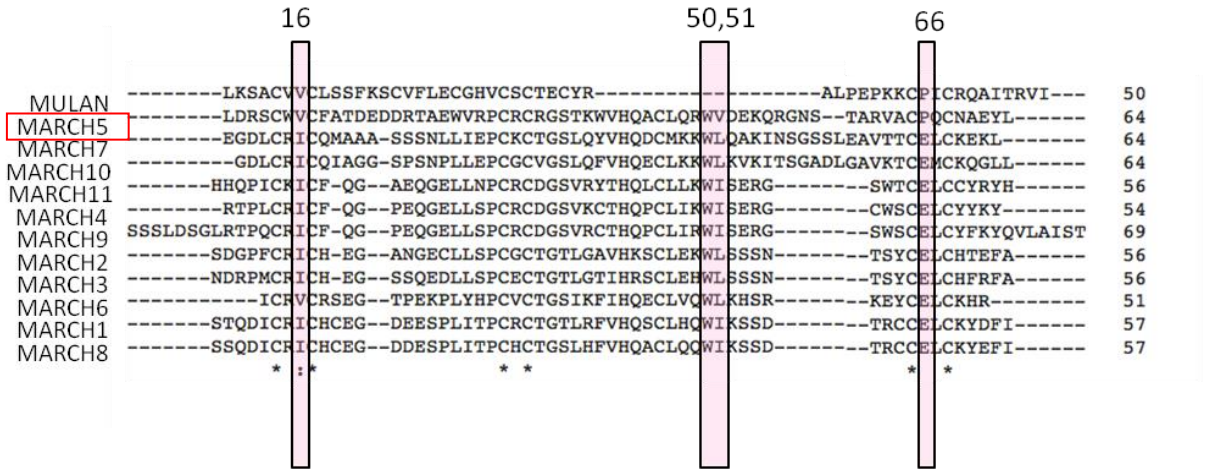
16
50,51
66
MULAN --------LKSACVVCLSSFKSCVFLECGHVCSCTECYR----------ALPEPKKCPICRQAITRVI--- 50
MARCH5 --------LDRSCWVCFATDEDDRTAEWVRPCRCRGSTKWVHQACLQRWVDEKQRGNS--TARVACPQCNAEYL------ 64
MARCH7 --------EGDLCRICQMAAA-SSSNLLIEPCKCTGSLQYVHQDCMKKWLQAKINSGSSLEAVTTCELCKEKL------- 64
MARCH10 ---------GDLCRICQIAGG-SPSNPLLEPCGCVGSLQFVHQECLKKWLKVKITSGADLGAVKTCEMCKQGLL------ 64
MARCH11 -------HHQPICRICF-QG--AEQGELLNPCRCDGSVRYTHQLCLLKWISERG--------SWTCELCCYRYH------ 56
MARCH4 --------RTPLCRICF-QG--PEQGELLSPCRCDGSVKCTHQPCLIKWISERG--------CWSCELCYYKY------- 54
MARCH9 SSSLDSGLRTPQCRICF-QG--PEQGELLSPCRCDGSVRCTHQPCLIRWISERG--------SWSCELCYFKYQVLAIST 69
MARCH2 -------SDGPFCRICH-EG--ANGECLLSPCGCTGTLGAVHKSCLEKWLSSSN--------TSYCELCHTEFA------ 56
MARCH3 -------NDRPMCRICH-EG--SSQEDLLSPCECTGTLGTIHRSCLEHWLSSSN--------TSYCELCHFRFA------ 56
MARCH6 -----------ICRVCRSEG--TPEKPLYHPCVCTGSIKFIHQECLVQWLKHSR--------KEYCELCKHR-------- 51
MARCH1 -------STQDICRICHCEG--DEESPLITPCRCTGTLRFVHQSCLHQWIKSSD--------TRCCELCKYDFI------ 57
MARCH8 -------SSQDICRICHCEG--DDESPLITPCHCTGSLHFVHQACLQQWIKSSD--------TRCCELCKYEFI------ 57

b

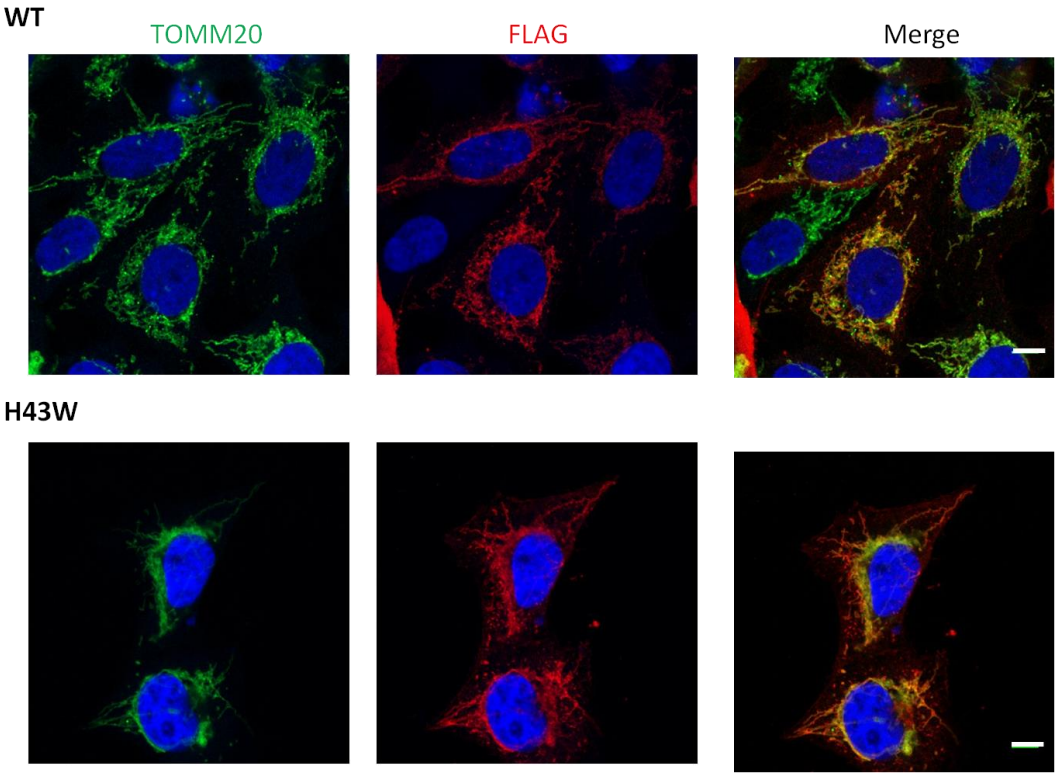
WT
TOMM20
FLAG
Merge
H43W

C65SC68S

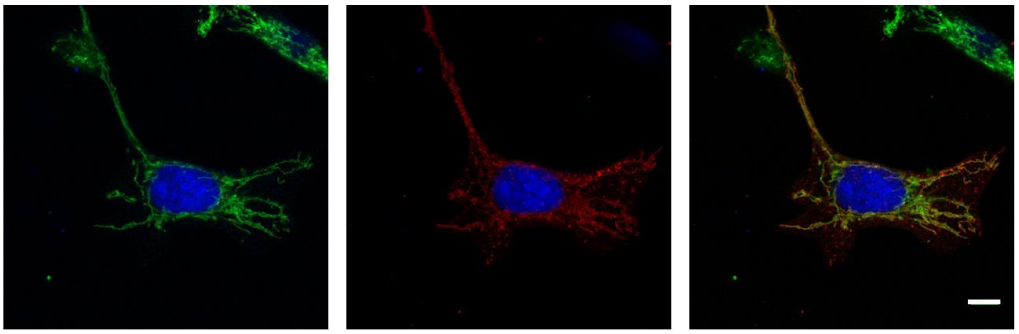

V16A

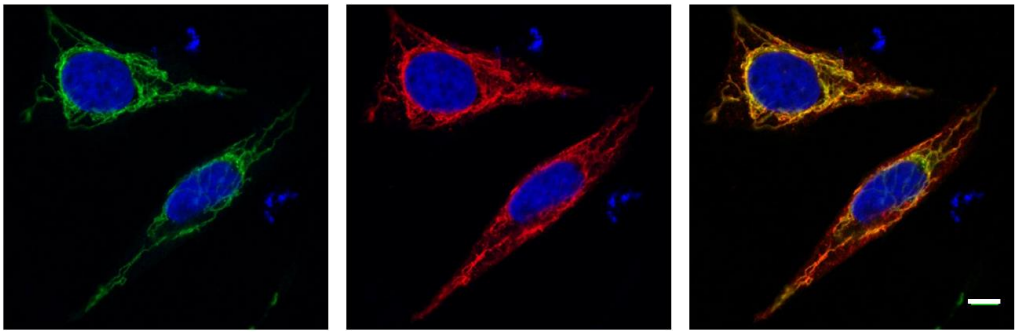

V51A

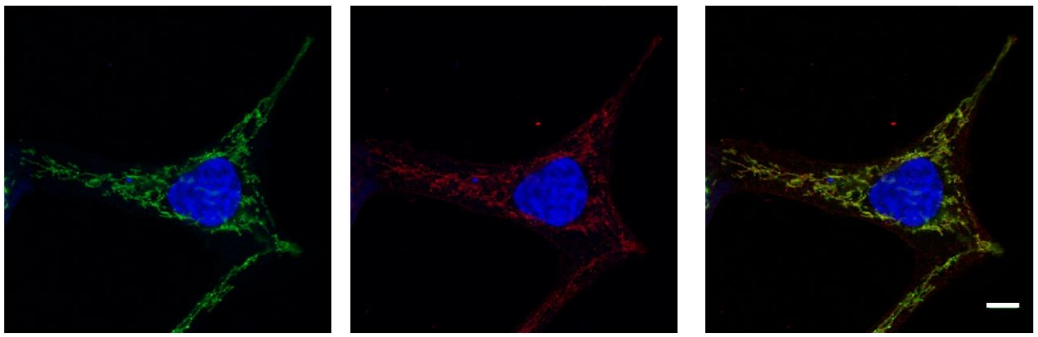

P66A

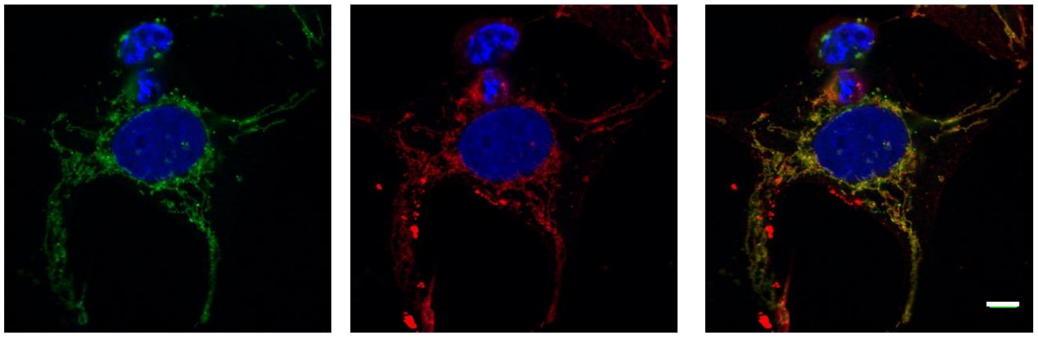

D202G

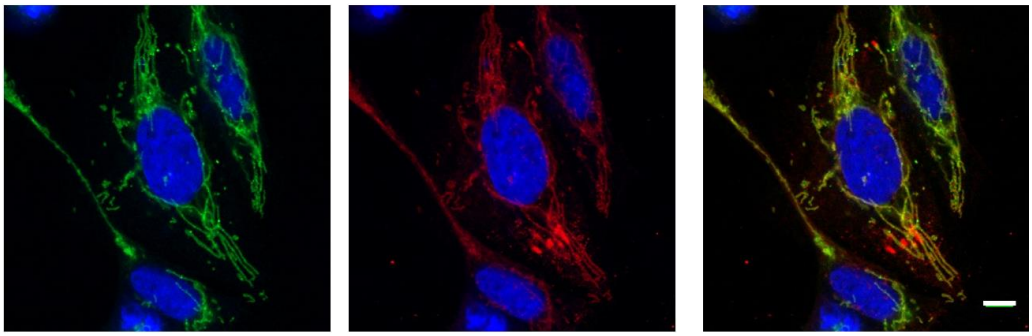

D202Y

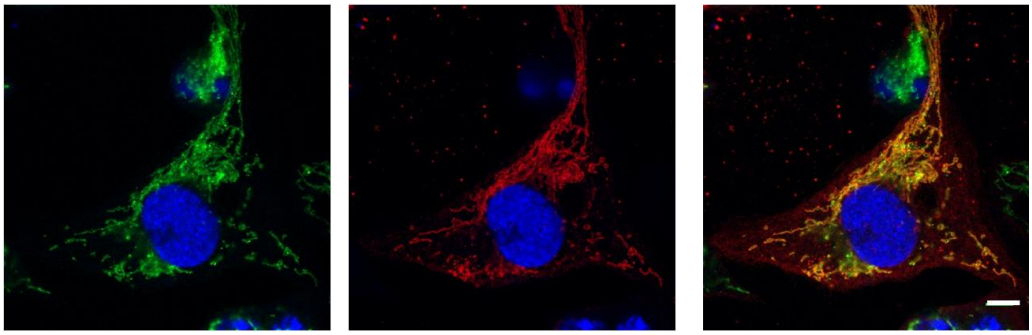

C

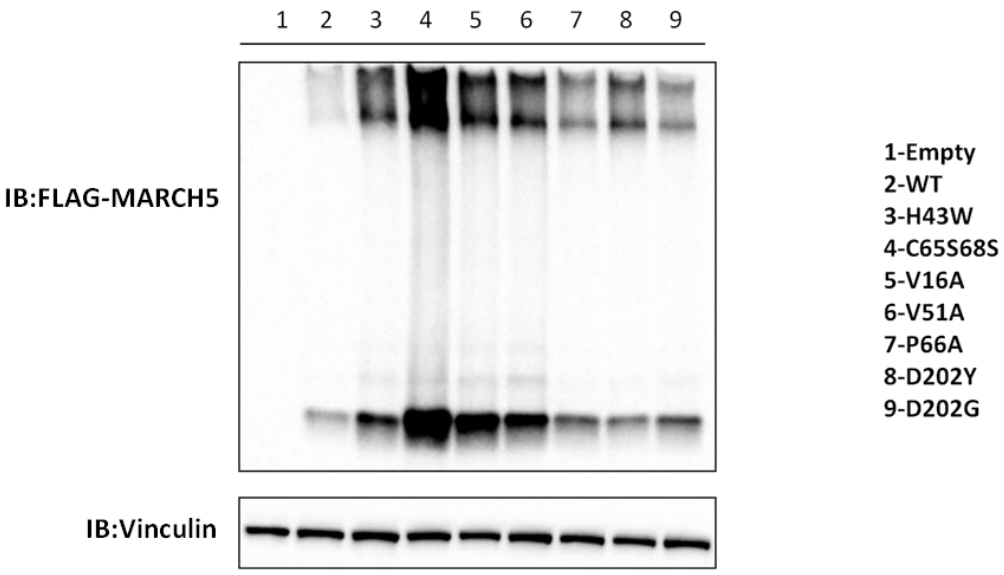

Figure 3.19. MARCH5 mutants alter mitochondrial morphology

(a) Schematic representation of conserved functional residues in MARCH5

(b) U2OS cells were plated on coated coverslips and transfected with the indicated FLAG-MARCH5 constructs for 48 h. Cells were then fixed in 4% paraformaldehyde and immunostained with anti-TOMM20 to stain mitochondria, anti-FLAG to stain MARCH5 and DAPI for nuclear staining. Scale bars represent 20 μm.

(c) Whole cell lysates from U2OS cells transfected with the indicated constructs were subjected to SDS-PAGE and immunoblotted with the indicated antibodies.

MCL1 stabilization occurs independently of changes in mitochondrial morphology

We observed two different phenomena upon the loss of MARCH5. This included the stabilization of MCL1 and the accumulation of perinuclear mitochondria. In order to assess if the changes in mitochondrial morphology were related to the stabilization of MCL1, U2OS cells were treated with two compounds that induce identical perinuclear morphology to that observed in the absence of MARCH5. Treatment with CCCP (an uncoupler of oxidative phosphorylation)[164] and mdivi-1 (a DRP1 inhibitor)[91] did not affect MCL-1 levels despite inducing changes in mitochondrial morphology (Fig. 3.20).

Together with our BH3 profiling results, these data indicate that MCL1 stabilization upon MARCH5 knockdown is mediated via regulation of NOXA, rather than by changes in mitochondrial morphology *per se*.

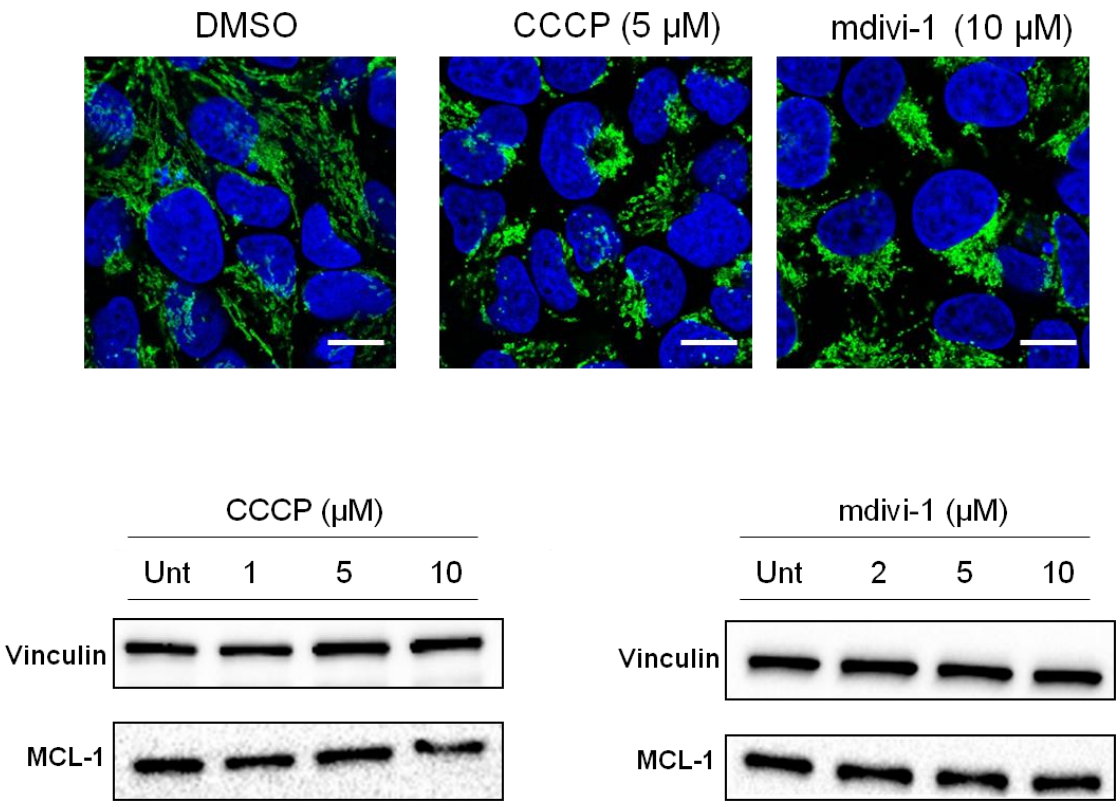

Figure 3.20. **MCL1 stabilization occurs independent of changes in mitochondrial morphology**

(a) U2OS cells were plated on coverslips and transfected with the siRLuc, siMARCH5 for 72 h or treated with CCCP (5 μM) for 4 h and mdivi-1 (10 μM) for 48 h. Cells were then fixed in 4% paraformaldehyde and immunostained with anti-TOMM20 to stain mitochondria and DAPI for nuclear staining. Scale bars represent 10 μm.

(b) Whole cell lysates from U2OS cells treated with CCCP and mdivi-1 at the indicated concentrations were subjected to SDS-PAGE and immunoblotted with the indicated antibodies.

CHAPTER 4. DISCUSSION

Summary: Mitochondrial ubiquitin ligases and regulation of apoptosis

At least four RING E3 ligases (MULAN, RNF144B, TRIM59, and MARCH5) are constitutively localized to the mitochondrial outer membrane. MULAN is a regulator of mitochondrial morphology. In addition, during stress-induced mitochondrial hyperfusion, MULAN ubiquitinates TRAF2 to activate NF-κB signaling, possibly enabling cell survival under stress conditions[127,165]. In contrast, MULAN is also a negative regulator of AKT and suppresses its signaling by targeting phosphorylated AKT for degradation[166]. These opposing functions of MULAN may signify specific roles in different cellular contexts. RNF144B is a critical regulator of epithelial homeostasis and its over-expression reduced the stability of pro-apoptotic BAX, thus protecting cells from undergoing apoptosis[124]. TRIM59 can negatively regulate p53, and is upregulated in gastric tumours, suggesting that it may facilitate tumorigenesis[167].

Here, we demonstrate that MARCH5 is a regulator of sensitivity to the BH3-mimetic ABT-737, and that this occurs via NOXA-dependent functional inactivation of MCL1. This is, to the best of our knowledge, the first report of direct regulation of the NOXA/MCL1 axis by a mitochondrial ligase. Furthermore, it is the first clear demonstration that a member of the MARCH family can regulate intrinsic apoptosis. Our results provide a conceptual framework for follow-on studies to identify additional targets of mitochondrial ligases that may be involved in tumorigenesis or drug resistance. Below, the key results of this study are discussed in a wider context.

(i) MARCH5 and BCL-2 family-mediated apoptosis

MARCH5 specifically and selectively interacts with members of the BCL-2 family of proteins, and these interactions determine the sensitivity to BH3 mimetics. Mechanistically, a NOXA/MCL1 axis is activated upon MARCH5 loss, and NOXA is required for both MARCH5-dependent stabilization of MCL1 as well as the enhanced BH3-dependent apoptosis. Notably, BIM and PUMA were dispensable for this response. Both these proteins are capable of binding and functionally inhibiting MCL1[153,44,168]; however, the MARCH5-dependent regulation of MCL1 specifically requires NOXA.

The co-stabilization of NOXA and MCL1 following MARCH5 depletion appears paradoxical, as sensitization to ABT-737 has been associated with the NOXA-dependent degradation of MCL1. However, it is possible that following the loss of MARCH5, the increase in MCL1 levels serves as a protective mechanism that guards against apoptosis that would be otherwise induced by NOXA upregulation. This concomitant upregulation could provide a "decision" point for entry into apoptosis, which can be triggered by a shift in the stoichiometry of NOXA levels over MCL1 or by activation of additional pro-apoptotic BH3 proteins by compounds such as ABT-737.

In support of this concept, camptothecin (CPT) treatment of cancer cells leads to upregulation of both MCL1 and NOXA, yet the propensity to undergo apoptosis depends on the precise ratio between NOXA and MCL1 levels[169]. This phenomenon was also observed in small cell lung cancers where the NOXA/MCL1 axis was a critical determinant of ABT-737 sensitivity[170]. Furthermore, despite concomitant upregulation of NOXA and MCL1, squamous cell carcinomas retain sensitivity to ABT-737, since treatment with the drug increases the NOXA:MCL1 ratio[171].

NOXA is a critical regulator of MCL1 stability at the mitochondrial outer membrane, and the formation of a NOXA-MCL1 complex is reportedly essential for the initiation of

proteasome-dependent MCL1 degradation and apoptosis[44,168]. However, in this study, the enhanced stabilization of MCL1 upon MARCH5 loss was actually dependent on a concomitant increase in NOXA levels.

These data clearly indicate that the proposed model in which NOXA upregulation leads to MCL1 degradation does not always hold true. We infer that the binding of NOXA via its BH3 domain serves to functionally inhibit MCL1. In support of this, there are reports that MCL1 is also stabilized by small molecule antagonists that bind to the same region of MCL1 as NOXA[157].

Apart from the requirement for NOXA during MARCH5-dependent regulation of MCL1, we also observed that the depletion of NOXA alone can moderately stabilize MCL1. Interestingly, this was accompanied by a destabilization of MARCH5. This is reminiscent of our RNAi data, where the loss of MARCH5 led to stabilization of MCL1. It is therefore apparent that MCL1 stability is tightly controlled by the levels of MARCH5, and that NOXA is critical for this regulation. It is probable that these three proteins exist in a complex at the mitochondria and changes in levels of one of the proteins impacts the stability of the others. This represents a novel mechanism by which a mitochondrial protein interacts with two BCL-2 family members in order to regulate their stability and function.

We observed a decrease in MCL1 ubiquitination upon expression of a ligase-defective MARCH5, suggesting that MARCH5 may be an MCL1 ubiquitin ligase. However, direct proof of this will require *in vitro* ubiquitination assays. Furthermore, our results indicate that NOXA levels might also be controlled at a post-translational level by MARCH5, and thus NOXA might also be a MARCH5 substrate. Again, whether this is direct or indirect will require in vitro studies; interpretation of these studies is complicated by the fact that NOXA stability can be regulated in an ubiquitin-independent manner[46]. Our finding that

MCL1 stabilization requires a physical interaction between NOXA and MCL1 itself suggests that a NOXA/MCL1/MARCH5 termolecular complex is present at some stage during the ubiquitination of MCL1. However, the precise mechanism by which NOXA itself is regulated by MARCH5 as well as its importance in mediating the ubiquitination of MCL1 warrants further study.

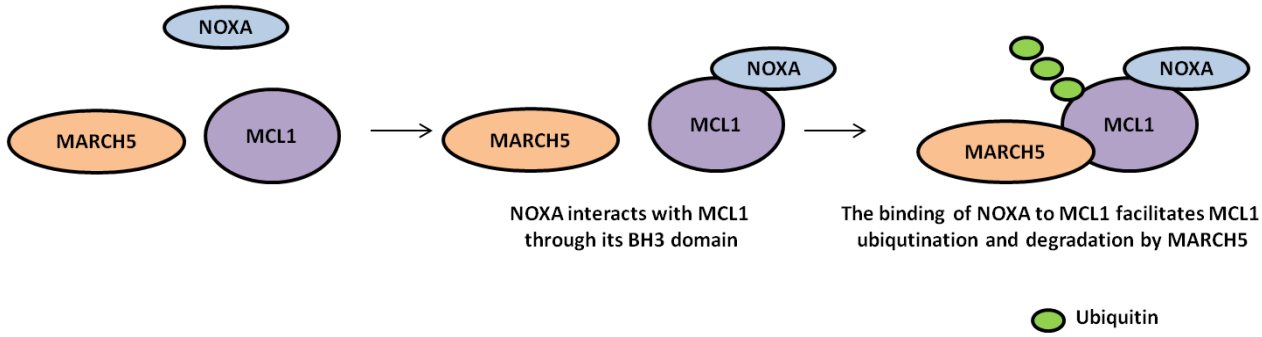

Figure 4.1. MARCH5, MCL1 and NOXA co-regulation

MARCH5 is the key regulator of a MCL1/NOXA complex through the ubiquitination of MCL1 in a NOXA-dependent manner.

The terminal effectors of ABT-737-induced apoptosis are BAX and BAK. Both proteins form oligomers on the mitochondrial outer membrane in response to diverse apoptotic stimuli, thereby triggering the release of apoptogenic factors from mitochondria[52].

Here, we found that sensitization to ABT-737 upon MARCH5 loss was dependent on BAX, but not BAK. The activity of BAX and BAK is held in check by the anti-apoptotic proteins BCL2, BCLXL, and MCL1 and this interaction is disrupted upon upregulation of pro-apoptotic PUMA, BIM and NOXA[26]. In this context, the MARCH5-dependent upregulation of NOXA could serve to disrupt MCL1-BAX/BAK interactions thereby

sensitizing to apoptosis; although BAK was dispensable for this response. This is consistent with prior studies demonstrating that BAK is dispensable for the response to ABT-737 in the HCT116 cell line[172].

Given our findings, we propose a model for the role of MARCH5 in regulation of BH3 protein-dependent apoptosis (Fig. 4.2). Under steady state conditions, MARCH5 is required to maintain an MCL1/NOXA ratio compatible with viability. This requires MARCH5 E3 ligase activity, and is NOXA-dependent. The loss of MARCH5 disrupts this balance and causes concomitant up-regulation of MCL1 and NOXA. However, MARCH5 depletion alone is not lethal in these cells. This could be attributed to the presence of the other anti-apoptotic proteins (i.e., BCL2 and BCLXL), which protect from apoptosis even when MCL1 is neutralized. The increase in NOXA serves to inhibit MCL1's anti-apoptotic activity, thereby allowing for the activation of BAX and sensitization to apoptosis upon administration of ABT-737 or other selective BH3 mimetics.

Whether the MARCH5/NOXA/MCL1 axis also modulates the sensitivity to other chemotherapeutics remains to be determined. The levels of NOXA and MCL1 are critical determinants of the sensitivity to DNA-damaging agents such as cisplatin in solid tumors[173]. It would be of interest to assess how the activation of the NOXA/MCL1 axis through the loss of MARCH5 could modulate the sensitivity to these chemotherapeutics.

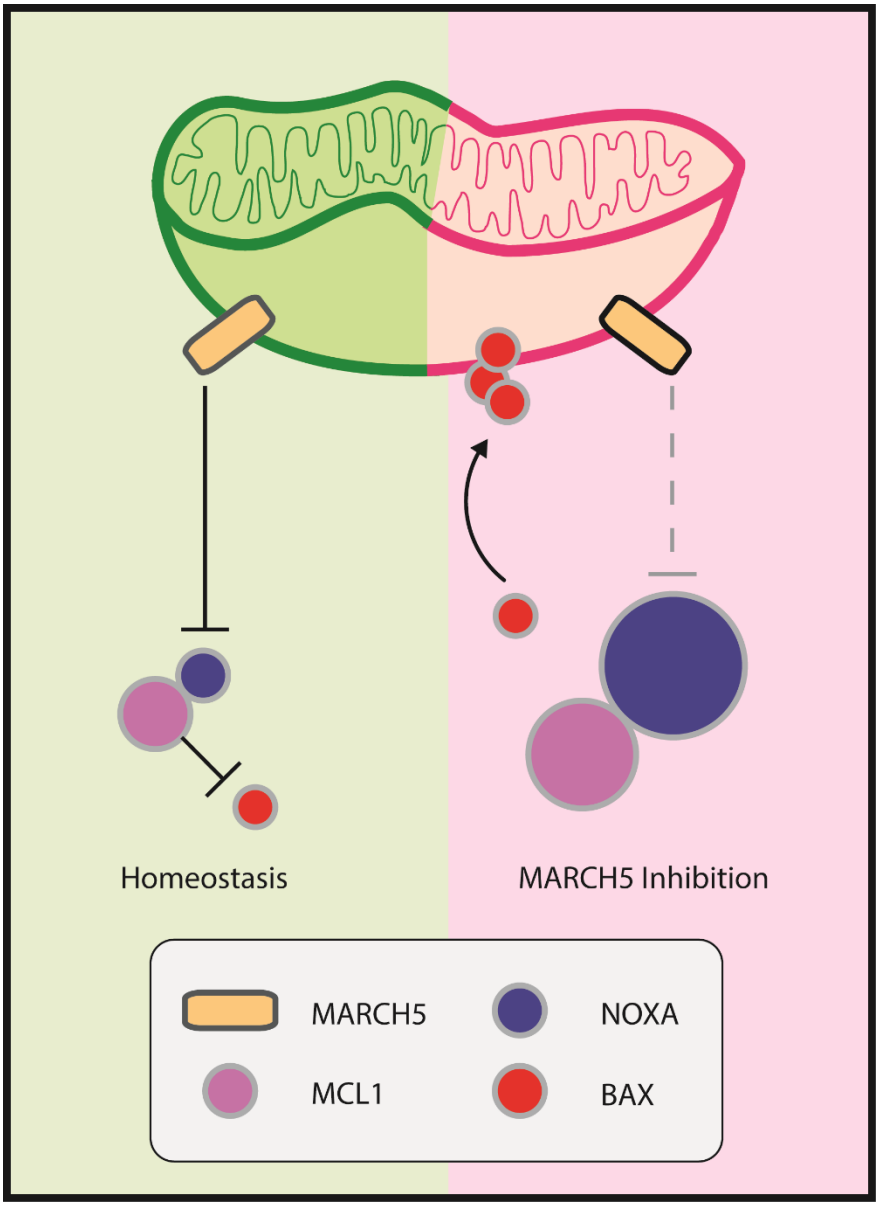

Figure 4.2. Proposed working model

MARCH5 is a key regulator of a MCL1/NOXA complex under steady-state conditions. The loss of MARCH5 leads to a co-stabilization of both NOXA and MCL1. The stoichiometric shift in levels of NOXA to MCL1 functionally inhibit MCL1, thereby freeing the downstream effector protein BAX to mediate apoptosis. This process cumulatively serves as a "priming" mechanism and additional stress stimuli are required to trigger cell death.

(ii) MARCH5 chemical and genetic synthetic lethality

WEHI-539, a BCLXL-selective inhibitor, had no effect on HCT116 cell viability when given as a single agent, but was synthetic lethal with MARCH5 loss. This phenocopies the effect observed when MCL1-null cells are treated with WEHI-539, as cells in which MCL1 is functionally inactivated rely on BCLXL for survival[49,62] . Together, these data provide further evidence that the concomitant upregulation of NOXA with MCL1 following MARCH5 loss is a 'priming event' for apoptosis, most likely due to functional inactivation of MCL1 through the concomitant upregulation of NOXA.

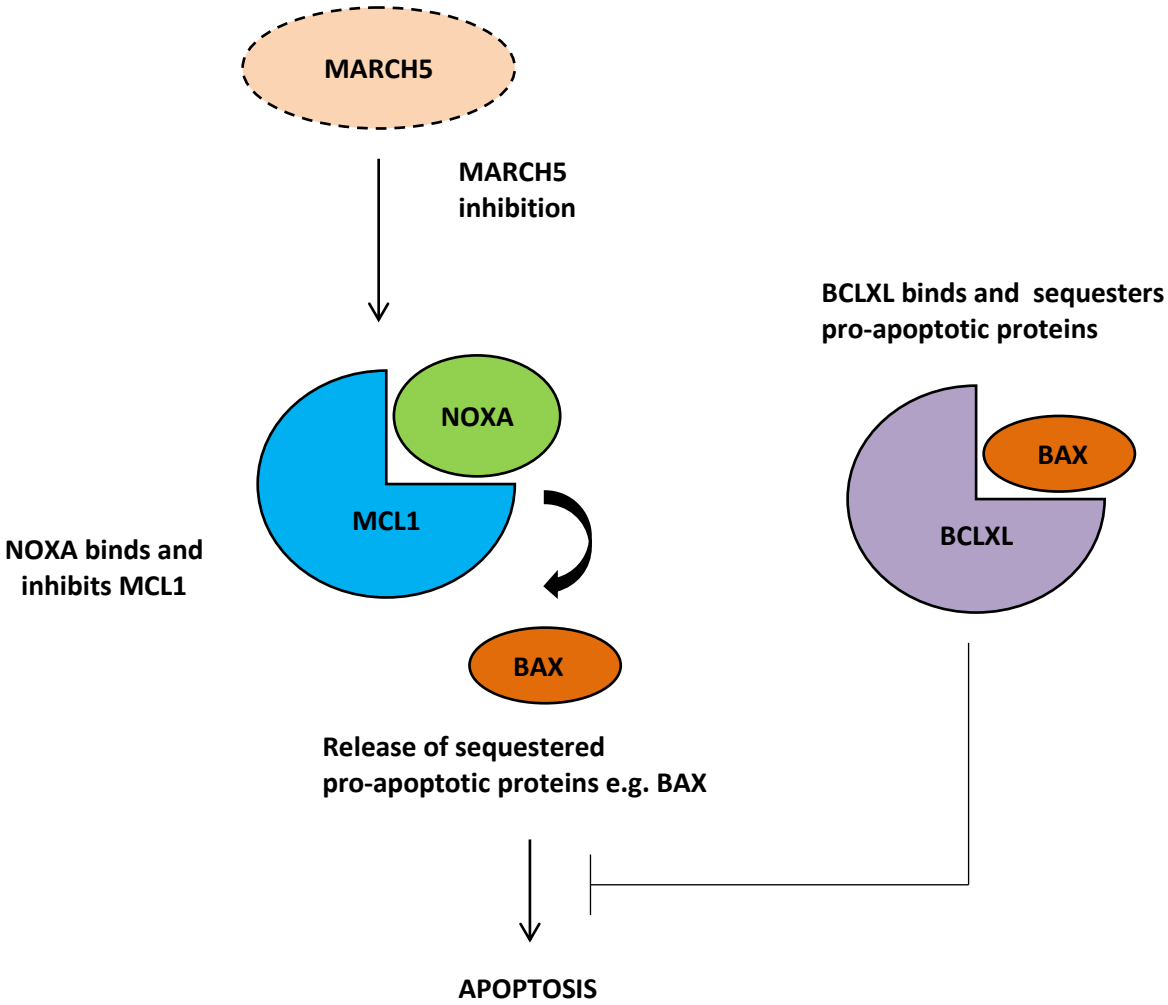

Figure 4.3. BCLXL protects against apoptosis once MCL1 is neutralized

The loss of MARCH5 leads to increase in NOXA, which binds and functionally inhibits MCL1. Under these conditions, the presence of BCLXL protects cells against apoptosis. Therefore, dual inhibition of MCL1 and BCLXL is required to induce cell death.

On the other hand the loss of MARCH5 did not sensitize cells to the BCL2-specific inhibitor, ABT-199. This suggests that MCL1 and BCLXL are the critical determinants of sensitization to cell death in our experimental setting. The concomitant loss of MARCH5 and MCL1 displays synthetic lethality in MCL1-dependent breast cancers. This provides further evidence that targeting MCL1 both with MCL1 specific inhibitors and through MARCH5 depletion would be effective in tumors with high MCL1 levels.

Our experiments have been conducted using a limited number of breast cancer cell lines. Therefore, testing this hypothesis in a larger panel of MCL1-dependent cancer cell lines from different tissue types would provide valuable insight into the efficacy of targeting MCL1 and MARCH5 in a broader context. Certain c-MYC-driven mouse lymphomas also show dependency on MCL1 for growth[174]. These mouse models could also be employed to validate the in vivo efficacy of MARCH5 and/or MCL1 inhibition.

In addition to regulating the MCL1/NOXA axis, the loss of MARCH5 also led to transcriptional upregulation of the p53 targets *p21* and *PUMA*. This suggests that there may be some form of mitochondria to nucleus communication. This could be a result of disruption in mitochondrial homeostasis upon MARCH5 loss and an initiation of a retrograde signaling response which is discussed below.

MARCH5 and mitochondrial retrograde signaling

Mitochondrial retrograde signaling is the process of signal transduction from mitochondria to the nucleus to co-ordinate transcriptional responses. The retrograde signaling response in yeast is induced in response to altered metabolic states, while in mammalian cells is associated with changes in Ca^{2+} dynamics within the mitochondrial compartment. Other factors such as oxidative stress, mitochondrial DNA damage, and disruptions in mitochondrial membrane potential are also associated with retrograde signaling. This signaling activity ensures that cells can rapidly adapt to both internal and external environmental changes[3,175].

In the present study, the transcriptional upregulation of p53 targets was accompanied by collapse of mitochondria around the perinuclear region as well as loss of mitochondrial membrane potential. This type of stress could explain the stabilization and activation of p53 we observed following MARCH5 depletion[176]. It has been also been demonstrated that MARCH5 mediates mitochondrial-endoplasmic reticulum contacts through MFN2, and that disruption of these interactions lead to defective uptake of calcium from the ER to mitochondria[137]. It is possible that these changes could contribute to the retrograde activation of p53.

Moreover, MARCH5-mediated sensitization to BH3 mimetics is partially p53-dependent. Thus, it is likely that MARCH5 loss lowers the threshold for apoptosis through both induction of mitochondrial stress and subsequent stress-related transcriptional changes as well as through altering protein-protein interactions at the mitochondria that allow for regulation of the MCL1/NOXA axis. NOXA, a p53 target, was a key determinant of ABT-737 sensitivity. However, there was no significant change in *NOXA* mRNA following loss of MARCH5. We infer that the presence of p53 sets the basal level of NOXA, and that this

in turn will determine the absolute level of NOXA protein that is stabilized following loss of MARCH5.

p53 was also required for maximal sensitization to ABT-737, it was dispensable for the synthetic lethal interaction between MARCH5 and MCL1. This is supported by experiments with MDA-MB-468 and MDA-MB-231: both these lines carry mutant p53, and were not sensitized to ABT-737 by MARCH5 knockdown, yet MCL1/MARCH5 synthetic lethality was retained in MCL1-dependent MDA-MB-468. Together, these data suggest that MARCH5 loss requires p53 for maximal sensitization to BH3 mimetics; however, factors beyond p53 (including MCL1 dependency as we show here) determine the intrinsic cellular sensitivity to depletion of MARCH5

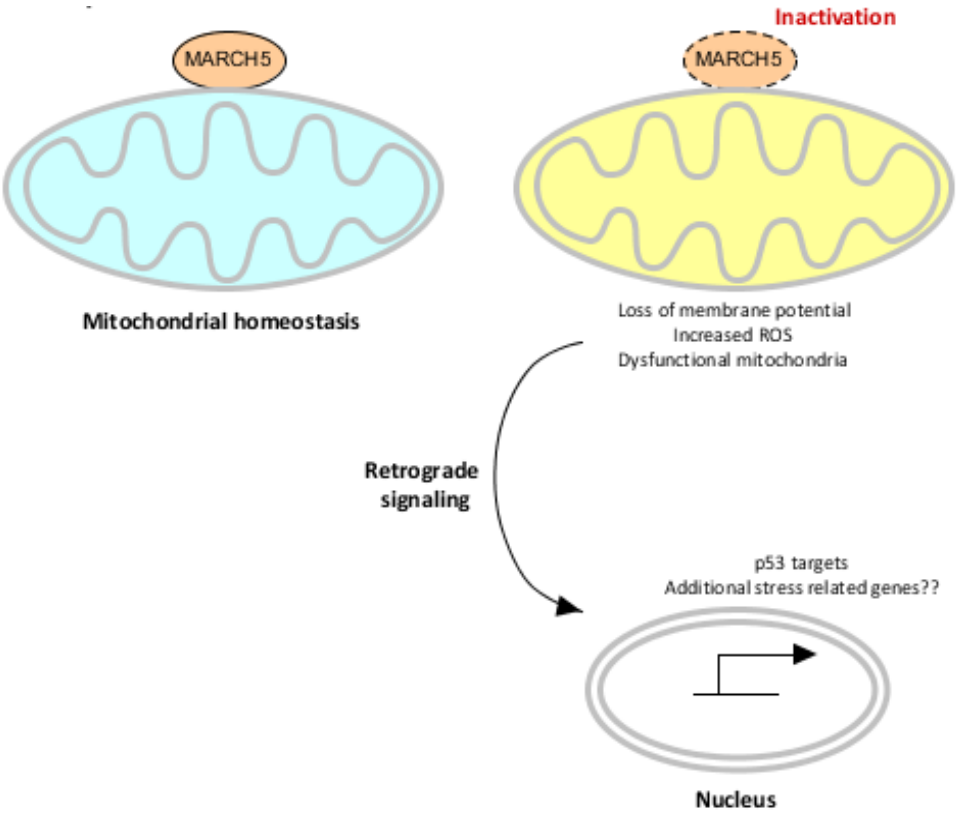

Figure 4.4. Alterations in mitochondrial morphology upon MARCH5 loss could activate retrograde signaling responses

The collapse of the mitochondrial network, loss of membrane potential and production of ROS observed upon depletion of MARCH5 could serve as a trigger for retrograde signaling from the mitochondria to the nucleus to activate stress-related signaling pathways.

Targeting MARCH5 in diseases

(i) MARCH5 and cancer

The present study has demonstrated that MARCH5 has an anti-apoptotic role in cancer cells. A survey of the COSMIC database indicates that *MARCH5* mRNA is overexpressed in a restricted set of tumor types. However, the frequency of MARCH5 mutations in primary tumor samples and in tumor cell lines is low. Thus it can be inferred that MARCH5 does not necessarily fall into the class of traditional oncogenes but is still important for cancer cell survival during tumorigenesis or following treatment with therapeutic compounds. Consistent with this hypothesis, we found that *MARCH5* expression contributed to an 8-gene index that correlated with sensitivity to ABT-263 (Navitoclax) in hematological malignancies. Indeed, its contribution was as significant as that of MCL1, a well-validated determinant of sensitivity to BH3 mimetics.

Due to low sample sizes in the publically available databases, we were unable to extend our analyses to other tissue types. Therefore, further in vivo studies with appropriate tumor models are now required to determine whether targeted inhibition of MARCH5 will have a therapeutic benefit in cancer. As with all cancer targets, this is likely to depend on the precise genetic

makeup of individual tumors. Furthermore (as recently reported for MCL1 in the case of triple-negative breast cancer[177]), predictive signatures should additionally take into account not only mRNA expression, but also protein levels of MARCH5 and BCL-2 family members.

The MARCH5-dependent sensitization to BH3 mimetics was strictly p53-dependent as this effect was attenuated in cell lines lacking p53 or harboring mutant p53. Thus a combination of factors must be taken into account while potentially targeting MARCH5 for therapeutic purposes. It is probable that MARCH5 loss requires p53 for sensitization to certain chemotherapeutics; however the subset of tumors that are MCL1-driven could be targeted through the combined depletion of MCL1 and MARCH5.

Breakthroughs in the design of selective MCL1 inhibitors indicate that direct targeting of this oncogene to induce cell death is now possible. Current data indicate that these compounds are effective in MCL1-dependent tumors, but have variable results in other cell lines[157]. Observations in the present study indicate that combined treatment with high doses of ABT-737 and A1210477 induce cell death in HCT116, but that this was no more effective than a combination of ABT-737 and MARCH5 knockdown. Together, these data clearly indicate that targeting MARCH5 will be particularly effective in combination with broad spectrum BH3 mimetics, or with the next generation of MCL1-selective antagonists.

Further studies are required in order to determine the feasibility and efficacy of therapeutically targeting MARCH5 in cancer. The targeting of E3 ubiquitin ligases for cancer therapeutics is still at an early stage. There is a clear need for development of specific E3 ligase inhibitors, since many of them play critical roles in cancer development and progression. The general proteasome inhibitor, Velcade (Bortezomib) is an FDA-approved compound that targets the ubiquitin-proteasome system[178]. In addition, the possibility of inhibiting SCF cullin-RING ligase with small molecules has been

demonstrated in chemical screens. MLN4924, a small molecule inhibitor of NEDD8-activating enzyme also has potential to be developed as a novel class of anti-cancer agents by restricting the neddylation of the SCF complex[179]. The challenge of targeting ubiquitin ligases lies in their extended flat surfaces, which disfavours the binding of small molecules[180]. Thus, identification of pathways regulated by specific E3 ligases or their substrates becomes crucial. This would offer an indirect route to target and inhibit biological function(s) of the ligase.

In line with above strategies, in depth studies into additional MARCH5 substrates as well as upstream regulators of MARCH5 expression in tumor cells would provide additional strategies by which this ligase could be potentially inhibited.

(ii) MARCH5 and neurodegenerative disorders

Given the roles of MARCH5 in apoptotic signaling and maintenance of mitochondrial homeostasis, it is conceivable that MARCH5 could play a role in the context of neurological disorders. For example, the accumulation of dysfunctional mitochondria, defective mitophagy (i.e., clearance of damaged mitochondria), increased ROS production and cellular stress all contribute to the development and/or progression of neurodegenerative disorders such as Parkinson's disease[128,132,164].

In contrast to its pro-survival role in tumor cells, however, MARCH5 appears to exacerbate neurodegenerative stress via disrupting mitochondrial membrane potential and increasing the levels of ROS[181,182]. Thus MARCH5 appears to possess opposing roles in different tissue types. This "yin-yang" phenomenon has been described in the functions of proteins such as Notch, which can behave as an oncogene or tumor suppressor depending on the cellular context[183].

Interestingly, the loss of MARCH5 in cancer cells led to perinuclear accumulation of mitochondria, which is reminiscent of the phenotype observed upon the treatment of CCCP. This phenotype has been associated with the induction of mitophagy through recruitment of PARKIN[164]. Thus, it would be interesting to observe whether the loss of MARCH5 could also trigger the translocation of PARKIN to mitochondria. MARCH5 has been identified as a PARKIN substrate in a proteomic screen following induction of mitophagy in HCT116 cells with CCCP, again indicative of a link with the mitophagy pathway[131]. Together, these data suggest that further studies are warranted to determine the role of MARCH5 in mitophagy and neurodegeneration.

FUTURE DIRECTIONS

Apart from activation of the p53 pathway, there may be global changes in transcription in response to the perturbation of MARCH5. Further studies are thus warranted in order to gain a better understanding of how MARCH5 disruption alters gene expression. RNA-seq in the presence and absence of MARCH5, or with the expression of MARCH5 functional mutants will be valuable in this regard. Genome-wide synthetic lethal screens would also allow for discovery of specific pathways regulated by MARCH5. From a therapeutic standpoint, chemical screens would enable the identification of compounds that sensitize cancer cells to cell death in combination with the loss of MARCH5.

The effects of the somatic mutations described in cancer databases on MARCH5 function remain unclear. Data presented herein show that the D202Y and D202G mutants promote hyperfusion of the mitochondrial network. This suggests that these could be gain-of-function mutations as certain cancers rely on hyperfused mitochondria to increase metabolic rates[184]. This however requires further study to clearly define the contributions

of these mutations to tumorigenesis. A proteomic approach could also be employed to identify proteins that differentially associate with the wild-type and mutant forms of MARCH5. This in turn would facilitate the functional characterization of these mutants in cancer.

The ubiquitination process occurs in a reversible manner. Deubiquitinating enzymes (DUBS) are a family of proteases that cleave ubiquitin from proteins. However, the precise mechanisms by which deubiquitinating enzymes (DUBS) regulate mitochondrial signaling events is largely unknown. USP30 and USP35 are two DUBS that have displayed mitochondrial specific localization and regulate mitophagy by deubiquitinating PARKIN substrates[185]. Intriguingly the depletion of USP30 sensitized cancer cells to the BH3 mimetic ABT-737[186]; indicative of a potential role of USP30 in the regulation of mitochondrial cell death. Further studies are warranted in order to determine whether MARCH5 and these two mitochondrial DUBS possess common substrates and function together to regulate the cell death process.

APPENDIX I

	WT-p53 (221)			WT-p53 Blood (41)		
Predictor	**Estimate**	**SE**	**pValue**	**Estimate**	**SE**	**pValue**
(Intercept)	2.17	0.24	**	1.67	1.87	0.39
MARCH5	-0.17	0.13	0.21	5.54	2.11	*
MCL1	0.42	0.22	0.06	6.62	2.44	*
BIM	0.14	0.21	0.49	0.68	0.83	0.43
BAX	-0.65	0.15	**	-3.07	0.87	*
HUWE1	-0.59	0.20	*	-1.92	1.56	0.25
BAK1	0.40	0.20	0.05	-8.85	2.79	*
NOXA	-0.81	0.17	**	-0.68	1.70	0.70
BCLXL	0.38	0.21	0.07	2.28	2.52	0.39
MARCH5:BAK1	-0.40	0.13	*			
MCL1:BAX	0.41	0.17	*	-3.46	1.57	0.05
MCL1:BAK1	-0.22	0.16	0.15	4.58	1.30	*
BAK1:BCLXL	-0.36	0.18	*	2.86	1.90	0.16
BIM:BAK1				5.35	1.72	*
HUWE1:BCLXL	0.51	0.19	*	-4.61	2.77	0.13
BAX:BAK1				-1.38	0.92	0.17
BIM:NOXA						
MARCH5:BAX				-1.80	0.74	*
MARCH5:BCLXL				-1.97	1.46	0.21
BIM:BAX	-0.38	0.17	*	-1.55	0.97	0.14
BAK1:NOXA				4.79	1.43	*
BIM:BCLXL				-6.41	2.35	*
MARCH5:MCL1				1.01	0.74	0.20
MCL1:BCLXL				4.03	1.81	*
MARCH5:NOXA	0.20	0.15	0.17	-3.20	1.25	*
MCL1:NOXA	-0.38	0.19	*			
BAX:BCLXL				1.91	1.37	0.19
BAX:HUWE1				3.62	1.54	*
BIM:HUWE1				5.81	1.55	*
MARCH5:BIM				0.78	0.99	0.45
MARCH5:HUWE1				3.06	1.26	*
MCL1:BIM				-3.60	1.39	*
NOXA:BCLXL				-5.08	1.69	*

Figure 5.1. Tabulation of results of multiple regression analysis

Results of optimized multiple linear regression analysis for all cell lines with wild type p53 (n = 221), and the wild type p53 blood subset. Each row shows the estimate value (i.e., the unit change in IC50) that is predicted for every unit increase in expression of the particular gene. SE, standard error of the estimate value. p values indicate whether each gene (or pairwise interaction) was deemed significant. An empty row indicates that the interaction was not considered significant in the relevant subset. Pairwise interactions discussed in Chapter 3 are highlighted in yellow.

APPENDIX II

Regulation of MARCH5 through the AKT pathway

INTRODUCTION

The activation of oncogenes often leads to the re-programming of mitochondrial function in order to facilitate tumor initiation or tumor maintenance. Chemotherapeutic resistance can also emerge due to oncogene-induced rewiring of mitochondria[1,4,7]. Thus, defining the key cytosolic and mitochondrial proteins that promote the re-programming of mitochondria is critical for the design of effective treatment strategies.

Oncogenes known to reprogram mitochondria during tumorigenesis include, *RAS*, *MYC*, and *AKT*[187,188,189]. These oncogenes can be activated via frank mutation, amplification, or deregulation of epigenetic control. However, they can also be activated indirectly via the loss of tumor suppressor protein function. A case in point is the activation of AKT that accompanies the loss of PTEN in many tumors[190].

Given that MARCH5 has a pro-survival role in cancer cells, we hypothesized that it might exhibit functional interactions with oncogenic signaling pathways. We initially focused our attention on the PTEN/AKT axis, as its deregulation has direct impacts on mitochondrial function[191].

RESULTS

Loss of PTEN is associated with increased MARCH5 expression

A panel of breast cancer lines that differed in PTEN status was interrogated along with MCF10A isogenic lines that were PTEN hetero- or homozygous knockout. Fig. 6.1a shows that although there was no direct relationship between the *absolute level* of PTEN protein and the level of MARCH5, the specific loss of PTEN in genetically engineered MCF10A cells was associated with an increase in MARCH5 levels (compare lanes 1-3). Furthermore, MARCH5 levels were increased in 6/7 of a panel of human breast cancer cell lines compared to non-tumorigenic MCF10A (compare lane 1 to lanes 4–10). MARCH5 upregulation is post-translational, since the level of *MARCH5* mRNA does not correlate with the absolute amount of MARCH5 protein (Fig. 6.1b).

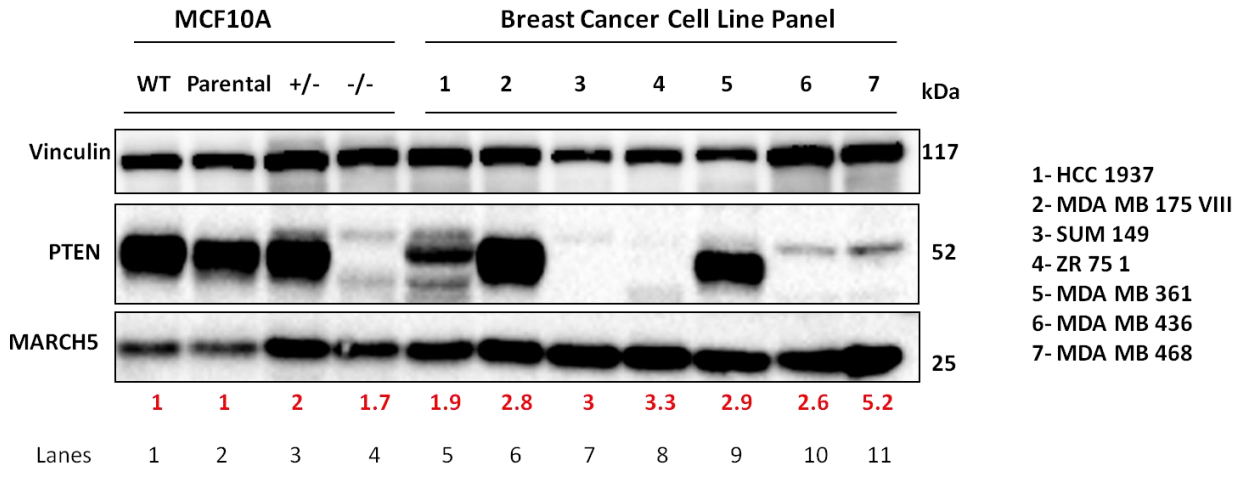

.

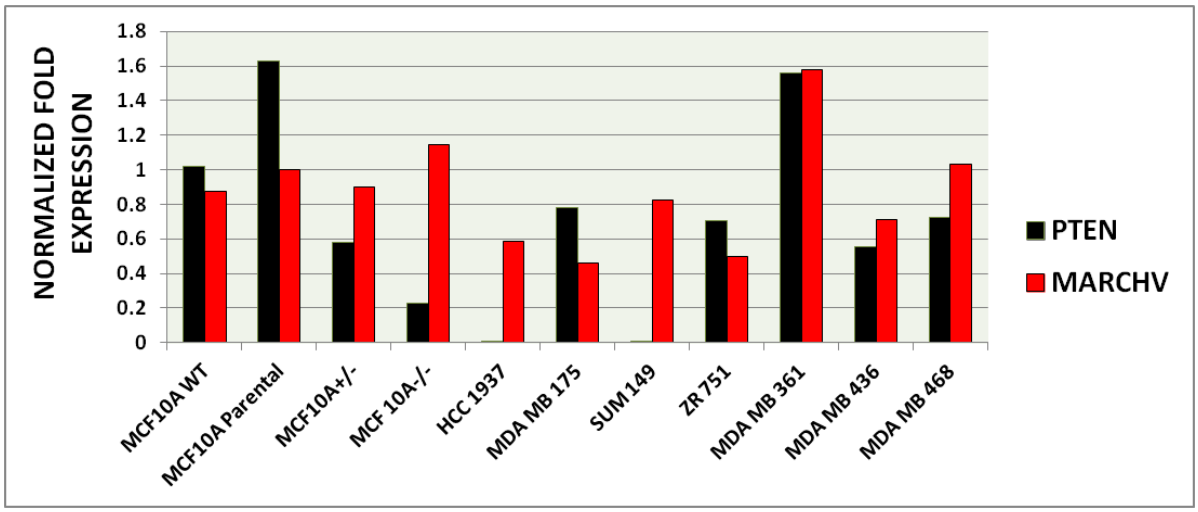

Figure 6.1. PTEN loss is associated with increased MARCH5 expression

(a) Whole cell lysates from the MCF10A isogenics and a panel of breast cancer lines were subjected to SDS-PAGE and immunoblotted with the indicated antibodies.

(b) *PTEN* and *MARCH5* levels in MCF10A isogenic lines and breast cancer cell lines were assessed using qRT-PCR. *18S* mRNA was used as loading control.

Chemical inhibition of the AKT pathway leads to destabilization of MARCH5 protein

Since AKT is activated upon loss of PTEN, we reasoned that AKT might regulate MARCH5 steady state levels. To test this, MCF10A isogenic cells were treated with SH6, a small molecule inhibitor of AKT. The phosphorylation of AKT at S473 and T308 activates the protein and thus measuring the phosphorylated forms of AKT is used a readout of AKT activation[192]. However we were unable to detect AKT or its phosphorylated forms in the MCF10A cell lines, probably due to low basal expression.

Strikingly, the compound downregulated MARCH5 protein but did not affect *MARCH5* mRNA (Fig. 6.2a). Importantly, the levels of TOMM20 were unchanged under these conditions, indicating that the SH6 inhibitor does not have a 'global' effect on MOM proteins. This demonstrated that the inhibition of AKT signaling was specifically destabilizing MARCH5.

Interestingly, scanning of the MARCH5 amino acid sequence reveals a highly conserved AKT phosphorylation site within the functionally important RING domain of the protein. Our prior results demonstrate that the RING domain is critical for regulating MARCH5 stability, and that mutations in this domain lead to stabilization of the protein. Thus, it would be of interest to assess how phosphorylation events within this domain determine the auto-regulation of MARCH5 levels.

a

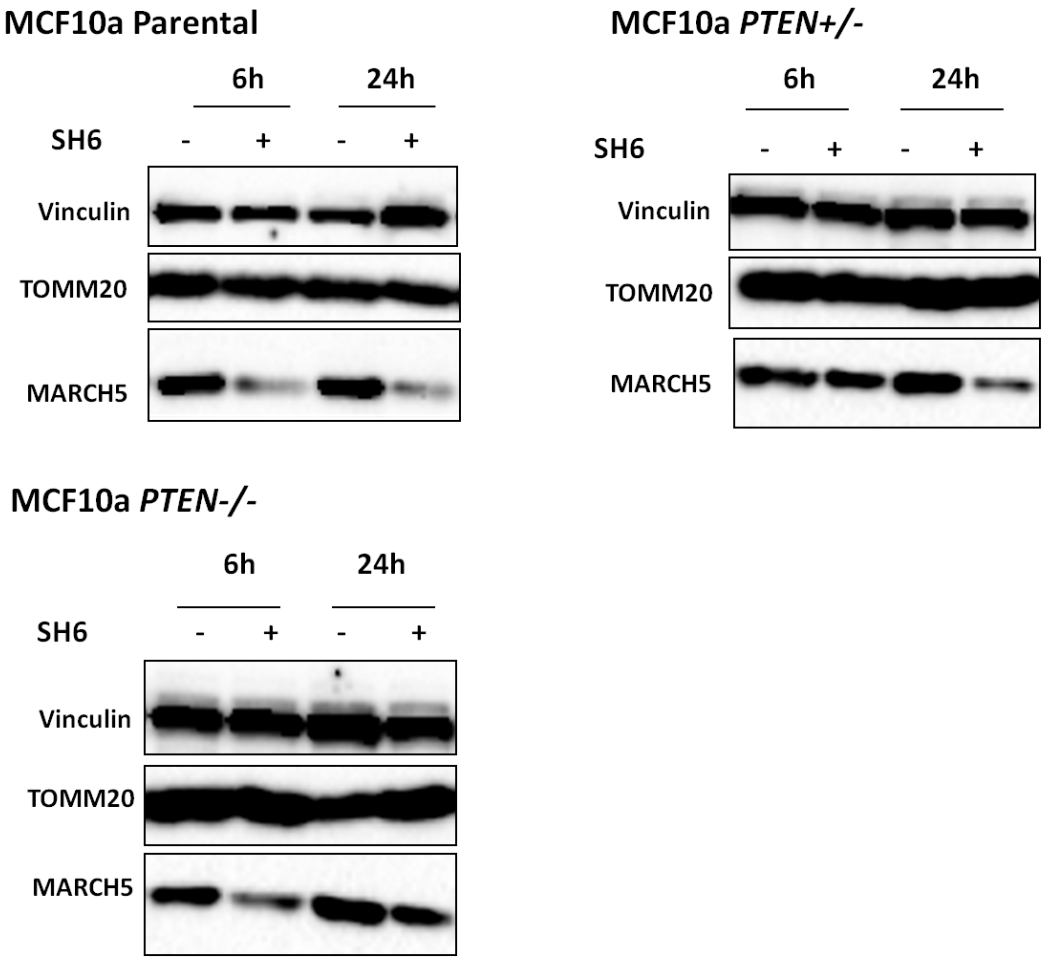
MCF10a Parental
6h
24h
SH6
- + - +
Vinculin
TOMM20
MARCH5
MCF10a PTEN+/-
6h
24h
SH6
- + - +
Vinculin
TOMM20
MARCH5
MCF10a PTEN-/-
6h
24h
SH6
- + - +
Vinculin
TOMM20
MARCH5

b

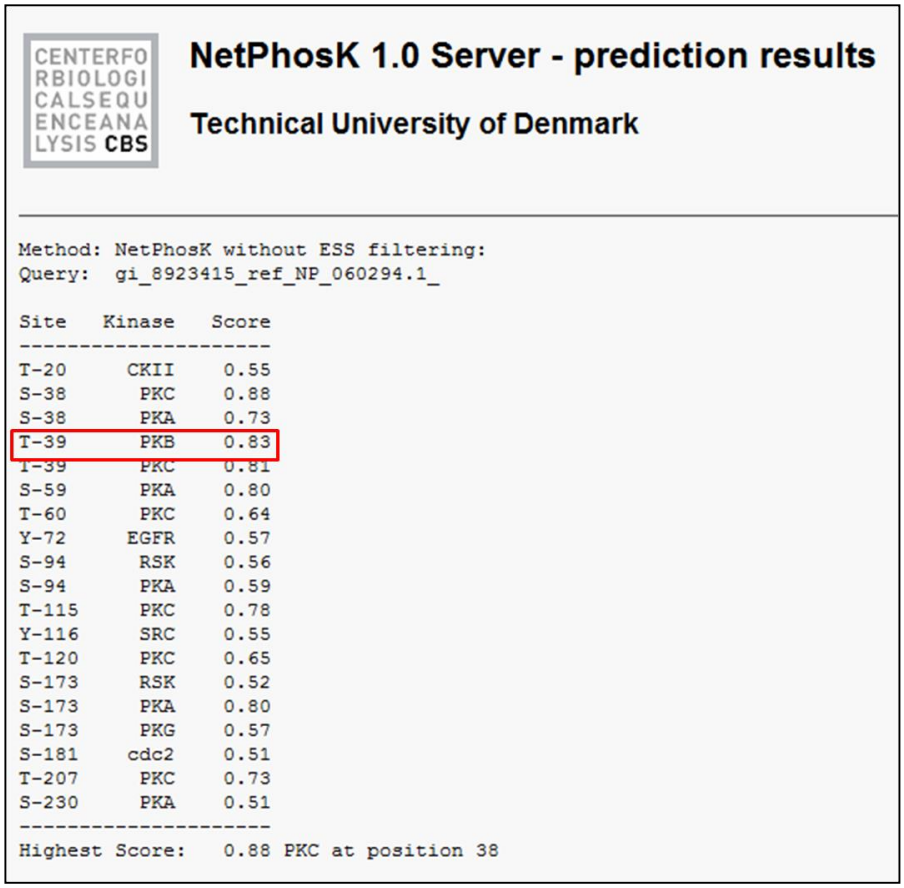

NetPhosK 1.0 Server - prediction results

Technical University of Denmark

Method: NetPhosK without ESS filtering:
Query: gi_8923415_ref_NP_060294.1_

Site	Kinase	Score
T-20	CKII	0.55
S-38	PKC	0.88
S-38	PKA	0.73
T-39	PKB	0.83
T-39	PKC	0.81
S-59	PKA	0.80
T-60	PKC	0.64
Y-72	EGFR	0.57
S-94	RSK	0.56
S-94	PKA	0.59
T-115	PKC	0.78
Y-116	SRC	0.55
T-120	PKC	0.65
S-173	RSK	0.52
S-173	PKA	0.80
S-173	PKG	0.57
S-181	cdc2	0.51
T-207	PKC	0.73
S-230	PKA	0.51

Highest Score: 0.88 PKC at position 38

Figure 6.2. Inhibition of AKT destabilizes MARCH5 protein

(a) MCF10A isogenic cell lines were treated with 10 μM of SH6 inhibitor for the indicated timepoints. Whole cell lysates were then harvested and subjected to SDS-PAGE and immunoblotted with the indicated antibodies.

(b) Scanning of phosphorylation sites on MARCH5 using the NetPhosK server revealed a potential AKT phosphorylation site.

DISCUSSION

The upregulation of MARCH5 observed in the engineered MCF10A and breast cancer cell line panel is likely associated with the re-wiring of cell signaling networks upon PTEN loss such as the hyper-activation of the AKT pathway. Chemical inhibition of AKT signaling also led to destabilization of MARCH5 protein suggesting that AKT is a potential upstream regulator of MARCH5 expression.

Interestingly, the predicted AKT phosphorylation site in MARCH5 falls within the important functional RING domain. Thus, the phosphorylation of MARCH5 could serve as an important regulatory mechanism. In this regard, similar phosphorylation-dependent regulatory events have been reported for the MDM2 E3 ligase. The phosphorylation of MDM2 near the C terminus inhibits RING domain oligomerization by the ATM kinase results in p53 stabilization after DNA damage[193]. The TRAF2 E3 ligase is also phosphorylated within its RING domain and this in turn induces NF-κB signaling[194].

Clearly, further studies are required to fully understand the mechanism by which AKT regulates MARCH5. In this regard, generation of phospho-mutants of MARCH5 will provide further insight into whether AKT (or indeed other kinases) control MARCH5 stability and/or function.

In addition, the AKT family is comprised of three different homologous isoforms. Studies in AKT isoform-specific knockout mice have shown that the different isoforms possess distinct functions[195]. Thus RNAi directed against specific isoforms would provide an indication of which isoform modulates MARCH5 levels and the significance of this regulation.

The functional interaction between MARCH5 and other oncogenes or tumor suppressors remains unclear. A literature survey revealed that MARCH5 scored as a synthetic lethal hit with RAS in a functional genomics screen, although this was not followed up by the authors. Furthermore, MARCH5 is mutated or upregulated in several primary tumors that carry RAS mutations[196].

Thus it appears that MARCH5 could be regulated at different levels during the course of tumorigenesis. Having observed a pro-survival role for MARCH5 in cancer, it is critical to identify upstream regulators in order to devise potential therapeutic strategies to target MARCH5. Furthermore, identification of the upstream regulators or the oncogenes that depend on MARCH5 would be useful for potential patient stratification if MARCH5 becomes a fully validated oncology target.

MATERIALS AND METHODS

Cell Culture

MCF10A WT and isogenic cell lines were cultured in DMEM/HAM's F12 supplemented with 5% horse serum, 4 mM L-glutamine, 100 U/ml penicillin, and 100 U/ml of streptomycin, 20 ng/ml EGF, 0.5 mg/ml hydrocortisone, 100ng/ml cholera toxin and 10μg/ml insulin in a humidified atmosphere of 5% CO_2 at 37°C. Cells were passaged prior to reaching full confluency for general maintenance. DMEM, HAM's F12, L-glutamine, penicillin and streptomycin were purchased from Lonza (Basel, Switzerland). EGF was purchased from Peprotech (UK), hydrocortisone, cholera toxin and insulin were purchased from Sigma-Aldrich (St. Louis, MO, USA). Breast cancer cell line pellets were provided by the IEO tissue culture facility.

Compound treatments

SH6 inhibitor was purchased from Calbiochem and used at a concentration of 10 μM for 48 h.

Western blot and antibodies

Cells were lyzed in 0.5% NP-40 lysis buffer (50 mM Tris, pH 8.0, 5 mM EDTA, 150 mM NaCl, 0.5% NP-40, 1 mM phenylmethylsulfonyl fluoride, 1 mM Na_3VO_4, 10 mM NaF and Complete Mini Protease Inhibitors (Roche, Nutley, NJ, USA), at 4°C for 30 min. Following SDS-PAGE electrophoresis, proteins were transferred onto nitrocellulose membranes. Membranes were incubated with the following antibodies: anti-MARCH5 (gifted by Dr. Nakamura, Tokyo Institute of Technology), anti-PTEN (Cell Signaling Technologies) , anti-vinculin (Sigma-Aldrich) and anti-TOMM20 (Santa Cruz Biotechnologies).

RT-qPCR

Total RNA was extracted using RNeasy Mini Kit (Qiagen) and complementary DNA (cDNA) was synthesized using the ImProm-II Reverse Transcription System (Promega). Ten nanograms cDNA was used per PCR reaction with SYBR Green PCR Master Mix (Applied Biosystems, ABI) and quantified on the BIORAD CFX96 Real Time System. Fold changes in mRNA expression was quantified using the Δ-ΔCt algorithm with *18S* ribosomal RNA as loading control. qPCR primers are tabulated below.

	Forward (5'-3')	Reverse (5'-3')
18S	GATTAAGTCCCTGCCCTTTGTACA	GATCCGAGGGCCTCACTAAAC
MARCHV	GATGCTGGACAGAAGTTGCTGG	CCACTCTGGCTGTACTGTTTCC
PTEN	AATGTTCAGTGGCGGAACTTGC	ACATGAACTTGTCTTCCCGTCG

Phosphorylation site prediction analysis

MARCH5 phosphorylation site prediction was performed using the NetPhosK server- http://www.cbs.dtu.dk/services/NetPhosK/ as described by Blom et al., 2004[197].

REFERENCES

1. Chan, D. C. Mitochondria: dynamic organelles in disease, aging, and development. *Cell* **125,** 1241–52 (2006).

2. Arnoult, D., Soares, F., Tattoli, I. & Girardin, S. E. Mitochondria in innate immunity. *EMBO Rep.* **12,** 901–10 (2011).

3. Butow, R. A. & Avadhani, N. G. Mitochondrial SignalingThe Retrograde Response. *Mol. Cell* **14,** 1–15 (2004).

4. Nunnari, J. & Suomalainen, A. Mitochondria: in sickness and in health. *Cell* **148,** 1145–59 (2012).

5. Vander Heiden, M. G., Cantley, L. C. & Thompson, C. B. Understanding the Warburg effect: the metabolic requirements of cell proliferation. *Science* **324,** 1029–33 (2009).

6. Ward, P. S. & Thompson, C. B. Metabolic reprogramming: a cancer hallmark even warburg did not anticipate. *Cancer Cell* **21,** 297–308 (2012).

7. Gogvadze, V., Orrenius, S. & Zhivotovsky, B. Mitochondria in cancer cells: what is so special about them? *Trends Cell Biol.* **18,** 165–73 (2008).

8. Carew, J. S. & Huang, P. Mitochondrial defects in cancer. **12,** 1–12 (2002).

9. Hanahan, D. & Weinberg, R. A. The hallmarks of cancer. *Cell* **100,** 57–70 (2000).

10. Hanahan, D. & Weinberg, R. A. Hallmarks of cancer: the next generation. *Cell* **144,** 646–74 (2011).

11. Tait, S. W. G. & Green, D. R. Mitochondria and cell death: outer membrane permeabilization and beyond. *Nat. Rev. Mol. Cell Biol.* **11,** 621–632 (2010).

12. Fulda, S. & Debatin, K.-M. Extrinsic versus intrinsic apoptosis pathways in anticancer chemotherapy. *Oncogene* **25,** 4798–811 (2006).

13. Taylor, R. C., Cullen, S. P. & Martin, S. J. Apoptosis: controlled demolition at the cellular level. *Nat. Rev. Mol. Cell Biol.* **9,** 231–41 (2008).

14. Galluzzi, L. & Kroemer, G. Necroptosis: a specialized pathway of programmed necrosis. *Cell* **135,** 1161–3 (2008).

15. Pasparakis, M. & Vandenabeele, P. Necroptosis and its role in inflammation. *Nature* **517,** 311–320 (2015).

16. Silke, J., Rickard, J. A. & Gerlic, M. The diverse role of RIP kinases in necroptosis and inflammation. *Nat. Immunol.* **16,** 689–697 (2015).

17. Kroemer, G., Galluzzi, L. & Brenner, C. Mitochondrial membrane permeabilization in cell death. *Physiol. Rev.* **87,** 99–163 (2007).

18. Czabotar, P. E., Lessene, G., Strasser, A. & Adams, J. M. Control of apoptosis by the BCL-2 protein family: implications for physiology and therapy. *Nat. Rev. Mol. Cell Biol.* **15,** 49–63 (2014).

19. Hardwick, J. M. & Soane, L. Multiple Functions of BCL-2 Family Proteins. *Cold Spring Harb. Perspect. Biol.* **5,** a008722–a008722 (2013).

20. Cleland, M. M. *et al.* Bcl-2 family interaction with the mitochondrial morphogenesis machinery. *Cell Death Differ.* **18,** 235–47 (2011).

21. Neuspiel, M., Zunino, R., Gangaraju, S., Rippstein, P. & McBride, H. Activated mitofusin 2 signals mitochondrial fusion, interferes with Bax activation, and reduces susceptibility to radical induced depolarization. *J. Biol. Chem.* **280,** 25060–70 (2005).

22. Wasiak, S., Zunino, R. & McBride, H. M. Bax/Bak promote sumoylation of DRP1 and its stable association with mitochondria during apoptotic cell death. *J. Cell Biol.* **177,** 439–50 (2007).

23. Eichhorn, J. M., Alford, S. E., Sakurikar, N. & Chambers, T. C. Molecular analysis of functional redundancy among anti-apoptotic Bcl-2 proteins and its role in cancer cell survival. *Exp. Cell Res.* **322,** 415–24 (2014).

24. Follis, A. V. *et al.* PUMA binding induces partial unfolding within BCL-xL to disrupt p53 binding and promote apoptosis. *Nat. Chem. Biol.* **9,** 163–8 (2013).

25. Brunelle, J. K. & Letai, A. Control of mitochondrial apoptosis by the Bcl-2 family. *J. Cell Sci.* **122,** 437–41 (2009).

26. Shamas-Din, A., Kale, J., Leber, B. & Andrews, D. W. Mechanisms of action of Bcl-2 family proteins. *Cold Spring Harb. Perspect. Biol.* **5,** a008714 (2013).

27. Youle, R. J. & Strasser, A. The BCL-2 protein family: opposing activities that mediate cell death. *Nat. Rev. Mol. Cell Biol.* **9,** 47–59 (2008).

28. Vrana, J. A., Cleaveland, E. S., Eastman, A. & Craig, R. W. Inducer-and cell type-specific regulation of antiapoptotic MCL1 in myeloid leukemia and multiple myeloma cells exposed to differentiation-inducing or microtubule-disrupting agents. *Apoptosis* **11,** 1275–88 (2006).

29. Opferman, J. T. *et al.* Obligate role of anti-apoptotic MCL-1 in the survival of hematopoietic stem cells. *Science* **307,** 1101–4 (2005).

30. Thomas, L. W., Lam, C. & Edwards, S. W. Mcl-1; the molecular regulation of protein function. *FEBS Lett.* **584,** 2981–9 (2010).

31. Ertel, F., Nguyen, M., Roulston, A. & Shore, G. C. Programming cancer cells for high expression levels of Mcl1. *EMBO Rep.* **14,** 328–36 (2013).

32. Zhong, Q., Gao, W., Du, F. & Wang, X. Mule/ARF-BP1, a BH3-only E3 ubiquitin ligase, catalyzes the polyubiquitination of Mcl-1 and regulates apoptosis. *Cell* **121,** 1085–95 (2005).

33. Inuzuka, H. *et al.* SCF(FBW7) regulates cellular apoptosis by targeting MCL1 for ubiquitylation and destruction. *Nature* **471,** 104–9 (2011).

34. Magiera, M. M. *et al.* Trim17-mediated ubiquitination and degradation of Mcl-1 initiate apoptosis in neurons. *Cell Death Differ.* **20,** 281–92 (2013).

35. Schwickart, M. *et al.* Deubiquitinase USP9X stabilizes MCL1 and promotes tumour cell survival. *Nature* **463,** 103–7 (2010).

36. Beroukhim, R. *et al.* The landscape of somatic copy-number alteration across human cancers. *Nature* **463,** 899–905 (2010).

37. Zhang, H. *et al.* Mcl-1 is critical for survival in a subgroup of non-small-cell lung cancer cell lines. *Oncogene* **30,** 1963–8 (2011).

38. Perciavalle, R. M. *et al.* Anti-apoptotic MCL-1 localizes to the mitochondrial matrix and couples mitochondrial fusion to respiration. *Nat. Cell Biol.* **14,** 575–83 (2012).

39. Hijikata, M., Kato, N., Sato, T., Kagami, Y. & Shimotohno, K. Molecular cloning and characterization of a cDNA for a novel phorbol-12-myristate-13-acetate-responsive gene that is highly expressed in an adult T-cell leukemia cell line. *J. Virol.* **64,** 4632–9 (1990).

40. Oda, E. *et al.* Noxa, a BH3-only member of the Bcl-2 family and candidate mediator of p53-induced apoptosis. *Science* **288,** 1053–8 (2000).

41. Sun, Y. & Leaman, D. W. Involvement of Noxa in cellular apoptotic responses to interferon, double-stranded RNA, and virus infection. *J. Biol. Chem.* **280,** 15561–8 (2005).

42. Ploner, C., Kofler, R. & Villunger, A. Noxa: at the tip of the balance between life and death. *Oncogene* **27,** S84–S92 (2008).

43. Baou, M. *et al.* Role of NOXA and its ubiquitination in proteasome inhibitor-induced apoptosis in chronic lymphocytic leukemia cells. *Haematologica* **95,** 1510–8 (2010).

44. Gomez-Bougie, P. *et al.* Noxa up-regulation and Mcl-1 cleavage are associated to apoptosis induction by bortezomib in multiple myeloma. *Cancer Res.* **67,** 5418–24 (2007).

45. Tonino, S. H. *et al.* ROS-mediated upregulation of Noxa overcomes chemoresistance in chronic lymphocytic leukemia. *Oncogene* **30,** 701–13 (2011).

46. Craxton, A. *et al.* NOXA, a sensor of proteasome integrity, is degraded by 26S proteasomes by an ubiquitin-independent pathway that is blocked by MCL-1. *Cell Death Differ.* **19,** 1424–34 (2012).

47. Zhang, H. *et al.* Genomic analysis and selective small molecule inhibition identifies BCL-X(L) as a critical survival factor in a subset of colorectal cancer. *Mol. Cancer* **14,** 126 (2015).

48. Kharbanda, S. *et al.* Translocation of SAPK/JNK to mitochondria and interaction with Bcl-x(L) in response to DNA damage. *J. Biol. Chem.* **275,** 322–7 (2000).

49. Lessene, G. *et al.* Structure-guided design of a selective BCL-X(L) inhibitor. *Nat. Chem. Biol.* **9,** 390–7 (2013).

50. Vela, L. & Marzo, I. Bcl-2 family of proteins as drug targets for cancer chemotherapy: the long way of BH3 mimetics from bench to bedside. *Curr. Opin. Pharmacol.* **23,** 74–81 (2015).

51. Mills, J. R. *et al.* RNAi screening uncovers Dhx9 as a modifier of ABT-737 resistance in an Eμ-myc/Bcl-2 mouse model. *Blood* **121,** 3402–12 (2013).

52. Van Delft, M. F. *et al.* The BH3 mimetic ABT-737 targets selective Bcl-2 proteins and efficiently induces apoptosis via Bak/Bax if Mcl-1 is neutralized. *Cancer Cell* **10,** 389–99 (2006).

53. Harper, M. T. & Poole, A. W. Bcl-xL-inhibitory BH3 mimetic ABT-737 depletes platelet calcium stores. *Blood* **119,** 4337–8 (2012).

54. Vandenberg, C. J. & Cory, S. ABT-199, a new Bcl-2-specific BH3 mimetic, has in vivo efficacy against aggressive Myc-driven mouse lymphomas without provoking thrombocytopenia. *Blood* **121,** 2285–8 (2013).

55. Tao, Z.-F. *et al.* Discovery of a Potent and Selective BCL-XL Inhibitor with in Vivo Activity. *ACS Med. Chem. Lett.* **5,** 1088–93 (2014).

56. Yecies, D., Carlson, N. E., Deng, J. & Letai, A. Acquired resistance to ABT-737 in lymphoma cells that up-regulate MCL-1 and BFL-1. *Blood* **115,** 3304–13 (2010).

57. Reuland, S. N. *et al.* ABT-737 synergizes with Bortezomib to kill melanoma cells. *Biol. Open* **1,** 92–100 (2012).

58. Tromp, J. M. *et al.* Tipping the Noxa/Mcl-1 balance overcomes ABT-737 resistance in chronic lymphocytic leukemia. *Clin. Cancer Res.* **18,** 487–98 (2012).

59. Nguyen, M. *et al.* Small molecule obatoclax (GX15-070) antagonizes MCL-1 and overcomes MCL-1-mediated resistance to apoptosis. *Proc. Natl. Acad. Sci. U. S. A.* **104,** 19512–7 (2007).

60. Vogler, M. *et al.* Different forms of cell death induced by putative BCL2 inhibitors. *Cell Death Differ.* **16,** 1030–1039 (2009).

61. Varadarajan, S. *et al.* Maritoclax and dinaciclib inhibit MCL-1 activity and induce apoptosis in both a MCL-1-dependent and -independent manner. *Oncotarget* **6,** 12668–81 (2015).

62. Xiao, Y. *et al.* MCL-1 Is a Key Determinant of Breast Cancer Cell Survival: Validation of MCL-1 Dependency Utilizing a Highly Selective Small Molecule Inhibitor. *Mol. Cancer Ther.* **14,** 1837–47 (2015).

63. Fridman, J. S. & Lowe, S. W. Control of apoptosis by p53. *Oncogene* **22,** 9030–40 (2003).

64. Gu, Z. T. *et al.* Heat stress induces apoptosis through transcription-independent p53-mediated mitochondrial pathways in human umbilical vein endothelial cell. *Sci. Rep.* **4,** 4469 (2014).

65. Miyashita, T. *et al.* Tumor suppressor p53 is a regulator of bcl-2 and bax gene expression in vitro and in vivo. *Oncogene* **9,** 1799–805 (1994).

66. Gartel, A. L. & Tyner, A. L. The Role of the Cyclin-dependent Kinase Inhibitor p21 in Apoptosis. *Mol. Cancer Ther.* **1,** 639–649 (2002).

67. He, G. *et al.* Induction of p21 by p53 following DNA damage inhibits both Cdk4 and Cdk2 activities. *Oncogene* **24,** 2929–2943 (2005).

68. Andrysik, Z., Kim, J., Tan, A. C. & Espinosa, J. M. A genetic screen identifies TCF3/E2A and TRIAP1 as pathway-specific regulators of the cellular response to p53 activation. *Cell Rep.* **3,** 1346–54 (2013).

69. Green, D. R. & Kroemer, G. Cytoplasmic functions of the tumour suppressor p53. *Nature* **458,** 1127–30 (2009).

70. Hagn, F. *et al.* BclxL changes conformation upon binding to wild-type but not mutant p53 DNA binding domain. *J. Biol. Chem.* **285,** 3439–50 (2010).

71. Wolff, S., Erster, S., Palacios, G. & Moll, U. M. p53's mitochondrial translocation and MOMP action is independent of Puma and Bax and severely disrupts mitochondrial membrane integrity. *Cell Res.* **18,** 733–44 (2008).

72. Deng, X., Gao, F., Flagg, T., Anderson, J. & May, W. S. Bcl2's flexible loop domain regulates p53 binding and survival. *Mol. Cell. Biol.* **26,** 4421–34 (2006).

73. Petros, A. M., Gunasekera, A., Xu, N., Olejniczak, E. T. & Fesik, S. W. Defining the p53 DNA-binding domain/Bcl-x(L)-binding interface using NMR. *FEBS Lett.* **559,** 171–4 (2004).

74. Detmer, S. A. & Chan, D. C. Functions and dysfunctions of mitochondrial dynamics. *Nat. Rev. Mol. Cell Biol.* **8,** 870–9 (2007).

75. Westermann, B. Mitochondrial fusion and fission in cell life and death. *Nat. Rev. Mol. Cell Biol.* **11,** 872–84 (2010).

76. Berman, S. B., Pineda, F. J. & Hardwick, J. M. Mitochondrial fission and fusion dynamics: the long and short of it. *Cell Death Differ.* **15,** 1147–52 (2008).

77. Chan, D. C. Mitochondrial fusion and fission in mammals. *Annu. Rev. Cell Dev. Biol.* **22,** 79–99 (2006).

78. Chen, H. *et al.* Mitofusins Mfn1 and Mfn2 coordinately regulate mitochondrial fusion and are essential for embryonic development. *J. Cell Biol.* **160,** 189–200 (2003).

79. Züchner, S. *et al.* Mutations in the mitochondrial GTPase mitofusin 2 cause Charcot-Marie-Tooth neuropathy type 2A. *Nat. Genet.* **36,** 449–51 (2004).

80. Mai, S., Klinkenberg, M., Auburger, G., Bereiter-Hahn, J. & Jendrach, M. Decreased expression of Drp1 and Fis1 mediates mitochondrial elongation in senescent cells and enhances resistance to oxidative stress through PINK1. *J. Cell Sci.* **123,** 917–26 (2010).

81. Chang, C.-R. & Blackstone, C. Dynamic regulation of mitochondrial fission through modification of the dynamin-related protein Drp1. *Ann. N. Y. Acad. Sci.* **1201,** 34–9 (2010).

82. Lee, Y., Jeong, S., Karbowski, M., Smith, C. L. & Youle, R. J. Roles of the Mammalian Mitochondrial Fission and Fusion Mediators Fis1 , Drp1 , and Opa1 in Apoptosis. **15,** 5001–5011 (2004).

83. Jahani-Asl, A. & Slack, R. S. The phosphorylation state of Drp1 determines cell fate. *EMBO Rep.* **8,** 912–3 (2007).

84. Karbowski, M. *et al.* Spatial and temporal association of Bax with mitochondrial fission sites, Drp1, and Mfn2 during apoptosis. *J. Cell Biol.* **159,** 931–8 (2002).

85. Parone, P. a & Martinou, J.-C. Mitochondrial fission and apoptosis: an ongoing trial. *Biochim. Biophys. Acta* **1763,** 522–30 (2006).

86. Karbowski, M., Norris, K. L., Cleland, M. M., Jeong, S.-Y. & Youle, R. J. Role of Bax and Bak in mitochondrial morphogenesis. *Nature* **443,** 658–62 (2006).

87. Dewson, G. & Kluck, R. M. Mechanisms by which Bak and Bax permeabilise mitochondria during apoptosis. *J. Cell Sci.* **122,** 2801–2808 (2009).

88. Brooks, C. *et al.* Bak regulates mitochondrial morphology and pathology during apoptosis by interacting with mitofusins. *Proc. Natl. Acad. Sci. U. S. A.* **104,** 11649–54 (2007).

89. Chen, Y.-B. *et al.* Bcl-xL regulates mitochondrial energetics by stabilizing the inner membrane potential. *J. Cell Biol.* **195,** 263–76 (2011).

90. Renault, T. T. *et al.* Mitochondrial Shape Governs BAX-Induced Membrane Permeabilization and Apoptosis. *Mol. Cell* 1–14 (2015). doi:10.1016/j.molcel.2014.10.028

91. Cassidy-Stone, A. *et al.* Chemical inhibition of the mitochondrial division dynamin reveals its role in Bax/Bak-dependent mitochondrial outer membrane permeabilization. *Dev. Cell* **14,** 193–204 (2008).

92. Taguchi, N., Ishihara, N., Jofuku, A., Oka, T. & Mihara, K. Mitotic phosphorylation of dynamin-related GTPase Drp1 participates in mitochondrial fission. *J. Biol. Chem.* **282,** 11521–9 (2007).

93. Ryan, M. T. & Stojanovski, D. Mitofusins 'bridge' the gap between oxidative stress and mitochondrial hyperfusion. *EMBO Rep.* **13,** 870–871 (2012).

94. Tondera, D. *et al.* SLP-2 is required for stress-induced mitochondrial hyperfusion. *EMBO J.* **28,** 1589–600 (2009).

95. Rambold, A. S., Kostelecky, B., Elia, N. & Lippincott-Schwartz, J. Tubular network formation protects mitochondria from autophagosomal degradation during nutrient starvation. *Proc. Natl. Acad. Sci. U. S. A.* **108,** 10190–5 (2011).

96. Komander, D. The emerging complexity of protein ubiquitination. *Biochem. Soc. Trans.* **37,** 937–53 (2009).

97. Grabbe, C., Husnjak, K. & Dikic, I. The spatial and temporal organization of ubiquitin networks. *Nat. Rev. Mol. Cell Biol.* **12,** 295–307 (2011).

98. Ye, Y. & Rape, M. Building ubiquitin chains: E2 enzymes at work. *Nat. Rev. Mol. Cell Biol.* **10,** 755–64 (2009).

99. Deshaies, R. J. & Joazeiro, C. a P. RING domain E3 ubiquitin ligases. *Annu. Rev. Biochem.* **78,** 399–434 (2009).

100. Bernassola, F., Karin, M., Ciechanover, A. & Melino, G. The HECT family of E3 ubiquitin ligases: multiple players in cancer development. *Cancer Cell* **14,** 10–21 (2008).

101. Wade, M. *et al.* Functional analysis and consequences of Mdm2 E3 ligase inhibition in human tumor cells. *Oncogene* **31,** 4789–97 (2012).

102. Lamothe, B. *et al.* Site-specific Lys-63-linked tumor necrosis factor receptor-associated factor 6 auto-ubiquitination is a critical determinant of I kappa B kinase activation. *J. Biol. Chem.* **282,** 4102–12 (2007).

103. Hicke, L. PROTEIN REGULATION BY MONOUBIQUITIN. **2,** (2001).

104. Istituto, F. & Molecolare, O. Monoubiquitination in Endocytosis Raghunath Peesari and Simona Polo. 1–8

105. Birsa, N. *et al.* Lysine 27 ubiquitination of the mitochondrial transport protein Miro is dependent on serine 65 of the Parkin ubiquitin ligase. *J. Biol. Chem.* **289,** 14569–82 (2014).

106. Yuan, W.-C. *et al.* K33-Linked Polyubiquitination of Coronin 7 by Cul3-KLHL20 Ubiquitin E3 Ligase Regulates Protein Trafficking. *Mol. Cell* **54,** 586–600 (2014).

107. Stieglitz, B. *et al.* Structural basis for ligase-specific conjugation of linear ubiquitin chains by HOIP. *Nature* **503,** 422–6 (2013).

108. Iwai, K., Fujita, H. & Sasaki, Y. Linear ubiquitin chains: NF-κB signalling, cell death and beyond. *Nat. Rev. Mol. Cell Biol.* **15,** 503–8 (2014).

109. Berndsen, C. E. & Wolberger, C. New insights into ubiquitin E3 ligase mechanism. *Nat. Struct. Mol. Biol.* **21,** 301–7 (2014).

110. Rotin, D. & Kumar, S. Physiological functions of the HECT family of ubiquitin ligases. *Nat. Rev. Mol. Cell Biol.* **10,** 398–409 (2009).

111. Dominguez, C., Folkers, G. E. & Boelens, R. Biological Introduction: RING domain proteins. **3,** 338–351 (2004).

112. Nakatani, Y. *et al.* Regulation of ubiquitin transfer by XIAP, a dimeric RING E3 ligase. *Biochem. J.* **450,** 629–38 (2013).

113. Linke, K. *et al.* Structure of the MDM2/MDMX RING domain heterodimer reveals dimerization is required for their ubiquitylation in trans. *Cell Death Differ.* **15,** 841–8 (2008).

114. Petroski, M. D. & Deshaies, R. J. Function and regulation of cullin-RING ubiquitin ligases. *Nat. Rev. Mol. Cell Biol.* **6,** 9–20 (2005).

115. Hoeller, D. & Dikic, I. Targeting the ubiquitin system in cancer therapy. *Nature* **458,** 438–44 (2009).

116. Kirkin, V. & Dikic, I. Ubiquitin networks in cancer. *Curr. Opin. Genet. Dev.* **21,** 21–8 (2011).

117. Komander, D., Clague, M. J. & Urbé, S. Breaking the chains: structure and function of the deubiquitinases. *Nat. Rev. Mol. Cell Biol.* **10,** 550–63 (2009).

118. Wickström, S. A., Masoumi, K. C., Khochbin, S., Fässler, R. & Massoumi, R. CYLD negatively regulates cell-cycle progression by inactivating HDAC6 and increasing the levels of acetylated tubulin. *EMBO J.* **29,** 131–44 (2010).

119. Nakagawa, T. *et al.* Deubiquitylation of histone H2A activates transcriptional initiation via trans-histone cross-talk with H3K4 di- and trimethylation. *Genes Dev.* **22,** 37–49 (2008).

120. Shembade, N., Ma, A. & Harhaj, E. W. Inhibition of NF-kappaB signaling by A20 through disruption of ubiquitin enzyme complexes. *Science* **327,** 1135–9 (2010).

121. Tollini, L. A., Jin, A., Park, J. & Zhang, Y. Regulation of p53 by Mdm2 E3 ligase function is dispensable in embryogenesis and development, but essential in response to DNA damage. *Cancer Cell* **26,** 235–47 (2014).

122. Escobar-henriques, M. & Langer, T. Dynamic survey of mitochondria by ubiquitin. 1–13 (2014).

123. Oberoi-Khanuja, T. K., Murali, A. & Rajalingam, K. IAPs on the move: role of inhibitors of apoptosis proteins in cell migration. *Cell Death Dis.* **4,** e784 (2013).

124. Benard, G. *et al.* IBRDC2, an IBR-type E3 ubiquitin ligase, is a regulatory factor for Bax and apoptosis activation. *EMBO J.* **29,** 1458–71 (2010).

125. Breitschopf, K., Haendeler, J., Malchow, P., Zeiher, A. M. & Dimmeler, S. Posttranslational modification of Bcl-2 facilitates its proteasome-dependent degradation: molecular characterization of the involved signaling pathway. *Mol. Cell. Biol.* **20,** 1886–96 (2000).

126. Niu, J., Shi, Y., Iwai, K. & Wu, Z.-H. LUBAC regulates NF-κB activation upon genotoxic stress by promoting linear ubiquitination of NEMO. *EMBO J.* **30,** 3741–53 (2011).

127. Zemirli, N. *et al.* Mitochondrial hyperfusion promotes NF-κB activation via the mitochondrial E3 ligase MULAN. *FEBS J.* **281,** 3095–112 (2014).

128. Narendra, D., Walker, J. E. & Youle, R. Mitochondrial quality control mediated by PINK1 and Parkin: links to parkinsonism. *Cold Spring Harb. Perspect. Biol.* **4,** a011338– (2012).

129. Neutzner, A., Benard, G., Youle, R. J. & Karbowski, M. Role of the ubiquitin conjugation system in the maintenance of mitochondrial homeostasis. *Ann. N. Y. Acad. Sci.* **1147,** 242–53 (2008).

130. Chen, Y. & Dorn, G. W. PINK1-phosphorylated mitofusin 2 is a Parkin receptor for culling damaged mitochondria. *Science* **340,** 471–5 (2013).

131. Sarraf, S. A. *et al.* Landscape of the PARKIN-dependent ubiquitylome in response to mitochondrial depolarization. *Nature* **496,** 372–6 (2013).

132. Dawson, T. M. & Dawson, V. L. The role of parkin in familial and sporadic Parkinson's disease. *Mov. Disord.* **25 Suppl 1,** S32–9 (2010).

133. Matsuda, S., Nakanishi, A., Minami, A., Wada, Y. & Kitagishi, Y. Functions and characteristics of PINK1 and Parkin in cancer. *Front. Biosci. (Landmark Ed.* **20,** 491–501 (2015).

134. Karbowski, M., Neutzner, A. & Youle, R. J. The mitochondrial E3 ubiquitin ligase MARCH5 is required for Drp1 dependent mitochondrial division. *J. Cell Biol.* **178,** 71–84 (2007).

135. Nathan, J. a & Lehner, P. J. The trafficking and regulation of membrane receptors by the RING-CH ubiquitin E3 ligases. *Exp. Cell Res.* **315,** 1593–600 (2009).

136. Yonashiro, R. *et al.* A novel mitochondrial ubiquitin ligase plays a critical role in mitochondrial dynamics. *EMBO J.* **25,** 3618–26 (2006).

137. Sugiura, A. *et al.* MITOL regulates endoplasmic reticulum-mitochondria contacts via Mitofusin2. *Mol. Cell* **51,** 20–34 (2013).

138. Park, Y.-Y., Nguyen, O. T. K., Kang, H. & Cho, H. MARCH5-mediated quality control on acetylated Mfn1 facilitates mitochondrial homeostasis and cell survival. *Cell Death Dis.* **5,** e1172 (2014).

139. Park, Y.-Y. *et al.* Loss of MARCH5 mitochondrial E3 ubiquitin ligase induces cellular senescence through dynamin-related protein 1 and mitofusin 1. *J. Cell Sci.* **123,** 619–26 (2010).

140. Sugiura, A. *et al.* A mitochondrial ubiquitin ligase MITOL controls cell toxicity of polyglutamine-expanded protein. *Mitochondrion* **11,** 139–46 (2011).

141. Yonashiro, R. *et al.* Mitochondrial ubiquitin ligase MITOL ubiquitinates mutant SOD1 and attenuates mutant SOD1-induced reactive oxygen species generation. *Mol. Biol. Cell* **20,** 4524–30 (2009).

142. Yonashiro, R. *et al.* Mitochondrial ubiquitin ligase MITOL blocks S-nitrosylated MAP1B-light chain 1-mediated mitochondrial dysfunction and neuronal cell death. *Proc. Natl. Acad. Sci. U. S. A.* **109,** 2382–7 (2012).

143. Shi, H.-X. *et al.* Mitochondrial ubiquitin ligase MARCH5 promotes TLR7 signaling by attenuating TANK action. *PLoS Pathog.* **7,** e1002057 (2011).

144. Yoo, Y.-S. *et al.* The mitochondrial ubiquitin ligase MARCH5 resolves MAVS aggregates during antiviral signalling. *Nat. Commun.* **6,** 7910 (2015).

145. Gu, H. *et al.* Mitochondrial E3 ligase March5 maintains stemness of mouse ES cells via suppression of ERK signalling. *Nat. Commun.* **6,** 7112 (2015).

146. Nagashima, S., Tokuyama, T., Yonashiro, R., Inatome, R. & Yanagi, S. Roles of mitochondrial ubiquitin ligase MITOL/MARCH5 in mitochondrial dynamics and diseases. *J. Biochem.* **155,** 273–9 (2014).

147. Ricci, F., Subramanian, A. & Wade, M. Open Access to High-Content Clonogenic Analysis. *J. Biomol. Screen.* (2014). doi:10.1177/1087057114557775

148. Li, Y.-C. *et al.* A versatile platform to analyze low-affinity and transient protein-protein interactions in living cells in real time. *Cell Rep.* **9,** 1946–58 (2014).

149. Wong, E. T. *et al.* Reproducible doxycycline-inducible transgene expression at specific loci generated by Cre-recombinase mediated cassette exchange. *Nucleic Acids Res.* **33,** e147 (2005).

150. Wiley: Applied Regression Analysis, 3rd Edition - Norman R. Draper, Harry Smith. at <http://eu.wiley.com/WileyCDA/WileyTitle/productCd-0471170828.html>

151. Keuling, A. M. *et al.* RNA silencing of Mcl-1 enhances ABT-737-mediated apoptosis in melanoma: role for a caspase-8-dependent pathway. *PLoS One* **4,** e6651 (2009).

152. Wade, M., Rodewald, L. W., Espinosa, J. M. & Wahl, G. M. BH3 activation blocks Hdmx suppression of apoptosis and cooperates with Nutlin to induce cell death. *Cell Cycle* **7,** 1973–82 (2008).

153. Lee, E. F. *et al.* A novel BH3 ligand that selectively targets Mcl-1 reveals that apoptosis can proceed without Mcl-1 degradation. *J. Cell Biol.* **180,** 341–55 (2008).

154. Haschka, M. D. *et al.* The NOXA–MCL1–BIM axis defines lifespan on extended mitotic arrest. *Nat. Commun.* **6,** 6891 (2015).

155. Touzeau, C. *et al.* The Bcl-2 specific BH3 mimetic ABT-199: a promising targeted therapy for t(11;14) multiple myeloma. *Leukemia* **28,** 210–2 (2014).

156. Goodwin, C. M., Rossanese, O. W., Olejniczak, E. T. & Fesik, S. W. Myeloid cell leukemia-1 is an important apoptotic survival factor in triple-negative breast cancer. *Cell Death Differ.* (2015). doi:10.1038/cdd.2015.73

157. Leverson, J. D. *et al.* Potent and selective small-molecule MCL-1 inhibitors demonstrate on-target cancer cell killing activity as single agents and in combination with ABT-263 (navitoclax). *Cell Death Dis.* **6,** e1590 (2015).

158. Stamelos, V. A., Redman, C. W. & Richardson, A. Understanding sensitivity to BH3 mimetics: ABT-737 as a case study to foresee the complexities of personalized medicine. *J. Mol. Signal.* **7,** 12 (2012).

159. Huskey, N. E. *et al.* CDK1 inhibition targets the p53-NOXA-MCL1 axis, selectively kills embryonic stem cells, and prevents teratoma formation. *Stem cell reports* **4,** 374–89 (2015).

160. Nakamura, N., Kimura, Y., Tokuda, M., Honda, S. & Hirose, S. MARCH-V is a novel mitofusin 2- and Drp1-binding protein able to change mitochondrial morphology. *EMBO Rep.* **7,** 1019–22 (2006).

161. Rovini, A., Savry, A., Braguer, D. & Carré, M. Microtubule-targeted agents: when mitochondria become essential to chemotherapy. *Biochim. Biophys. Acta* **1807,** 679–88 (2011).

162. Matsuda, N. *et al.* PINK1 stabilized by mitochondrial depolarization recruits Parkin to damaged mitochondria and activates latent Parkin for mitophagy. *J. Cell Biol.* **189,** 211–221 (2010).

163. Gottlieb, E., Armour, S. M., Harris, M. H. & Thompson, C. B. Mitochondrial membrane potential regulates matrix configuration and cytochrome c release during apoptosis. *Cell Death Differ.* **10,** 709–17 (2003).

164. Narendra, D., Tanaka, A., Suen, D.-F. & Youle, R. J. Parkin is recruited selectively to impaired mitochondria and promotes their autophagy. *J. Cell Biol.* **183,** 795–803 (2008).

165. Li, W. *et al.* Genome-wide and functional annotation of human E3 ubiquitin ligases identifies MULAN, a mitochondrial E3 that regulates the organelle's dynamics and signaling. *PLoS One* **3,** e1487 (2008).

166. Bae, S. *et al.* Akt is negatively regulated by the MULAN E3 ligase. *Cell Res.* **22,** 873–85 (2012).

167. Zhou, Z. *et al.* TRIM59 is up-regulated in gastric tumors, promoting ubiquitination and degradation of p53. *Gastroenterology* **147,** 1043–54 (2014).

168. Nakajima, W., Hicks, M. A., Tanaka, N., Krystal, G. W. & Harada, H. Noxa determines localization and stability of MCL-1 and consequently ABT-737 sensitivity in small cell lung cancer. *Cell Death Dis.* **5,** e1052 (2014).

169. Mei, Y. *et al.* Noxa/Mcl-1 balance regulates susceptibility of cells to camptothecin-induced apoptosis. *Neoplasia* **9,** 871–81 (2007).

170. Hauck, P., Chao, B. H., Litz, J. & Krystal, G. W. Alterations in the Noxa/Mcl-1 axis determine sensitivity of small cell lung cancer to the BH3 mimetic ABT-737. *Mol. Cancer Ther.* **8,** 883–92 (2009).

171. Geserick, P., Wang, J., Feoktistova, M. & Leverkus, M. The ratio of Mcl-1 and Noxa determines ABT737 resistance in squamous cell carcinoma of the skin. *Cell Death Dis.* **5,** e1412 (2014).

172. Wang, C. & Youle, R. J. Predominant requirement of Bax for apoptosis in HCT116 cells is determined by Mcl-1's inhibitory effect on Bak. *Oncogene* **31,** 3177–89 (2012).

173. Nakajima, W. *et al.* Abstract 1657: The role of Noxa/MCL-1 axis in solid tumors treated with DNA damaging agents. *Cancer Res.* **75,** 1657–1657 (2015).

174. Kelly, G. L. *et al.* Targeting of MCL-1 kills MYC-driven mouse and human lymphomas even when they bear mutations in p53. *Genes Dev.* **28,** 58–70 (2014).

175. Freije, W. A., Mandal, S. & Banerjee, U. Expression profiling of attenuated mitochondrial function identifies retrograde signals in Drosophila. *G3 (Bethesda).* **2,** 843–51 (2012).

176. Karawajew, L., Rhein, P., Czerwony, G. & Ludwig, W.-D. Stress-induced activation of the p53 tumor suppressor in leukemia cells and normal lymphocytes requires mitochondrial activity and reactive oxygen species. *Blood* **105,** 4767–75 (2005).

177. Goodwin, C. M., Rossanese, O. W., Olejniczak, E. T. & Fesik, S. W. Myeloid cell leukemia-1 is an important apoptotic survival factor in triple-negative breast cancer. *Cell Death Differ.* 1–9 (2015). doi:10.1038/cdd.2015.73

178. Kane, R. C., Bross, P. F., Farrell, A. T. & Pazdur, R. Velcade: U.S. FDA approval for the treatment of multiple myeloma progressing on prior therapy. *Oncologist* **8,** 508–13 (2003).

179. Jia, L. & Sun, Y. SCF E3 ubiquitin ligases as anticancer targets. *Curr. Cancer Drug Targets* **11,** 347–56 (2011).

180. Landré, V., Rotblat, B., Melino, S., Bernassola, F. & Melino, G. Screening for E3-ubiquitin ligase inhibitors: challenges and opportunities. *Oncotarget* **5,** 7988–8013 (2014).

181. Fang, L., Li, J., Flammer, J. & Neutzner, A. MARCH5 inactivation supports mitochondrial function during neurodegenerative stress. *Front. Cell. Neurosci.* **7,** 176 (2013).

182. Fang, L. *et al.* Inactivation of MARCH5 prevents mitochondrial fragmentation and interferes with cell death in a neuronal cell model. *PLoS One* **7,** e52637 (2012).

183. Lobry, C., Oh, P. & Aifantis, I. Oncogenic and tumor suppressor functions of Notch in cancer: it's NOTCH what you think. *J. Exp. Med.* **208,** 1931–5 (2011).

184. Boland, M. L., Chourasia, A. H. & Macleod, K. F. Mitochondrial dysfunction in cancer. *Front. Oncol.* **3,** 292 (2013).

185. Wang, Y. *et al.* Deubiquitinating enzymes regulate PARK2-mediated mitophagy. *Autophagy* **11,** 595–606 (2015).

186. Liang, J.-R. *et al.* USP30 deubiquitylates mitochondrial Parkin substrates and restricts apoptotic cell death. *EMBO Rep.* **16,** 618–27 (2015).

187. Hu, Y. *et al.* K-ras(G12V) transformation leads to mitochondrial dysfunction and a metabolic switch from oxidative phosphorylation to glycolysis. *Cell Res.* **22,** 399–412 (2012).

188. Li, F. *et al.* Myc stimulates nuclearly encoded mitochondrial genes and mitochondrial biogenesis. *Mol. Cell. Biol.* **25,** 6225–34 (2005).

189. Guha, M., Fang, J.-K., Monks, R., Birnbaum, M. J. & Avadhani, N. G. Activation of Akt is essential for the propagation of mitochondrial respiratory stress signaling and activation of the transcriptional coactivator heterogeneous ribonucleoprotein A2. *Mol. Biol. Cell* **21,** 3578–89 (2010).

190. Carnero, A., Blanco-Aparicio, C., Renner, O., Link, W. & Leal, J. F. M. The PTEN/PI3K/AKT signalling pathway in cancer, therapeutic implications. *Curr. Cancer Drug Targets* **8,** 187–98 (2008).

191. Li, Y. *et al.* Phosphatase and tensin homolog deleted on chromosome 10 (PTEN) signaling regulates mitochondrial biogenesis and respiration via estrogen-related receptor α (ERRα). *J. Biol. Chem.* **288,** 25007–24 (2013).

192. Liu, P. *et al.* Cell-cycle-regulated activation of Akt kinase by phosphorylation at its carboxyl terminus. *Nature* **508,** 541–5 (2014).

193. Maya, R. *et al.* ATM-dependent phosphorylation of Mdm2 on serine 395: role in p53 activation by DNA damage. *Genes Dev.* **15,** 1067–77 (2001).

194. Thomas, G. S., Zhang, L., Blackwell, K. & Habelhah, H. Phosphorylation of TRAF2 within its RING domain inhibits stress-induced cell death by promoting IKK and suppressing JNK activation. *Cancer Res.* **69,** 3665–72 (2009).

195. Gonzalez, E. & McGraw, T. E. The Akt kinases: isoform specificity in metabolism and cancer. *Cell Cycle* **8,** 2502–8 (2009).

196. Luo, J. *et al.* A genome-wide RNAi screen identifies multiple synthetic lethal interactions with the Ras oncogene. *Cell* **137,** 835–48 (2009).

197. Blom, N., Sicheritz-Pontén, T., Gupta, R., Gammeltoft, S. & Brunak, S. Prediction of post-translational glycosylation and phosphorylation of proteins from the amino acid sequence. *Proteomics* **4,** 1633–49 (2004).